



# Relay based spectrum sharing designs for cognitive radio networks

**Author:**

Zhai, Chao

**Publication Date:**

2013

**DOI:**

<https://doi.org/10.26190/unsworks/16403>

**License:**

<https://creativecommons.org/licenses/by-nc-nd/3.0/au/>

Link to license to see what you are allowed to do with this resource.

Downloaded from <http://hdl.handle.net/1959.4/52958> in <https://unsworks.unsw.edu.au> on 2024-05-02

# Relay Based Spectrum Sharing Designs for Cognitive Radio Networks

Chao Zhai

A dissertation submitted to the Graduate Research School of  
The University of New South Wales  
in partial fulfillment of the requirements for the degree of

Doctor of Philosophy



School of Electrical Engineering and Telecommunications  
Faculty of Engineering

August 2013



PLEASE TYPE

THE UNIVERSITY OF NEW SOUTH WALES  
Thesis/Dissertation Sheet

Surname or Family name: Zhai

First name: Chao

Other name/s:

Abbreviation for degree as given in the University calendar: PhD

School: Electrical Engineering and Telecommunications

Faculty: Engineering

Title: Relay Based Spectrum Sharing Designs  
for Cognitive Radio Networks

Abstract 350 words maximum: (PLEASE TYPE)

With ever-growing wireless data transmission requirements, there is a dramatic increase in the demand for radio spectrum. Within the current spectrum regulatory framework, all of the frequency bands are exclusively allocated to specific services. However, the licensed spectrum is often under-utilized across time and space dimensions. In this context, cognitive radio (CR) has emerged as a promising technology to deal with the stringent requirement and scarcity of the spectrum. Cooperative relaying can allow distributed terminals to collaborate so as to realize the space diversity to combat the detrimental effects of channel fading. This thesis focuses on designing the bandwidth efficient relay based spectrum sharing solutions to improve the capacity of CR networks while guaranteeing the performance of licensed users.

A cognitive two-path successive relaying (TPSR) scheme is proposed to facilitate the spectrum sharing, where the superposition coding and successive interference cancellation techniques are used to realize the primary signal relaying and secondary signal transmission simultaneously. The optimal power allocation is determined to maximize the secondary success probability without violating the primary outage performance. For the multiuser CR network, an adaptive spectrum leasing scheme with the best secondary user (SU) selection is proposed. The SU can intelligently switch between the TPSR and decode-and-forward relay modes to assist the primary data transmission in exchange for the spectrum release for a fraction of time to transmit the secondary data. The cooperative diversity gain of primary system and the multiuser diversity of secondary system are studied.

For large wireless network, it is nontrivial to select the relay in a coordinated fashion, as the heavy signalling overhead may negate the cooperation gains. Three uncoordinated relay selection schemes are proposed, where each relay can determine whether to cooperate or not independently according to the local channel or geo-location information. To address the uncertain interference problem in spatially random network, a cooperative spectrum sharing scheme between cellular network downlink and ad-hoc network is designed. The transmission capacity of ad-hoc network and the average throughput of cellular network are analysed by using the stochastic geometry theory, based on which the optimal system parameters are determined.

Declaration relating to disposition of project thesis/dissertation

I hereby grant to the University of New South Wales or its agents the right to archive and to make available my thesis or dissertation in whole or in part in the University libraries in all forms of media, now or here after known, subject to the provisions of the Copyright Act 1968. I retain all property rights, such as patent rights. I also retain the right to use in future works (such as articles or books) all or part of this thesis or dissertation.

I also authorise University Microfilms to use the 350 word abstract of my thesis in Dissertation Abstracts International (this is applicable to doctoral thesis only).

*Chao Zhai*

Signature

*Chenxi Liu*

Witness

*23/10/2013*

Date

The University recognises that there may be exceptional circumstances requiring restrictions on copying or conditions on use. Requests for restriction for a period of up to 2 years must be made in writing. Requests for a longer period of restriction may be considered in exceptional circumstances and require the approval of the Dean of Graduate Research.

FOR OFFICE USE ONLY

Date of completion of requirements for Award:

**COPYRIGHT STATEMENT**

'I hereby grant the University of New South Wales or its agents the right to archive and to make available my thesis or dissertation in whole or part in the University libraries in all forms of media, now or here after known, subject to the provisions of the Copyright Act 1968. I retain all proprietary rights, such as patent rights. I also retain the right to use in future works (such as articles or books) all or part of this thesis or dissertation.

I also authorise University Microfilms to use the 350 word abstract of my thesis in Dissertation Abstract International (this is applicable to doctoral theses only).

I have either used no substantial portions of copyright material in my thesis or I have obtained permission to use copyright material; where permission has not been granted I have applied/will apply for a partial restriction of the digital copy of my thesis or dissertation.'

Signed ..... *Chaozhew* .....

Date ..... *23/10/2013* .....

**AUTHENTICITY STATEMENT**

'I certify that the Library deposit digital copy is a direct equivalent of the final officially approved version of my thesis. No emendation of content has occurred and if there are any minor variations in formatting, they are the result of the conversion to digital format.'

Signed ..... *Chaozhew* .....

Date ..... *23/10/2013* .....

**ORIGINALITY STATEMENT**

'I hereby declare that this submission is my own work and to the best of my knowledge it contains no materials previously published or written by another person, or substantial proportions of material which have been accepted for the award of any other degree or diploma at UNSW or any other educational institution, except where due acknowledgement is made in the thesis. Any contribution made to the research by others, with whom I have worked at UNSW or elsewhere, is explicitly acknowledged in the thesis. I also declare that the intellectual content of this thesis is the product of my own work, except to the extent that assistance from others in the project's design and conception or in style, presentation and linguistic expression is acknowledged.'

Signed ..... *Chowzhen* .....

Date ..... *23/10/2013* .....

## ABSTRACT

With ever-growing wireless data transmission requirements, there is a dramatic increase in the demand for radio spectrum. Within the current spectrum regulatory framework, all of the frequency bands are exclusively allocated to specific services. However, the licensed spectrum is often under-utilized across time and space dimensions. In this context, cognitive radio (CR) has emerged as a promising technology to deal with the stringent requirement and scarcity of the spectrum. Cooperative relaying can allow distributed terminals to collaborate so as to realize the space diversity to combat the detrimental effects of channel fading. This thesis focuses on designing the bandwidth efficient relay based spectrum sharing solutions to improve the capacity of CR networks while guaranteeing the performance of licensed users.

A cognitive two-path successive relaying (TPSR) scheme is proposed to facilitate the spectrum sharing, where the superposition coding and successive interference cancellation techniques are used to realize the primary signal relaying and secondary signal transmission simultaneously. The optimal power allocation is determined to maximize the secondary success probability without violating the primary outage performance. For the multiuser CR network, an adaptive spectrum leasing scheme with the best secondary user (SU) selection is proposed. The SU can intelligently switch between the TPSR and decode-and-forward relay modes to assist the primary data transmission in exchange for the spectrum release for a fraction of time to transmit the secondary data.

The cooperative diversity gain of primary system and the multiuser diversity of secondary system are studied.

For large wireless network, it is nontrivial to select the relay in a coordinated fashion, as the heavy signaling overhead may negate the cooperation gains. Three uncoordinated relay selection schemes are proposed, where each relay can determine whether to cooperate or not independently according to the local channel or geo-location information. To address the uncertain interference problem in spatially random network, a cooperative spectrum sharing scheme between cellular network downlink and ad-hoc network is designed. The transmission capacity of ad-hoc network and the average throughput of cellular network are analyzed by using the stochastic geometry theory, based on which the optimal system parameters are determined.

## ACKNOWLEDGEMENTS

My deepest gratitude goes first and foremost to my supervisor Prof. Wei Zhang for his constant encouragement and guidance. During my PhD study, I have learnt lots of things from him, particularly about how to think critically, write logically, work efficiently, and network actively. I am much indebted for his patience, criticism, encouragement, and support over the years. Without his enthusiastic help, I would have never attain the academic progress.

I would like to thank Prof. Guoqiang Mao of Sydney University for his supervision and comments on my work in developing the uncoordinated cooperation and spectrum sharing schemes in large wireless network. I sincerely thank Prof. P. C. Ching of the Chinese University of Hong Kong (CUHK) for his support on my visit to CUHK and his inspiring discussions about the bandwidth efficient spectrum sharing designs. I would like to thank Prof. K. B. Letaief of the Hong Kong University of Science and Technology (HKUST) for his support on my visit to HKUST and his constructive suggestions on the spectrum sharing designs with energy harvesting. I am also grateful to the valuable suggestions given by Prof. Jun Zhang and Prof. Shenghui Song of HKUST in refining the spectrum sharing model with energy harvesting.

Many thanks go to my friends and colleagues at UNSW, Long Shi, Yi Lu, Zhe Wang, Lu Yang, Shihao Yan, Chenxi Liu, Nan Yang, Yixuan Xie, Mengyu Huang, Tao Huang, Giovanni, Rui Ma, Xiaochen Wang, Chiya Zhang, and Wei Wang. Thanks them all for the enjoyable time spent together. Wish all of them

have a brilliant future.

I would like to express my ultimate gratitude and love to my wife Jianing. When I studied abroad, she lived in China and has taken good care of our son Hongyu. They give me the strongest motivation to work hard. Especially, I would like to thank my parents for their continuous support and encouragement throughout the PhD study period.

Finally, I would like to acknowledge the Tuition Fee Remission (TFR) scholarship and the Postgraduate Research Student Support (PRSS) conference travel funds awarded by the University of New South Wales as well as the living allowance awarded by China Scholarship Council (CSC).

# Contents

<b>Table of Contents</b>	<b>vii</b>
<b>Abbreviations</b>	<b>x</b>
<b>List of Notations</b>	<b>xii</b>
<b>List of Figures</b>	<b>xiii</b>
<b>List of Publications</b>	<b>xv</b>
<b>1 Introduction</b>	<b>1</b>
1.1 Cooperative Spectrum Sharing . . . . .	2
1.2 Challenges and Motivations . . . . .	5
1.3 Thesis Outline and Contributions . . . . .	8
<b>2 Cooperative Spectrum Sharing Based on TPSR</b>	<b>11</b>
2.1 Introduction . . . . .	11
2.2 Cognitive Spectrum Sharing . . . . .	13
2.2.1 Cognitive Relay for Spectrum Sharing . . . . .	14
2.2.2 Signal Model . . . . .	15
2.3 Outage Performance and Power Allocation . . . . .	17
2.3.1 Spectrum Sharing Probability . . . . .	17
2.3.2 Outage Probability of the Primary System . . . . .	19
2.3.3 Outage Probability of the Secondary System . . . . .	21
2.3.4 Optimal Power Allocation . . . . .	23
2.4 Numerical and Simulation Results . . . . .	26
2.4.1 Comparison with Other Schemes . . . . .	26
2.4.2 Outage Performance vs. Secondary Transmission Power . . . . .	29
2.4.3 Outage Performance vs. Primary Transmission Power . . . . .	31
2.4.4 Outage Performance vs. Small-Scale Distance . . . . .	33
2.5 Summary . . . . .	34
2.6 Appendix I: Derivation of Spectrum Sharing Probability . . . . .	34
2.7 Appendix II: Derivation of Approximate Rate . . . . .	36
2.8 Appendix III: Power Allocation Factor $\hat{\beta}$ . . . . .	37

<b>3</b>	<b>Adaptive Spectrum Leasing with Secondary User Scheduling</b>	<b>39</b>
3.1	Introduction . . . . .	39
3.2	System Model . . . . .	41
3.3	Adaptive Spectrum Leasing with User Scheduling . . . . .	43
3.3.1	Secondary User Scheduling . . . . .	43
3.3.2	Optimal Time Allocation for TPSR based Scheme . . . . .	45
3.3.3	Optimal Time Allocation for DF based Scheme . . . . .	49
3.4	Diversity Performance Analysis . . . . .	51
3.4.1	Cooperative Diversity of Primary System . . . . .	51
3.4.2	Selection Diversity of Secondary System . . . . .	53
3.5	Multiuser Diversity: Throughput Scaling Law . . . . .	56
3.5.1	Throughput Lower Bound . . . . .	56
3.5.2	Throughput Upper Bound . . . . .	58
3.6	Numerical and Simulation Results . . . . .	59
3.6.1	Outage Probability . . . . .	60
3.6.2	Secondary Throughput . . . . .	63
3.7	Summary . . . . .	64
3.8	Appendix I: Proof of the Rate Upper Bound . . . . .	65
3.9	Appendix II: Proof of the Condition . . . . .	68
<b>4</b>	<b>Uncoordinated Cooperation with Spatially Random Relays</b>	<b>71</b>
4.1	Introduction . . . . .	71
4.2	System Model and Relay Protocol . . . . .	73
4.2.1	System Model . . . . .	73
4.2.2	Relay Protocol . . . . .	74
4.3	Uncoordinated Cooperation Schemes . . . . .	75
4.3.1	Distance Based Scheme . . . . .	77
4.3.2	Sectorized Scheme . . . . .	80
4.3.3	Local SNR Based Scheme . . . . .	82
4.4	System Success Probability . . . . .	84
4.4.1	For the Sectorized Scheme . . . . .	85
4.4.2	For the Local SNR Based Scheme . . . . .	87
4.5	Numerical and Simulation Results . . . . .	89
4.6	Summary . . . . .	95
<b>5</b>	<b>Cooperative Spectrum Sharing in Ad-Hoc Network</b>	<b>96</b>
5.1	Introduction . . . . .	96
5.2	System Description . . . . .	99
5.2.1	Spectrum Sharing Model . . . . .	100
5.2.2	Cooperation Model . . . . .	101
5.3	Transmission Capacity of Secondary System . . . . .	103
5.4	Average Throughput of Primary System . . . . .	104
5.4.1	Distance Distribution and Interference Model . . . . .	104

---

5.4.2	Success Probability of Cell-Interior Communication . . . . .	105
5.4.3	Success Probability of Cell-Edge Communication . . . . .	107
5.4.4	Average Throughput of Primary System . . . . .	110
5.5	Solution to the Optimization Problem . . . . .	112
5.6	Numerical and Simulation Results . . . . .	113
5.6.1	Average Throughput of Primary System . . . . .	114
5.6.2	Transmission Capacity of Secondary System . . . . .	117
5.7	Summary . . . . .	120
5.8	Appendix I: Success Probability of Case II . . . . .	121
5.9	Appendix II: Success Probability of Case III . . . . .	123
<b>6</b>	<b>Conclusion and Future Work</b>	<b>125</b>
6.1	Thesis Conclusion . . . . .	125
6.2	Future Work . . . . .	127
	<b>Bibliography</b>	<b>129</b>

# Abbreviations

<b>ACK</b>	Acknowledgement
<b>AF</b>	Amplify-and-forward
<b>ARQ</b>	Automatic repeat request
<b>AWGN</b>	Additive white Gaussian noise
<b>BS</b>	Base station
<b>CDF</b>	Cumulative distribution function
<b>CCDF</b>	Complement cumulative distribution function
<b>CR</b>	Cognitive radio
<b>CSI</b>	Channel state information
<b>CSMA</b>	Carrier sense multiple access
<b>DF</b>	Decode-and-forward
<b>DOA</b>	Direction of arrival
<b>GPS</b>	Global positioning system
<b>MAC</b>	Media access control
<b>MAP</b>	Media access probability
<b>MIMO</b>	Multi-input multi-output
<b>ML</b>	Maximum-likelihood
<b>MRC</b>	Maximal ratio combining
<b>MU</b>	Mobile user
<b>NACK</b>	Negative acknowledgement
<b>OFDM</b>	Orthogonal frequency division multiplexing
<b>PDF</b>	Probability density function

<b>PGFL</b>	Probability generating functional
<b>PPP</b>	Poisson point process
<b>PR</b>	Primary receiver
<b>PT</b>	Primary transmitter
<b>PU</b>	Primary user
<b>QoS</b>	Quality of service
<b>SIC</b>	Successive interference cancelation
<b>SIFS</b>	Shorter inter-frame space
<b>SINR</b>	Signal to interference plus noise ratio
<b>SIR</b>	Signal to interference ratio
<b>SNR</b>	Signal to noise ratio
<b>SR</b>	Secondary receiver
<b>ST</b>	Secondary transmitter
<b>STBC</b>	Space-time block code
<b>SU</b>	Secondary user
<b>TDMA</b>	Time division multiple access
<b>TPSR</b>	Two-path successive relaying
<b>WLAN</b>	Wireless local-area network

# List of Notations

$\alpha$	path-loss exponent
$ \cdot $	magnitude of an element
$\ \cdot\ $	Euclidean norm for vectors
$\mathcal{CN}(0, a)$	complex Gaussian random variable with zero mean and variance $a$
$N_0$	variance of additive white Gaussian noise
$\mathbf{H}_{m \times n}$	channel matrix with size $m \times n$
$\mathbf{I}_n$	identity matrix with size $n \times n$
$i$	the imaginary unit $i = \sqrt{-1}$
$(\cdot)^{\mathcal{T}}$	transpose
$(\cdot)^{\mathcal{H}}$	conjugate transpose
$\mathbb{E}_{\mathcal{I}}[\cdot]$	mathematical expectation taken over random variable $\mathcal{I}$
$\text{mod}(\cdot, \cdot)$	modulo operation
$\log_2(\cdot)$	logarithm with base two
$\ln(\cdot)$	natural logarithm
$\max\{\cdot\}$	maximization
$\min\{\cdot\}$	minimization
$\sup\{\cdot\}$	supremum of a set
$\text{diag}(d_1, \dots, d_n)$	a diagonal matrix with diagonal entries $d_1, \dots, d_n$
$\det(\cdot)$	determinant of a matrix
$\mathcal{L}_{\mathcal{I}}(s)$	Laplace transform of random variable $\mathcal{I}$
$\Gamma(\cdot)$	Gamma function
$\Gamma(\cdot, \cdot)$	incomplete Gamma function

# List of Figures

1.1	DF based cooperative spectrum leasing schemes . . . . .	3
1.2	Two-path successive relaying protocol . . . . .	5
2.1	Transmission order of the TPSR based spectrum sharing scheme . . . . .	13
2.2	The approximate and exact power allocation factor $\beta$ . . . . .	24
2.3	The objective function with different values of $\beta$ . . . . .	25
2.4	Comparison to other schemes with different primary powers . . . . .	27
2.5	Comparison to other schemes with different large-scale distances . . . . .	28
2.6	Outage probability vs. secondary power for various large-scale distance . . . . .	29
2.7	Outage probability vs. secondary power for various transmission rates . . . . .	30
2.8	Outage probability vs. primary power for various large-scale distances . . . . .	31
2.9	Outage probability vs. primary power for various transmission rates . . . . .	32
2.10	Outage probability vs. secondary power for various small-scale distance . . . . .	33
3.1	Spectrum leasing schemes in the cognitive radio network . . . . .	41
3.2	Flow chart of the SU scheduling with adaptive mode selection . . . . .	44
3.3	Outage probability of primary system with $r_0 = 3$ and $m = 3$ . . . . .	60
3.4	Outage probability of primary system with $r_0 = 2$ and $m = 3$ . . . . .	61
3.5	Outage probability of secondary system with $r_0 = 2$ and $m = 3$ . . . . .	62
3.6	Outage probability of secondary system with $r_0 = 1.5$ and $m = 3$ . . . . .	62
3.7	Throughput of secondary system with different number of users . . . . .	63
3.8	Throughput scaling law of the secondary system . . . . .	64
4.1	Flow chart of the uncoordinated cooperative truncated ARQ . . . . .	76
4.2	The coordinate system with destination located at the origin . . . . .	78
4.3	Retransmission probability of the distance based scheme . . . . .	80
4.4	The coordinate system with source located at the origin . . . . .	81
4.5	Retransmission probability vs. node density . . . . .	90
4.6	Success probability vs. node density for different SNR thresholds . . . . .	91
4.7	Success probability vs. node density for different $S - D$ distances . . . . .	92
4.8	Success probability vs. $S - D$ distance for different SNR thresholds . . . . .	93
4.9	Success probability vs. average SNR at the destination . . . . .	94
5.1	The overlaid wireless network with PPP modeling . . . . .	99

---

5.2	Bandwidth division between primary and secondary systems . . . . .	100
5.3	The cooperation model for the cell-edge communication . . . . .	101
5.4	Primary average throughput vs. relative distance factor $\zeta$ . . . . .	114
5.5	Primary average throughput vs. bandwidth allocation factor $\beta$ . . . . .	115
5.6	Primary average throughput vs. secondary user density $\lambda_s$ . . . . .	116
5.7	Secondary transmission capacity vs. primary ratio $\rho$ for different $c_0$ . . . . .	117
5.8	Secondary transmission capacity vs. primary ratio $\rho$ for different $T_1$ . . . . .	118
5.9	Secondary transmission capacity vs. target outage for different $\xi$ . . . . .	119
5.10	Secondary transmission capacity vs. target outage for different $\rho$ . . . . .	120

# List of Publications

## Journal Papers:

1. **C. Zhai**, W. Zhang, and G. Mao, “Cooperative spectrum sharing between cellular and ad-hoc networks,” *IEEE Trans. Wireless Commun.*, submitted, Jul. 2013.
2. **C. Zhai** and W. Zhang, “Adaptive spectrum leasing with secondary user scheduling in cognitive radio networks,” *IEEE Trans. Wireless Commun.*, vol. 12, pp. 3388–3398, Jul. 2013.
3. **C. Zhai**, W. Zhang, and P. C. Ching, “Cooperative spectrum sharing based on two-path successive relaying,” *IEEE Trans. Commun.*, vol. 61, pp. 2260–2270, Jun. 2013.
4. **C. Zhai**, W. Zhang, and G. Mao, “Uncoordinated cooperative communications with spatially random relays,” *IEEE Trans. Wireless Commun.*, vol. 11, pp. 3126–3135, Sep. 2012.

## Conference Papers:

1. **C. Zhai**, W. Zhang, and G. Mao, “Cooperative spectrum sharing in wireless ad-hoc networks,” in *Proc. IEEE International Conference on Acoustics, Speech and Signal Processing (ICASSP)*, Vancouver, Canada, pp. 5293–5297, May 2013.
2. **C. Zhai** and W. Zhang, “Multiuser diversity of spectrum leasing in cognitive radio networks,” invited paper of the *IEEE International Wireless Symposium (IWS)*, Beijing, China, pp. 1–4, Apr. 2013.
3. **C. Zhai**, W. Zhang, and P. C. Ching, “Spectrum leasing based on bandwidth efficient relaying in cognitive radio networks,” in *Proc. IEEE Global Communications Conference (GLOBECOM)*, Anaheim, California, USA, pp. 4927–4932, Dec. 2012.

4. **C. Zhai** and W. Zhang, “Spectrum and energy efficient cognitive relay for spectrum leasing”, invited paper of the 13th *IEEE International Conference on Communication Systems (ICCS)*, Singapore, pp. 240–244, Nov. 2012.
5. **C. Zhai**, W. Zhang, and G. Mao, “Uncoordinated cooperative truncated ARQ schemes in wireless systems,” in *Proc. IEEE International Conference on Communications (ICC)*, Ottawa, Canada, pp. 3910–3914, Jun. 2012.
6. **C. Zhai**, W. Zhang, and P. C. Ching, “Spectrum sharing based on two-path successive relaying,” in *Proc. IEEE International Conference on Acoustics, Speech and Signal Processing (ICASSP)*, Kyoto, Japan, pp. 2909–2912, Mar. 2012.

# Chapter 1

## Introduction

Driven by the consumers' ever-growing interest in wireless services, the demand for radio spectrum is dramatically increasing and this trend is expected to continue in the coming years [1]. Within the current spectrum regulatory framework, most of the useful frequency bands are exclusively allocated to specific services and it becomes exceedingly difficult to find vacant bands to either deploy new services or to enhance the existing ones [2]. However, the licensed spectrum is often under-utilized across time and space dimensions. In this context, cognitive radio (CR) has emerged as a promising way to deal with the stringent requirement and scarcity of the spectrum.

Multi-input multi-output (MIMO) technology along with some channel coding techniques such as space-time/frequency coding [3] has been extensively studied to mitigate the multi-path fading of wireless channels. However, the implementation of multiple antennas on small terminals is quite difficult due to the limited device-size and the cost constraints [4]. In this context, cooperative communication has emerged that allows distributed terminals in a wireless network to collaborate through some distributed signal processing [5, 6] so as to realize the space diversity to combat the detrimental effect of channel fading [7].

Through taking advantage of both cognitive radio and cooperative techniques, the stringent requirement for the spectrum can be alleviated, as the capacity of wireless

networks can be greatly improved. In this chapter, the cooperative spectrum sharing in cognitive radio network is firstly introduced in Section 1.1. The motivations and challenging problems are outlined in Section 1.2. Finally, the thesis organization and contribution are presented in Section 1.3.

## 1.1 Cooperative Spectrum Sharing

Spectrum sharing in CR networks has been intensively studied to meet the increasing demand for wireless applications, as the exclusive usage of spectrum is inefficient [8]. Although the spectrum belongs to the primary system, it allows secondary system access under a strict performance constraint [9]. The spectrum sharing schemes can be categorized into three types [10, 11], i.e., interweave, underlay, and overlay.

- For the interweave spectrum sharing, the secondary users (SUs) can opportunistically access the channel when the primary users (PUs) are sensed to be idle. If the PUs are sensed to be active, the SUs should evacuate from the spectrum bands immediately to avoid causing interference to the PUs' transmission.
- For the underlay spectrum sharing, the SUs access the channel concurrently with the PUs under the interference constraint. The secondary transmitters should estimate the channel states between themselves and the primary receivers, based on which the transmission power should be carefully adjusted to avoid causing intolerable interference to the primary receiver (PR).
- For the overlay spectrum sharing, the secondary system can actively help the primary data transmission in the space/time/frequency domain in exchange for the opportunity of spectrum access. With the cooperation of SUs, the primary data transmission requirement can be satisfied more easily and the spectrum can thus be released to the secondary data transmission.

Since there is no interference between the primary and the secondary systems due to the explicit coordination, more benefits can be brought by the overlay spectrum

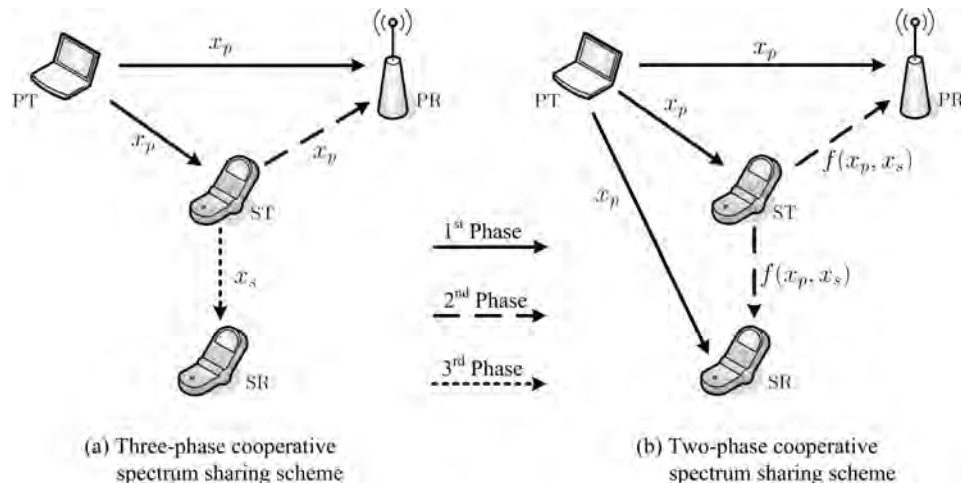


**Figure 1.1:** DF based cooperative spectrum sharing schemes.

sharing, which is the focus of this thesis.

In the cooperative communication system, packets transmitted by the source can be overheard by the nearby relays due to the broadcast nature of wireless channels. When the wireless link between source and destination undergoes deep fading, there is a high probability that the bad channel condition will continue for a period. However, if the relay is adopted to help the source transmission, the reliability of source data delivery can be enhanced, because the relay-destination and source-destination channels are independent and the probability that both of them undergo deep fading is very small [12]. This is a kind of space diversity achieved by the virtual antenna arrays formed through the cooperation of relays [13]. Through implementing the cooperative techniques in the cognitive radio network, the spectrum efficiency can be improved, which falls into the cooperative spectrum sharing category introduced as follows.

Based on the conventional decode-and-forward (DF) protocol, a three-phase cooperative spectrum sharing scheme, i.e., spectrum leasing, was proposed in [14] and shown in Fig. 1.1(a), where the secondary transmitter (ST) can actively help the primary data transmission in the first two communication phases to exchange for the opportunity of secondary data transmission over the licensed spectrum in the third

phase. Thanks to the advantage of cooperation, the primary rate target can be satisfied in a short time duration and the spectrum can thus be released to the secondary data transmission in the remaining time. The primary system has the instantaneous/statistical information of the whole network to determine the optimal time allocation. The cooperative automatic repeat request (ARQ) scheme with spectrum leasing was proposed in [15], where the PUs may handover the possible retransmission slots to the nearby SUs that can correctly decode the original primary data. A fraction of retransmission time is used to relay the primary data, while the remaining time is awarded to the secondary traffic. To regulate the coexistence of PUs and SUs in the multihop networks, the opportunistic routing algorithm with spectrum leasing was proposed in [16], where both the superposition coding and orthogonal multiplexing techniques are considered by the SUs to realize the primary data relaying and secondary data transmission. For the dynamic spectrum leasing [17], the PUs can adjust the willingness of leasing the spectrum by tuning the amount of interference it can bear. Since a better performance with less energy consumption can be expected for the primary system, and the secondary transmission requirement can be satisfied, the spectrum leasing is a win-win game for both systems [18].

To improve the spectrum efficiency, the two-phase cooperative spectrum sharing schemes based on DF and amplify-and-forward (AF) relaying as shown in Fig. 1.1(b) were proposed in [19] and [20], respectively. In the first communication phase, the primary signal is broadcasted from the primary transmitter (PT), and in the second phase, the primary data and secondary data are simultaneously transmitted by the ST using the superposition coding technique. Interference can be tolerated as space diversity can be introduced by the cooperation; thus, the performance of the primary system can be protected. The secondary receiver (SR) firstly cancels the primary signal before decoding its desired secondary signal. As an extension, the two-phase cooperative spectrum sharing scheme with SU selection was proposed in [21] for the multiuser network. The SU that can correctly receive the primary data in the first phase and has the best channel state towards the PR is selected to relay the primary

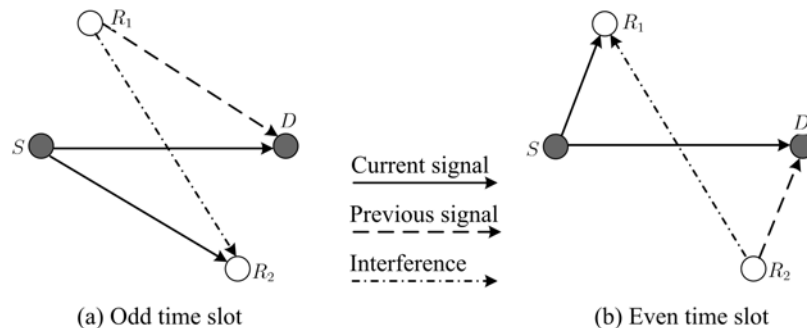


**Figure 1.2:** Two-path successive relaying protocol.

data in the second phase. With the cooperation of the best SU, the PR can tolerate a certain amount of interference. Among the remaining SUs, the one that can satisfy the interference constraint and bring the largest secondary rate is scheduled for the secondary data transmission.

## 1.2 Challenges and Motivations

In the CR network, a secondary system geographically coexists with the primary system that owns the licensed spectrum. The cooperative technique can be adopted as an effective way to realize the design goal of CR network as mentioned in the previous section. However, for the traditional DF/AF relaying protocols [22], multiple communication phases are included. To combat the low bandwidth efficiency of the multi-phase protocols, the two-path successive relaying (TPSR) protocol as shown in Fig. 1.2 has been proposed in [23, 24], where the two relays can alternately and successively forward the source signal to the destination. The source transmission is continuous without interruption from relays, so the bandwidth efficiency is much higher than the conventional cooperation protocols. It was recently shown that full diversity and full rate can be achieved with the cooperation of the two relays via space-time coding techniques [25, 26]. Moreover, the achievable rate of the TPSR scheme was investigated in [27], and the diversity-multiplexing tradeoff with AF and DF fashions were analyzed in [28] and [29], respectively. The full interference cancelation

algorithm was proposed to remove the inter-relay interference at the destination node in the AF-based two-path cooperative networks [30].

The TPSR scheme can be adopted in the spectrum sharing process to further improve the bandwidth efficiency. For the CR network with single primary link coexisting with two secondary communication pairs, the following challenging problems will be encountered in the TPSR based spectrum sharing design. i) How to simultaneously forward the primary data and transmit the secondary data without adversely affecting the transmission quality of each system by controlling the mutual interference? ii) In the spectrum sharing procedure, the primary system not only enjoys the benefits of cooperation but also suffers from the interference caused by the secondary data transmission. Then, at what point the benefits brought by the cooperation can negate the detrimental effect of interference? iii) The system performance needs to be analyzed, based on which the optimal system parameter designs should be determined to maximize the throughput of secondary system while guaranteeing the performance requirement of primary system.

In the multiuser CR network, one primary link coexists with multiple STs that intend to communicate with a common SR. To improve the spectrum utilization efficiency, the best ST should be selected for the cooperative spectrum sharing in the time domain, which is also known as the spectrum leasing. The motivations and challenging problems are listed as follows. i) The optimal ST should be selected in a distributed way to assist the primary data transmission for a time duration. So, the distributed MAC protocol needs to be designed to select the best ST with some necessary signaling exchange. ii) To efficiently utilize the spectrum, the cooperation mode can be dynamically switched between the traditional DF and the superior TPSR. The problem is how to select the relaying mode with optimal time allocation to maximize the capacity of secondary system under the primary performance constraint. iii) The multiuser diversity of the cooperative spectrum sharing system needs to be studied. It is not clear what is the impact of cognitive constraint on the cooperative diversity gain of primary link and on the multiuser diversity of secondary system.

The DF based incremental relaying [22], which is also known as the cooperative truncated ARQ, can greatly improve the system throughput because relaying is performed only when the original transmission fails [33]. In the conventional cooperative ARQ schemes, the locations of relays are usually fixed or restricted into a small area. It could select the best relay in a centralized way with global channel state information (CSI) or in a distributed way using the time back-off mechanism [34]. However, in a large wireless network, there are many spatially random relays. It is nontrivial to realize the relay selection in a coordinated fashion, because a huge amount of control-signal exchange overhead is required. The heavy overhead in the coordination may even negate the performance gains brought by the cooperation. It is desirable to develop effective uncoordinated methods to realize the relay selection in a large network to reduce the coordination overhead. Each potential relay should determine independently by itself whether to cooperate or not according to its local information.

For the large wireless ad-hoc network, there are many concurrent primary and secondary links. All the PUs and SUs are randomly distributed over the two-dimensional plane. Both the primary and secondary data transmissions suffer from interferences coming from other concurrent transmission links. It is challenging to accurately model the aggregate interference, as it bears the uncertainties caused by the random locations of users and the channel fading effects. The cooperative spectrum sharing can be implemented between cellular and ad-hoc networks that are geographically overlaid. For the cellular network downlink, the weak signal and strong interference at the cell-edge area cause a bottleneck to guarantee the overall quality of service (QoS) requirement. The ad-hoc users can assist the cell-edge data transmissions in exchange for the spectrum usage. The dependence of the interference at the cell-edge mobile user (MU) and at the cooperating SUs makes the exact performance analysis very difficult. In this case, the performance should be evaluated and verified through simulations, based on which the optimal system parameters could be determined.

## 1.3 Thesis Outline and Contributions

This thesis aims to develop bandwidth efficient relay based spectrum sharing schemes to improve the capacity of cognitive radio networks while satisfying the performance requirement of licensed users. The organization together with the contributions are presented as follows.

In Chapter 2, a spectrum sharing scheme based on TPSR is proposed for the overlaid wireless network, where one primary link coexists with two secondary links. In this scheme, two secondary transmitters can send secondary signal alternately to their respective receivers while relaying the primary signal at the same time. The transmission of the primary system is continuous, and the secondary system can opportunistically help the primary data transmission in exchange for the spectrum sharing. Superposition coding is used at the secondary transmitters, where the primary signal and secondary signal are linearly combined. Successive interference decoding and cancelation is performed by secondary users to extract their desired signals. For the primary system, joint decoding is performed by treating the secondary signal as noise at the receiver side. The optimal power allocation is determined to maximize the success probability of the secondary system without violating the outage performance of the primary system.

In Chapter 3, an adaptive spectrum-leasing scheme is proposed for the multiuser cognitive radio network. Based on the TPSR and DF protocols, each cognitive user can intelligently switch the spectrum leasing protocol to cooperate in the primary data transmission. Due to the advantage of cooperation, the primary data transmission time can be shortened and as a reward, the spectrum can be released to the secondary data transmission in the remaining time. For given  $m$  cognitive users, the best one that can achieve the largest secondary rate while satisfying primary rate target is scheduled for the spectrum leasing. It is shown that the cooperative diversity gain of  $m + 1$  can be achieved for the primary system and the selection diversity gain of  $m$  can be obtained for the secondary system. The multiuser diversity of secondary

system in terms of throughput scales as  $\log(\log m)$  when  $m$  is large. Therefore, the cognitive radio network does not lose diversity gain compared with the stand-alone multiuser wireless network without cognitive constraint.

In Chapter 4, three uncoordinated relay selection schemes are proposed for the large cooperative network to reduce the signaling overhead. The source-destination communication is assisted by the intermediate relays that are spatially randomly distributed over the two-dimensional plane. The cooperative truncated ARQ with one possible retransmission is adopted as the relaying protocol. In case the original data transmission between source and destination fails, without a central controller, all the potential relays that have correctly received the source data will contend for the channel to retransmit. The competition for the channel access is governed by the retransmission probability that is independently calculated by each potential relay according to the local information, such as distance, angle, and channel SNR towards the destination. The system success probabilities are analyzed and it shows that the proposed uncoordinated schemes significantly outperform the source retransmission scheme.

In Chapter 5, the cooperative relaying protocol is designed to realize the spectrum sharing between cellular network downlink and ad-hoc network coexisting in the same geographic region. In the cellular network, the weak signal and strong interference at cell-edge area often cause difficulty in guaranteeing the QoS requirement. The ad-hoc users can actively help the cell-edge data transmission to improve the average throughput of cellular network downlink. In return, a fraction of spectrum can be released to the ad-hoc network for its own data transmission. The transmission capacity of ad-hoc network is maximized subject to the constraints on the outage probability of ad-hoc network and on the throughput improvement ratio of cellular network. Both the transmission capacity of ad-hoc network and the average throughput of cellular network are analyzed using the stochastic geometry theory. The optimal ad-hoc user density and spectrum allocation are calculated through solving an optimization problem. It demonstrates that the proposed scheme can effectively facilitate ad-hoc

transmissions while conservatively improving the cellular network performance.

In Chapter 6, the thesis conclusion and perspectives for future work are presented.

# Chapter 2

## Cooperative Spectrum Sharing Based on TPSR

### 2.1 Introduction

Spectrum sharing schemes are widely studied in cognitive radio (CR) networks using the game theory [37–39], the stochastic geometry theory [40–42], or the MIMO techniques [43–45] to accommodate a growing demand for wireless applications. In the spectrum sharing process, the secondary system can either implicitly occupy the spectrum [46] without being noticed by the primary system or explicitly help the primary system’s data transmission in exchange for the spectrum access [19, 20]. Implicit spectrum sharing is performed by the secondary system opportunistically when the spectrum is sensed to be idle [47] or when the channel state of the primary link is sensed to be very good in tolerating a certain amount of interference [2]. Explicit spectrum sharing needs the primary system to coordinate its operation with the secondary system. Regardless of the sharing scheme used, the cooperative techniques [22] can be used to effectively improve the capacity of CR network [7].

In the traditional cooperative spectrum sharing schemes, multiple communication phases are required to transmit the same primary signal, resulting in a relatively low

spectrum efficiency of the primary system and low spectrum access opportunity of the secondary system. In this chapter, an opportunistic bandwidth-efficient two-path cognitive relaying scheme is developed for the overlaid wireless network to facilitate the spectrum sharing. The transmission of primary system is continuous without coordinating the transmission order with the secondary system [14, 19], while the transmission of secondary system is implicitly performed through all the time slots. Two cognitive transmitters serve as relays to help the primary system in a successive fashion, and they also send their own information to the intended receivers. It is achieved by employing superposition coding at secondary transmitters and successive decoding at the receivers. On one hand, the secondary signal transmission introduces interference to the primary system. On the other hand, the secondary users relay the primary signals to achieve the space diversity gain. By determining an optimal power allocation between primary signal relaying and secondary signal transmission, the interference imposed on the primary system can be greatly suppressed by taking advantage of cooperation, and the successive interference cancelation can be well performed by the secondary receivers to retrieve the desired secondary signals. The achievable rates and outage probabilities of the primary and secondary systems are analyzed. The optimal power allocation factor is determined to maximize the success probability of secondary system while protecting the outage performance of primary system. Simulation results show that the proposed one-phase cooperative spectrum sharing scheme greatly outperforms the conventional multi-phase schemes in terms of secondary throughput. The outage performance of the primary system can be greatly improved and the secondary transmission requirement can be well satisfied.

The rest of this chapter is organized as follows. In Section 2.2, the system model is introduced and a cognitive spectrum sharing scheme based on the two-path successive relaying (TPSR) is proposed. Section 2.3 analyzes the outage probabilities of both primary and secondary systems based on which the optimal power allocation is studied. Numerical and simulation results are presented in Section 2.4. Section 2.5 concludes this chapter.

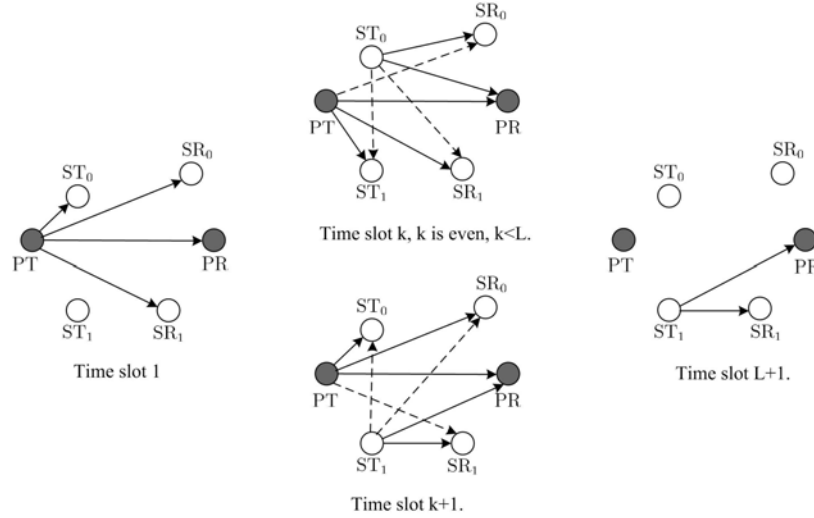


**Figure 2.1:** Transmission order of the spectrum sharing scheme based on two-path successive relaying. The solid lines represent the transmission link, while the dashed lines represent the interference channel.

## 2.2 Cognitive Spectrum Sharing

The overlaid wireless network shown in Fig. 2.1 is considered, where a pair of primary transmitter (PT) and receiver (PR) coexists with two pairs of secondary transmitters ( $ST_i, i = 0, 1$ ) and receivers ( $SR_i, i = 0, 1$ ) in the same channel. The positions of all transmitters and receivers are fixed. The distance for any pair of secondary transmitter and secondary receiver is much shorter than the distance between any primary user and any secondary user.

All channels are assumed to undergo independent Rayleigh block fading that remains invariant in one data frame but changes independently from one frame to another. Let  $h_{u,v}$  denote the channel from transmitter  $u$  to receiver  $v$ , and  $d_{u,v}$  the distance between  $u$  and  $v$ . The channel power gain is  $\mathcal{G}_{u,v} = |h_{u,v}|^2$ , which is exponentially distributed with mean  $\bar{\mathcal{G}}_{u,v} = d_{u,v}^{-\alpha}$  with  $\alpha$  being the path loss exponent. The channel between  $u$  and  $v$  is assumed to be symmetric, i.e.,  $h_{u,v} = h_{v,u}$ , and the channel state information is perfectly known at the receiver. Each user is equipped with only one omnidirectional antenna operating with half-duplex mode. The transmissions of PT and STs are assumed to be well synchronized.

### 2.2.1 Cognitive Relay for Spectrum Sharing

To facilitate spectrum sharing, the two secondary transmitters can send the secondary data to the secondary receivers while also serving as relays for primary data transmission based on the TPSR as follows. For a certain time slot  $k$ , the unit power signals  $x_p[k]$ ,  $x_0[k]$ , and  $x_1[k]$  represent the primary signal, the secondary signal of  $ST_0$ , and the secondary signal of  $ST_1$ , respectively.

- Time slot 1: PT transmits  $x_p[1]$ ;  $ST_0$ ,  $SR_0$ ,  $SR_1$  receive and detect  $x_p[1]$ ;  $ST_1$  keeps silent; PR receives  $x_p[1]$ .
- Time slot 2: PT transmits  $x_p[2]$ ;  $ST_0$  applies the superposition coding and transmits the composite signal  $x_c[2] = f(x_p[1], x_0[2])$ ;  $SR_0$  and  $SR_1$  first cancel  $x_p[1]$ , then detect and cancel  $x_0[2]$ , and finally detect  $x_p[2]$ ;  $ST_1$  first detects and cancels  $x_p[1]$ , then detects and cancels  $x_0[2]$ , and finally detects  $x_p[2]$ ; PR receives  $x_p[2]$  and  $x_c[2]$ .
- Time slot 3: PT transmits  $x_p[3]$ ;  $ST_1$  applies the superposition coding and transmits the composite signal  $x_c[3] = f(x_p[2], x_1[3])$ ;  $SR_0$  and  $SR_1$  first cancel  $x_p[2]$ , then detect and cancel  $x_1[3]$ , and finally detect  $x_p[3]$ ;  $ST_0$  first detects and cancels  $x_p[2]$ , then detects and cancels  $x_1[3]$ , and finally detects  $x_p[3]$ ; PR receives  $x_p[3]$  and  $x_c[3]$ .
- The operation of Time slot 2 and 3 repeats alternately until Time slot  $L$ .
- Time slot  $L+1$ :  $ST_1$  transmits the composite signal  $x_c[L+1] = f(x_p[L], x_1[L+1])$ ;  $SR_1$  cancels  $x_p[L]$ , detects  $x_1[L+1]$ ;  $ST_0$  and  $SR_0$  keep silent; PR receives  $x_c[L+1]$  and jointly decodes primary signals  $x_p[1], x_p[2], \dots, x_p[L]$  by regarding secondary signals as noise.

In the cognitive spectrum sharing, a total of  $L+1$  time slots are used to transmit  $L$  primary symbols. The spectral efficiency of the primary system is  $L/(L+1)$ , which approaches 1 for a large  $L$ . The joint maximum-likelihood (ML) decoding

is performed by PR at the end of the cooperation. For the secondary system, the successive interference decoding and cancelation is performed in each time slot to retrieve the desired signals. The advantages of the above cognitive relay strategy are summarized as follows. 1) No spectrum efficiency loss is induced for the primary system; 2) Concurrent data transmissions of both PUs and SUs are supported; 3) No coordination from the primary system is needed because the SU is oblivious to the primary user and the primary one continues to send data to its receiver.

### 2.2.2 Signal Model

We consider time slot  $k$  ( $k = 2, \dots, L$ ), when  $ST_i$ ,  $i = \text{mod}(k, 2)$  and PT simultaneously perform the transmissions. For  $ST_i$ , the transmitted composite signal is generated by linearly combining the previous primary signal and the current secondary signal, i.e.,

$$x_c[k] = f(x_p[k-1], x_i[k]) = \sqrt{\beta}x_p[k-1] + \sqrt{1-\beta}x_i[k], \quad (2.1)$$

where  $\beta \in [0, 1]$  is the power allocation factor. If  $\beta = 0$ ,  $ST_i$  is selfish and only transmits its own signal. If  $\beta = 1$ ,  $ST_i$  becomes selfless and only serves as a relay for the primary signal. To protect the primary signal from the interference of the secondary signal, we set  $\beta \geq 0.5$ . Thus, more power is allocated to relay the primary signal and less interference is generated from the secondary signal.

The signal received at  $SR_i$  and  $SR_j$  ( $j = 1 - i$ ) in time slot  $k$  is denoted as  $y_{SR_v}[k]$  ( $v = i$  or  $j$ ), which is given by

$$y_{SR_v}[k] = \sqrt{P_p}h_{PT,SR_v}x_p[k] + \sqrt{P_s}h_{ST_i,SR_v}x_c[k] + n_{SR_v}[k], \quad (2.2)$$

where  $P_p$  and  $P_s$  denote the transmission power of primary signal and secondary signal, respectively, and  $n_{SR_v}[k] \sim \mathcal{CN}(0, N_0)$  is the zero mean additive white Gaussian noise (AWGN) with power  $N_0$ . In fact, the first term of (2.2) is the received signal from PT and the second term is the received composite signal from  $ST_i$ . The successive decoding is performed as follows. First, the previous primary signal  $x_p[k-1]$

is canceled. Then, the secondary signal  $x_i[k]$  is decoded and canceled. Finally, the current primary signal  $x_p[k]$  is decoded.

The signal received at secondary transmitter  $ST_j$  ( $j = 1 - i$ ) is given by

$$y_{ST_j}[k] = \sqrt{P_p}h_{PT,ST_j}x_p[k] + \sqrt{P_s}h_{ST_i,ST_j}x_c[k] + n_{ST_j}[k], \quad (2.3)$$

where  $n_{ST_j}[k] \sim \mathcal{CN}(0, N_0)$  is the AWGN. The first term of (2.3) represents the received signal from PT and the second term is the received composite signal from  $ST_i$ . The channel between  $ST_0$  and  $ST_1$  is usually much stronger than the channel between PT and  $ST_j$  because the secondary users are close to one another. Hence, the composite signal  $x_c[k]$  can be firstly decoded and canceled. Then, the current primary signal is decoded. In the detection of  $x_c[k]$ , as  $\beta \geq 0.5$ , the previous primary signal  $x_p[k - 1]$  is first detected and canceled, and the secondary signal  $x_i[k]$  is then extracted.

At PR, all the received signals in  $L + 1$  time slots are written as

$$\mathbf{y} = \mathbf{H}\mathbf{x}_p + \mathbf{w}, \quad (2.4)$$

where  $\mathbf{x}_p = [x_p[1], x_p[2], \dots, x_p[L]]^T$  is the primary signal vector and the superscript  $\mathcal{T}$  denotes the transpose operation.  $\mathbf{H}$  is the equivalent MIMO channel with size  $(L + 1) \times L$ , given by

$$\mathbf{H} = \begin{bmatrix} \sqrt{P_p}h_{PT,PR} & 0 & \cdots & 0 & 0 & 0 \\ \sqrt{\beta P_s}h_{ST_0,PR} & \sqrt{P_p}h_{PT,PR} & \ddots & 0 & 0 & 0 \\ 0 & \sqrt{\beta P_s}h_{ST_1,PR} & \ddots & 0 & 0 & 0 \\ \vdots & \ddots & \ddots & \ddots & \ddots & \vdots \\ 0 & 0 & \ddots & \sqrt{\beta P_s}h_{ST_1,PR} & \sqrt{P_p}h_{PT,PR} & 0 \\ 0 & 0 & \cdots & 0 & \sqrt{\beta P_s}h_{ST_0,PR} & \sqrt{P_p}h_{PT,PR} \\ 0 & 0 & \cdots & 0 & 0 & \sqrt{\beta P_s}h_{ST_1,PR} \end{bmatrix}. \quad (2.5)$$

The vector  $\mathbf{w}$  denotes the interference plus noise, given by

$$\mathbf{w} = \sqrt{(1 - \beta)P_s} \begin{bmatrix} 0 \\ h_{\text{ST}_0, \text{PR}} x_0[2] \\ h_{\text{ST}_1, \text{PR}} x_1[3] \\ \vdots \\ h_{\text{ST}_0, \text{PR}} x_0[L] \\ h_{\text{ST}_1, \text{PR}} x_1[L + 1] \end{bmatrix} + \begin{bmatrix} n_{\text{PR}}[1] \\ n_{\text{PR}}[2] \\ n_{\text{PR}}[3] \\ \vdots \\ n_{\text{PR}}[L] \\ n_{\text{PR}}[L + 1] \end{bmatrix}. \quad (2.6)$$

## 2.3 Outage Performance and Power Allocation

Let  $E_c$  denote the event of both  $\text{ST}_0$  and  $\text{ST}_1$  correctly detecting the primary signal. In this case, the TPSR will be activated and the spectrum sharing is performed. Otherwise, both  $\text{ST}_0$  and  $\text{ST}_1$  will keep silent, and PR will only see the primary signal directly coming from PT without interference. For the opportunistic spectrum sharing, the outage probability of the primary system and the secondary system is denoted as  $P_{\text{out}}^{\text{p}}$  and  $P_{\text{out}}^{\text{s}}$ , respectively.

$$P_{\text{out}}^{\text{p}} = \Pr \{E_c\} P_{\text{out}}^{\text{pc}} + (1 - \Pr \{E_c\}) P_{\text{out}}^{\text{pd}}, \quad (2.7)$$

$$P_{\text{out}}^{\text{s}} = \Pr \{E_c\} P_{\text{out}}^{\text{sc}} + (1 - \Pr \{E_c\}) P_{\text{out}}^{\text{sd}}, \quad (2.8)$$

where  $P_{\text{out}}^{\text{pc}}$  and  $P_{\text{out}}^{\text{sc}}$  represent the outage probabilities of the primary system and the secondary system, respectively, when the cognitive TPSR is used.  $P_{\text{out}}^{\text{pd}}$  and  $P_{\text{out}}^{\text{sd}}$  denote the outage probabilities of the primary system and the secondary system when STs keep silent. As the secondary system is not activated in this case, it has  $P_{\text{out}}^{\text{sd}} = 1$ .

### 2.3.1 Spectrum Sharing Probability

For  $\text{ST}_j$  ( $j = 1 - i, i = 0$  or  $1$ ), before detecting the current primary signal, the previous primary signal forwarded from  $\text{ST}_i$  should be first decoded and canceled. To detect the previous primary signal correctly, the achievable rate  $R_{\text{ST}_j}^1$  should be

larger than the transmission rate  $R_p$  of the primary signal. From (2.3), we get

$$R_{ST_j}^1 = \log_2 \left( 1 + \frac{\beta \rho \eta \mathcal{G}_{ST_0, ST_1}}{\eta \mathcal{G}_{PT, ST_j} + (1 - \beta) \rho \eta \mathcal{G}_{ST_0, ST_1} + 1} \right), \quad (2.9)$$

where the numerator is the power of previous primary signal and the denominator is the power of interference plus noise. The parameters  $\eta = P_p/N_0$  and  $\rho = P_s/P_p$ .

After the successful detection and cancelation of the previous primary signal, the secondary signal is detected and canceled. To guarantee correct detection of the current secondary signal, the transmission rate  $R_s$  should not be larger than the achievable rate  $R_{ST_j}^2$ , which is given by

$$R_{ST_j}^2 = \log_2 \left( 1 + \frac{(1 - \beta) \rho \eta \mathcal{G}_{ST_0, ST_1}}{\eta \mathcal{G}_{PT, ST_j} + 1} \right). \quad (2.10)$$

After the successful detection and cancelation of the secondary signal, the achievable rate of the current primary signal becomes

$$R_{ST_j}^3 = \log_2 (1 + \eta \mathcal{G}_{PT, ST_j}). \quad (2.11)$$

Based on the above analysis, the spectrum sharing probability, i.e., probability of the TPSR being activated, is written as

$$\Pr \{E_c\} = \Pr \left\{ R_{ST_0}^1 \geq R_p, R_{ST_0}^2 \geq R_s, R_{ST_0}^3 \geq R_p, R_{ST_1}^1 \geq R_p, R_{ST_1}^2 \geq R_s, R_{ST_1}^3 \geq R_p \right\}, \quad (2.12)$$

where the first three and last three terms correspond to  $ST_0$  and  $ST_1$ , respectively.

The spectrum sharing probability can be derived as [see Appendix I],

$$\Pr \{E_c\} = \exp \left[ -\frac{T}{\eta} \left( \frac{1}{\bar{\mathcal{G}}_{PT, ST_0}} + \frac{1}{\bar{\mathcal{G}}_{PT, ST_1}} \right) - \frac{\mu}{\bar{\mathcal{G}}_{ST_0, ST_1}} \right] \left[ 1 - \frac{1}{1 + \xi \bar{\mathcal{G}}_{ST_0, ST_1} / \bar{\mathcal{G}}_{PT, ST_0}} - \frac{1}{1 + \xi \bar{\mathcal{G}}_{ST_0, ST_1} / \bar{\mathcal{G}}_{PT, ST_1}} \right], \quad (2.13)$$

where  $T = 2^{R_p} - 1$ ,  $U = 2^{R_s} - 1$ , and  $\xi = (T + 1)/(\mu\eta)$  with

$$\mu = \begin{cases} \frac{T(T+1)}{\rho\eta(\beta - T + T\beta)}, & \max \left\{ 0.5, \frac{T}{T+1} \right\} \leq \beta \leq \max \left\{ 0.5, \frac{T(U+1)}{T(U+1)+U} \right\} \\ \frac{U(T+1)}{\rho\eta(1-\beta)}, & \max \left\{ 0.5, \frac{T(U+1)}{T(U+1)+U} \right\} < \beta < 1. \end{cases} \quad (2.14)$$

If the distance between the primary transmitter and any secondary transmitter is the same, i.e.,  $\bar{\mathcal{G}}_{\text{PT,ST}} = \bar{\mathcal{G}}_{\text{PT,ST}_i}$  ( $i = 0, 1$ ), then (2.13) is reduced to

$$\Pr\{E_c\} = \exp\left(-\frac{2T}{\eta\bar{\mathcal{G}}_{\text{PT,ST}}} - \frac{\mu}{\bar{\mathcal{G}}_{\text{ST}_0,\text{ST}_1}}\right) \frac{2\bar{\mathcal{G}}_{\text{ST}_0,\text{ST}_1}^2}{(\bar{\mathcal{G}}_{\text{PT,ST}}/\xi + \bar{\mathcal{G}}_{\text{ST}_0,\text{ST}_1})(\bar{\mathcal{G}}_{\text{PT,ST}}/\xi + 2\bar{\mathcal{G}}_{\text{ST}_0,\text{ST}_1})}. \quad (2.15)$$

**Remarks:** From (2.15), the following observations are obtained: 1) With the increase of  $\rho$ ,  $\Pr\{E_c\}$  becomes larger. Hence, increasing the power ratio can help improve the cooperation opportunity. 2) With the increase of  $T$  and  $U$ , it becomes more difficult for ST to decode the primary and secondary signals. As a result,  $\Pr\{E_c\}$  turns smaller. 3) With shorter distance between  $\text{ST}_0$  and  $\text{ST}_1$ ,  $\bar{\mathcal{G}}_{\text{ST}_0,\text{ST}_1}$  becomes larger. Due to the strong signal strength between secondary transmitters, more interference from the primary system can be tolerated in the successive decoding. Consequently,  $\Pr\{E_c\}$  turns larger. 4) With  $\eta \rightarrow \infty$ ,  $R_{\text{ST}_j}^1$  and  $R_{\text{ST}_j}^2$  become unrelated with  $\eta$  and  $R_{\text{ST}_j}^3$  approaches infinity, so  $\Pr\{E_c\}$  turns to be a constant related with  $\rho$  and  $\beta$ .

### 2.3.2 Outage Probability of the Primary System

The rate for direct transmission between PT and PR is  $R_{\text{pd}} = \log_2(1 + \eta\mathcal{G}_{\text{PT,PR}})$ . Then, the outage probability is derived as

$$P_{\text{out}}^{\text{pd}} = \Pr\{R_{\text{pd}} < R_p\} = 1 - \exp\left(-\frac{T}{\eta\bar{\mathcal{G}}_{\text{PT,PR}}}\right). \quad (2.16)$$

For the two-path successive relaying, from (2.4) the achievable rate of the primary system is expressed as

$$\begin{aligned} R_{\text{pc}} &= \frac{1}{L+1} \log_2 \left[ \det(\mathbf{I}_L + \mathbf{H}^{\mathcal{H}}(\mathbf{C}^{-\frac{1}{2}})^{\mathcal{H}}\mathbf{C}^{-\frac{1}{2}}\mathbf{H}) \right] \\ &= \frac{1}{L+1} \log_2 \left[ \det(\mathbf{I}_{L+1} + \tilde{\mathbf{H}}\tilde{\mathbf{H}}^{\mathcal{H}}) \right], \end{aligned} \quad (2.17)$$

where  $\mathbf{C} = \mathbb{E}[\mathbf{w}\mathbf{w}^{\mathcal{H}}] = \text{diag}\{N_0, \lambda_0, \lambda_1, \dots, \lambda_0, \lambda_1\}$ , with  $\lambda_0 = (1 - \beta)P_s\mathcal{G}_{\text{ST}_0,\text{PR}} + N_0$ ,  $\lambda_1 = (1 - \beta)P_s\mathcal{G}_{\text{ST}_1,\text{PR}} + N_0$  and the superscript  $\mathcal{H}$  denoting the conjugate transpose

operation. The normalized channel matrix  $\tilde{\mathbf{H}} = \mathbf{C}^{-1/2}\mathbf{H}$  is written as

$$\tilde{\mathbf{H}} = \begin{bmatrix} \frac{\sqrt{P_p}h_{\text{PT,PR}}}{\sqrt{N_0}} & 0 & \cdots & 0 & 0 & 0 \\ \frac{\sqrt{\beta P_s}h_{\text{ST}_0,\text{PR}}}{\sqrt{\lambda_0}} & \frac{\sqrt{P_p}h_{\text{PT,PR}}}{\sqrt{\lambda_0}} & \ddots & 0 & 0 & 0 \\ 0 & \frac{\sqrt{\beta P_s}h_{\text{ST}_1,\text{PR}}}{\sqrt{\lambda_1}} & \ddots & 0 & 0 & 0 \\ \vdots & \ddots & \ddots & \ddots & \ddots & \vdots \\ 0 & 0 & \ddots & \frac{\sqrt{\beta P_s}h_{\text{ST}_1,\text{PR}}}{\sqrt{\lambda_1}} & \frac{\sqrt{P_p}h_{\text{PT,PR}}}{\sqrt{\lambda_1}} & 0 \\ 0 & 0 & \cdots & 0 & \frac{\sqrt{\beta P_s}h_{\text{ST}_0,\text{PR}}}{\sqrt{\lambda_0}} & \frac{\sqrt{P_p}h_{\text{PT,PR}}}{\sqrt{\lambda_0}} \\ 0 & 0 & \cdots & 0 & 0 & \frac{\sqrt{\beta P_s}h_{\text{ST}_1,\text{PR}}}{\sqrt{\lambda_1}} \end{bmatrix} \quad (2.18)$$

The term  $\mathbf{I}_{L+1} + \tilde{\mathbf{H}}\tilde{\mathbf{H}}^H$  in (2.17) is a tridiagonal matrix, whose determinant is not easy to obtain. An approximation of the achievable rate is obtained as follows [see Appendix II].

$$R_{\text{pc}} \approx \tilde{R}_{\text{pc}} = \frac{L}{2(L+1)} \log_2 \left\{ \frac{\eta \mathcal{G}_{\text{PT,PR}}}{(1-\beta)\rho\eta \mathcal{G}_{\text{ST}_0,\text{PR}} + 1} \left[ 1 + \frac{\eta \mathcal{G}_{\text{PT,PR}}}{(1-\beta)\rho\eta \mathcal{G}_{\text{ST}_1,\text{PR}} + 1} \right] + \frac{\rho\eta \mathcal{G}_{\text{ST}_1,\text{PR}} + 1}{(1-\beta)\rho\eta \mathcal{G}_{\text{ST}_1,\text{PR}} + 1} \left[ \frac{\eta \mathcal{G}_{\text{PT,PR}}}{(1-\beta)\rho\eta \mathcal{G}_{\text{ST}_1,\text{PR}} + 1} + \frac{\rho\eta \mathcal{G}_{\text{ST}_0,\text{PR}} + 1}{(1-\beta)\rho\eta \mathcal{G}_{\text{ST}_0,\text{PR}} + 1} \right] \right\}. \quad (2.19)$$

Consequently, the approximate outage probability is derived as

$$P_{\text{out}}^{\text{pc}} \approx \tilde{P}_{\text{out}}^{\text{pc}} = \Pr \left\{ \tilde{R}_{\text{pc}} < R_p \right\} = \Pr \left\{ \mathcal{G}_{\text{PT,PR}}^2 + \left( \frac{\omega_1 \theta_0}{\theta_1 \eta} + \frac{\theta_1}{\eta} \right) \mathcal{G}_{\text{PT,PR}} < \frac{\omega_1 \theta_1 \varphi - \omega_0 \theta_0}{\eta^2} \right\}, \quad (2.20)$$

where  $\varphi = 4^{(L+1)R_p/L}$  and other parameters are given as

$$\begin{aligned} \omega_0 &= 1 + \rho\eta \mathcal{G}_{\text{ST}_0,\text{PR}}, & \omega_1 &= 1 + (1-\beta)\rho\eta \mathcal{G}_{\text{ST}_0,\text{PR}}, \\ \theta_0 &= 1 + \rho\eta \mathcal{G}_{\text{ST}_1,\text{PR}}, & \theta_1 &= 1 + (1-\beta)\rho\eta \mathcal{G}_{\text{ST}_1,\text{PR}}. \end{aligned} \quad (2.21)$$

As  $\mathcal{G}_{\text{PT,PR}}$  is exponentially distributed, (2.20) can be further derived as

$$\tilde{P}_{\text{out}}^{\text{pc}} = \mathbb{E} \left\{ 1 - \exp \left[ \frac{1}{2\bar{\mathcal{G}}_{\text{PT,PR}}} \left( \frac{\omega_1 \theta_0}{\theta_1 \eta} + \frac{\theta_1}{\eta} \right) - \frac{1}{\bar{\mathcal{G}}_{\text{PT,PR}}} \sqrt{\frac{\omega_1 \theta_1 \varphi - \omega_0 \theta_0}{\eta^2} + \frac{1}{4} \left( \frac{\omega_1 \theta_0}{\theta_1 \eta} + \frac{\theta_1}{\eta} \right)^2} \right] \right\}, \quad (2.22)$$

where the expectation is taken over random variables  $\mathcal{G}_{\text{ST}_0, \text{PR}}$  and  $\mathcal{G}_{\text{ST}_1, \text{PR}}$ , which are included in the parameter pair  $(\omega_0, \omega_1)$  and  $(\theta_0, \theta_1)$ , respectively. The integral regions of  $\mathcal{G}_{\text{ST}_1, \text{PR}}$  and  $\mathcal{G}_{\text{ST}_0, \text{PR}}$  are given as follows with respect to different values of  $\beta$ .

- For  $0.5 \leq \beta < \max \left\{ 0.5, 1 - \sqrt{1/\varphi} \right\}$ ,

$$0 < \mathcal{G}_{\text{ST}_1, \text{PR}} < \infty, 0 < \mathcal{G}_{\text{ST}_0, \text{PR}} < \infty. \quad (2.23)$$

- For  $\max \left\{ 0.5, 1 - \sqrt{1/\varphi} \right\} \leq \beta < \max \left\{ 0.5, 1 - 1/\varphi \right\}$ ,

$$\begin{cases} 0 < \mathcal{G}_{\text{ST}_1, \text{PR}} < \frac{\varphi(1-\beta) - 1}{\rho\eta[1 - \varphi(1-\beta)^2]}, & 0 < \mathcal{G}_{\text{ST}_0, \text{PR}} < \infty \\ \frac{\varphi(1-\beta) - 1}{\rho\eta[1 - \varphi(1-\beta)^2]} \leq \mathcal{G}_{\text{ST}_1, \text{PR}} < \infty, & 0 < \mathcal{G}_{\text{ST}_0, \text{PR}} < \frac{\theta_1\varphi - \theta_0}{\rho\eta[\theta_0 - (1-\beta)\theta_1\varphi]}. \end{cases} \quad (2.24)$$

- For  $\max \left\{ 0.5, 1 - 1/\varphi \right\} \leq \beta < 1$ ,

$$0 < \mathcal{G}_{\text{ST}_1, \text{PR}} < \frac{\varphi - 1}{\rho\eta[1 - (1-\beta)\varphi]}, 0 < \mathcal{G}_{\text{ST}_0, \text{PR}} < \frac{\theta_1\varphi - \theta_0}{\rho\eta[\theta_0 - (1-\beta)\theta_1\varphi]}. \quad (2.25)$$

Therefore, the approximate outage probability of the primary system with TPSR can be numerically computed by (2.22) with integral regions of  $\mathcal{G}_{\text{ST}_1, \text{PR}}$  and  $\mathcal{G}_{\text{ST}_0, \text{PR}}$  given by (2.23)–(2.25).

### 2.3.3 Outage Probability of the Secondary System

Consider a certain time slot  $k$  ( $2 \leq k \leq L - 1$ ), PT transmits the current primary signal and  $\text{ST}_i$ ,  $i = \text{mod}(k, 2)$  transmits the composite signal simultaneously. After the cancelation of the previous primary signal,  $\text{SR}_i$  should first detect its desired secondary signal by viewing the current primary signal as noise. To get the correct detection of the secondary signal,  $R_s$  should not be larger than the achievable rate  $R_{\text{SR}_i}^1$ , which is given by

$$R_{\text{SR}_i}^1 = \log_2 \left( 1 + \frac{(1-\beta)\rho\eta\mathcal{G}_{\text{ST}_i, \text{SR}_i}}{\eta\mathcal{G}_{\text{PT}, \text{SR}_i} + 1} \right). \quad (2.26)$$

In time slot  $k+1$ , PT and  $ST_j$  ( $j = 1-i$ ) transmit at the same time. After the cancellation of the previous primary signal,  $SR_i$  needs to detect and cancel the secondary signal of  $ST_j$  followed by the detection of the current primary signal. To guarantee the correct detection and cancellation of the secondary signal, the transmission rate  $R_s$  must be no larger than the achievable rate  $R_{SR_i}^2$ , which is given by

$$R_{SR_i}^2 = \log_2 \left( 1 + \frac{(1-\beta)\rho\eta\mathcal{G}_{ST_j,SR_i}}{\eta\mathcal{G}_{PT,SR_i} + 1} \right). \quad (2.27)$$

For any time slot, after the cancellation of the secondary signal, the primary signal needs to be detected; it will then be used for interference cancellation in the next time slot. Interference calculation requires the target rate  $R_p$  to be no larger than the achievable rate  $R_{SR_i}^3$  given by

$$R_{SR_i}^3 = \log_2 (1 + \eta\mathcal{G}_{PT,SR_i}). \quad (2.28)$$

Therefore, the outage probability of the secondary pair ( $ST_i, SR_i$ ) is obtained as

$$P_{\text{out}}^{s_i} = 1 - \Pr \{ R_{SR_i}^1 \geq R_s, R_{SR_i}^2 \geq R_s, R_{SR_i}^3 \geq R_p \}. \quad (2.29)$$

By substituting the related terms into (2.29) and after some mathematical manipulations, we have

$$P_{\text{out}}^{s_i} = 1 - \frac{\rho(1-\beta)}{\rho(1-\beta) + U\bar{\mathcal{G}}_{PT,SR_i}(1/\bar{\mathcal{G}}_{ST_i,SR_i} + 1/\bar{\mathcal{G}}_{ST_j,SR_i})} \times \exp \left[ -\frac{U(T+1)}{(1-\beta)\rho\eta} \left( \frac{1}{\bar{\mathcal{G}}_{ST_i,SR_i}} + \frac{1}{\bar{\mathcal{G}}_{ST_j,SR_i}} \right) - \frac{T}{\eta\bar{\mathcal{G}}_{PT,SR_i}} \right]. \quad (2.30)$$

In the spectrum sharing process, along with relaying one frame of primary signal,  $L/2$  codewords of  $ST_0$  and  $L/2$  codewords of  $ST_1$  are transmitted to  $SR_0$  and  $SR_1$ , respectively. The average outage probability of the whole secondary system is thus obtained as

$$P_{\text{out}}^{\text{sc}} = \frac{1}{2}(P_{\text{out}}^{s_0} + P_{\text{out}}^{s_1}). \quad (2.31)$$

Note that, (2.31) is the outage probability of the secondary system when the cognitive two-path successive relaying is successfully performed by the two secondary transmitters.

### 2.3.4 Optimal Power Allocation

For each time slot, the spectrum sharing model can be abstracted as the cognitive interference channels, where two senders are transmitting data to two receivers. Sender one, i.e., PT, intends to send the primary data to PR. Sender two, i.e., the cognitive relay  $ST_0$  or  $ST_1$ , needs to send the secondary data to the cognitive user while serving as a relay to forward the primary data to PR. The secondary system is oblivious to the primary one, but the cognitive relay can adapt its transmission power or data rate to maximize the benefits to the secondary system itself while not causing harmful interference to the primary system. In fact, the interference effect induced by the secondary data transmission can be compensated by the diversity gain resulted from the cognitive relay. If more power is allocated to relay the primary data, the primary system performance will be improved at the cost of losing secondary data rate. If more power is given to send the secondary data, the secondary system rate is enhanced, but the primary user may be subject to more interference which may not be suppressed by the relay diversity gain. Therefore, it is crucial to find the optimal power allocation for cognitive relays so that it is advantageous to both systems.

According to (2.7), (2.8), (2.16), and (2.31), the power allocation factor can be optimized by minimizing the outage probability of the secondary system ( $P_{\text{out}}^s$ ) without degrading the performance of the primary system ( $P_{\text{out}}^p \leq P_{\text{out}}^{\text{Pd}}$ ). The optimization problem can be equivalently written as

$$\begin{aligned} \max_{\beta \in [0.5, 1]} \quad & \frac{1}{2} \Pr(E_c) [(1 - P_{\text{out}}^{s_0}) + (1 - P_{\text{out}}^{s_1})] \\ \text{s. t.} \quad & P_{\text{out}}^{\text{Pc}} \leq P_{\text{out}}^{\text{Pd}}. \end{aligned} \tag{2.32}$$

This optimization problem aims to find the optimal power factor  $\beta$  that can maximize the success probability of secondary system while protecting the outage performance of primary system.

For mathematical tractability, the distance between any two secondary users is assumed to be the same, while the distance between any primary user and any secondary user is also assumed to be the same. Then, the secondary success probability

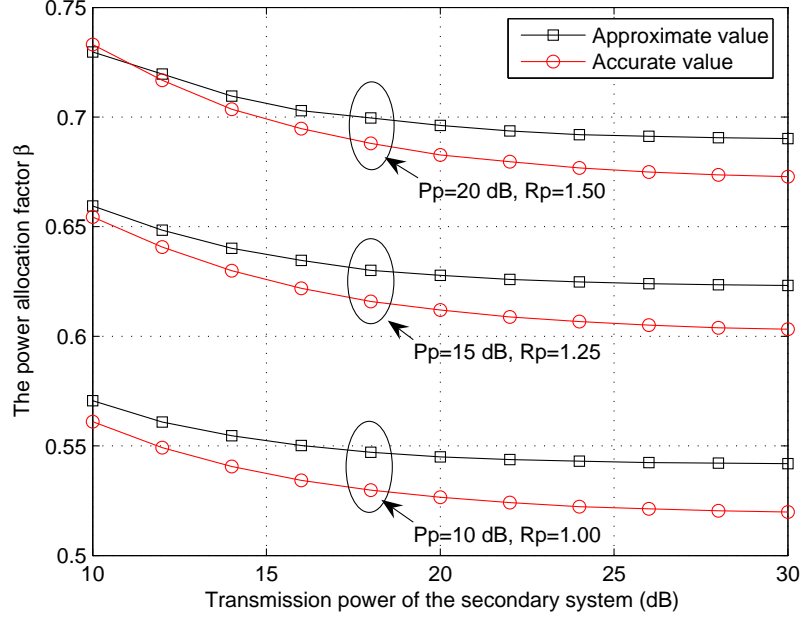


**Figure 2.2:** The approximate and exact power allocation factor  $\beta$ . The approximate value is obtained using  $\tilde{P}_{\text{out}}^{\text{Pc}} = P_{\text{out}}^{\text{Pd}}$ , while the exact value is obtained using  $P_{\text{out}}^{\text{Pc}} = P_{\text{out}}^{\text{Pd}}$ . The large-scale distance is set as 1.0 and the small-scale distance is 0.1.

$P_{\text{suc}}^{\text{s}} = 1 - P_{\text{out}}^{\text{s0}} = 1 - P_{\text{out}}^{\text{s1}}$  is written as follows.

$$P_{\text{suc}}^{\text{s}} = \exp\left(-\frac{T}{\eta K}\right) \exp\left(-\frac{2U(T+1)}{\rho\eta M(1-\beta)}\right) \frac{\rho M(1-\beta)}{\rho M(1-\beta) + 2UK}, \quad (2.33)$$

where  $K = \bar{\mathcal{G}}_{\text{PT,ST}} = \bar{\mathcal{G}}_{\text{PT,SR}}$ , and  $M = \bar{\mathcal{G}}_{\text{ST}_0, \text{ST}_1} = \bar{\mathcal{G}}_{\text{ST,SR}}$ . In conjunction with  $\Pr(E_c)$  given by (2.15), the optimization problem (2.32) can be rewritten as

$$\begin{aligned} \max_{\beta \in [0.5, 1]} \quad & f(\beta) = \Pr(E_c) P_{\text{suc}}^{\text{s}} \\ \text{s. t.} \quad & P_{\text{out}}^{\text{Pc}} \leq P_{\text{out}}^{\text{Pd}}. \end{aligned} \quad (2.34)$$

The more power is allocated for the relaying, the more cooperative advantage is brought to the primary system and the less interference is introduced. As a result,  $P_{\text{out}}^{\text{Pc}}$  monotonically decreases with  $\beta$  in the whole range of  $[0.5, 1]$ . By letting  $\tilde{P}_{\text{out}}^{\text{Pc}} = P_{\text{out}}^{\text{Pd}}$ , we can find the approximate critical point  $\tilde{\beta}$  from (2.22). In Fig. 2.2, the approximate critical point is compared with the exact critical point obtained by letting  $P_{\text{out}}^{\text{Pc}} = P_{\text{out}}^{\text{Pd}}$ .

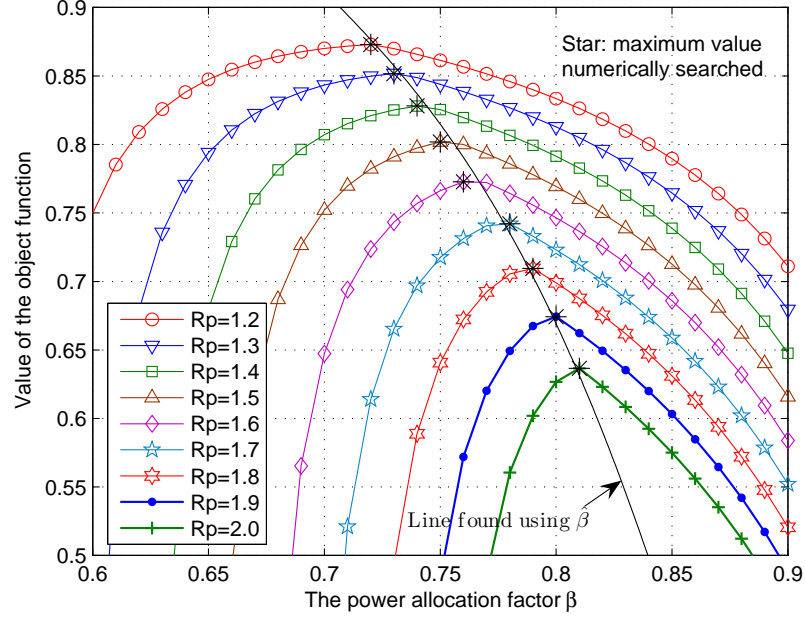


**Figure 2.3:** The value of objective function in (2.34) with different  $\beta$  values. The large-scale and small-scale distances are set as 1.0 and 0.1, respectively. The transmission power is  $P_p = 25$  dB,  $P_s = 15$  dB, and the secondary rate is set as  $R_s = R_p - 0.2$ .

The approximate value is numerically found and the exact value is obtained by Monte Carlo simulations. The result shows that the approximate value is an upper bound of the exact value for most of the cases, which is beneficial to protecting the primary performance conservatively. To satisfy the constraint of (2.34), the power allocation factor should be larger than or equal to  $\tilde{\beta}$ .

In the objective function,  $P_{\text{suc}}^s$  is a monotonically decreasing function of the power allocation factor  $\beta$  in the whole range of  $[0.5, 1]$ , which can be observed from (2.33). The spectrum sharing probability  $\Pr(E_c)$  given by (2.15) is always a monotonically increasing function of  $\beta$  when  $\max\{0.5, \frac{T}{T+1}\} \leq \beta \leq \max\{0.5, \frac{T(U+1)}{T(U+1)+U}\}$  and a monotonically decreasing function in the range of  $\max\{0.5, \frac{T(U+1)}{T(U+1)+U}\} < \beta < 1$ . Therefore, by jointly considering the monotonicity of  $P_{\text{suc}}^s$  and  $\Pr\{E_c\}$  in the whole range of  $\beta \in [0.5, 1]$ , the maximum value of the objective function should be in the lower range of  $\max\{0.5, \frac{T}{T+1}\} \leq \beta \leq \max\{0.5, \frac{T(U+1)}{T(U+1)+U}\}$ . As shown in Appendix

III, we can find the optimal power allocation factor  $\hat{\beta}$  that maximizes the objective function  $f(\beta)$ .

In fact, for almost all simulations, it can always find  $\hat{\beta} = \frac{T(U+1)}{T(U+1)+U}$ , of which the optimality is shown in Fig. 2.3. If  $\hat{\beta} \geq \tilde{\beta}$ , the optimal power allocation factor is  $\beta^* = \hat{\beta}$ ; otherwise, if  $\hat{\beta} < \tilde{\beta}$ , as the objective function  $f(\beta)$  is a continuously decreasing function in the range of  $[\hat{\beta}, 1]$ , the optimal power allocation factor is  $\beta^* = \tilde{\beta}$ . In general, the optimal power allocation factor can be suitably set as  $\beta^* = \max\{\tilde{\beta}, \hat{\beta}\}$ .

## 2.4 Numerical and Simulation Results

In the simulations, the path-loss exponent is set as  $\alpha = 3$  and the noise power is set as  $N_0 = 1$ . The frame length is set as  $L = 8$ , so the complexity of joint ML decoding at PR can be acceptable without obviously losing the bandwidth efficiency. The small-scale distance between any two secondary users is set the same, and the large-scale distance between any primary user and any secondary user is also set the same. The distance between any two users is normalized with respect to the distance between PT and PR, so the normalized distance between PT and PR is 1.

### 2.4.1 Comparison with Other Schemes

The proposed spectrum sharing scheme is first compared with other protocols based on the multi-phase cooperative techniques. For the DF based spectrum sharing protocol [19], only one pair of secondary users (ST, SR) coexists with the primary pair (PT, PR) and there are two communication phases. The primary signal is first broadcasted by PT. If ST correctly receives the primary signal in the first phase, it will forward a composite signal through linearly combining the primary signal and its own secondary signal. SR will detect the secondary signal by canceling the primary signal or treating it as noise. The joint decoding is performed by PR through viewing the secondary signal as noise. For the DF based spectrum leasing protocol [14], two

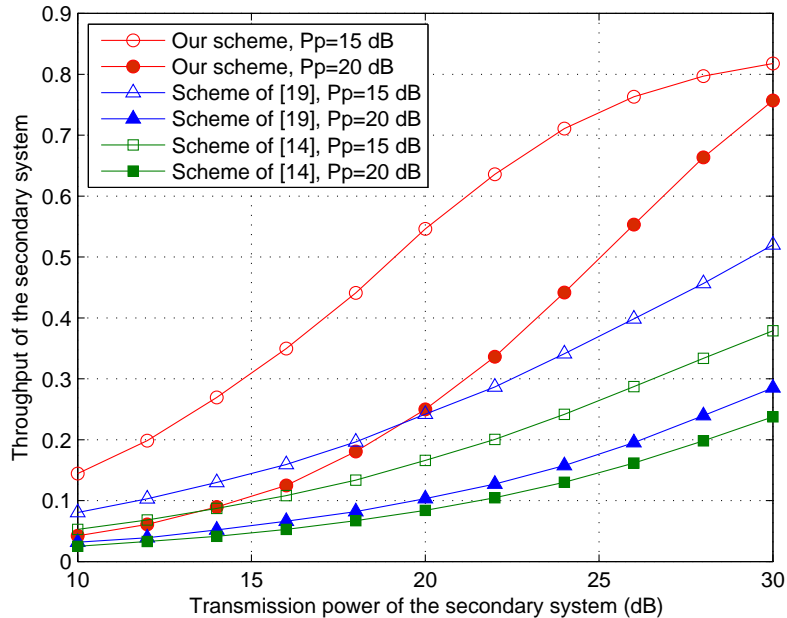


**Figure 2.4:** Throughput of secondary system with different primary transmission powers. The large-scale distance is 1.0, small-scale distance is 0.1, primary rate  $R_p = 1.5$  bits/s/Hz, and secondary rate  $R_s = 1.0$  bits/s/Hz.

secondary pairs  $(ST_0, SR_0)$  and  $(ST_1, SR_1)$  coexist with the primary pair  $(PT, PR)$ , and three communication phases are included. In the beginning,  $PT$  broadcasts its primary signal. If both  $ST_0$  and  $ST_1$  correctly receive the primary signal, they will jointly forward it using the distributed space-time coding technique. The maximal ratio combining (MRC) technique is adopted by  $PR$  to retrieve the primary signals. Finally,  $ST_0$  and  $ST_1$  transmit their own secondary signals to  $SR_0$  and  $SR_1$ , respectively in an orthogonal way and the primary users keep silent.

For the duration of each block fading, the achievable rate of primary system with SUs' cooperation is guaranteed no smaller than that of the stand-alone primary link without spectrum sharing. Therefore, the primary outage performance can be protected and the power/time allocation factor of each scheme can be numerically calculated. To make fair comparisons, the secondary transmission power of the proposed scheme and the scheme of [14] is set as  $P_s$ , while it is  $2P_s$  for the scheme of [19]. The throughput of secondary system with regard to different primary powers and

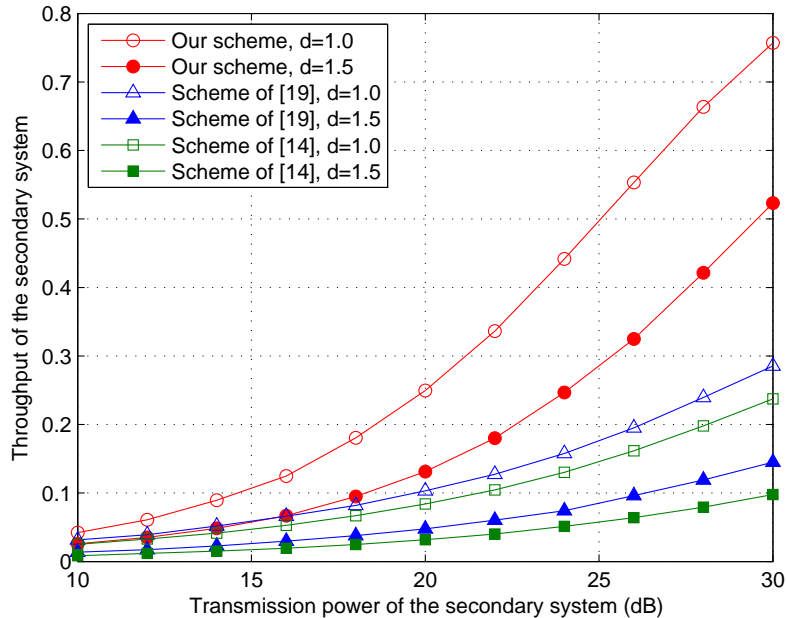


**Figure 2.5:** Throughput of secondary system with different large-scale distances  $d = d_{PT,ST} = d_{ST,PR} = d_{PT,SR} = d_{SR,PR}$ . The small-scale distance is 0.1, primary power  $P_p = 20$  dB, primary rate  $R_p = 1.5$  bits/s/Hz, and secondary rate  $R_s = 1.0$  bits/s/Hz.

different large-scale distances are plotted in Fig. 2.4 and Fig. 2.5, respectively.

The spectrum efficiency is high for the proposed scheme, as the transmission of primary and secondary signals is continuous over all the time slots. Therefore, the proposed scheme greatly outperforms the multi-phase schemes in terms of throughput of secondary system. The two-phase spectrum sharing scheme [19] outperforms the three-phase scheme [14]. With the increase of primary transmission power, the throughput gets smaller as shown by Fig. 2.4, because more resource (power/time) is allocated to help the primary data transmission to support the achievable rate and less resource is available for the secondary data transmission. The performance deteriorates with the increase of large-scale distance as shown by Fig. 2.5. The longer the distance, the lower the probability of STs correctly receiving the primary signal. When STs erroneously receive the primary signal, the opportunistic spectrum sharing is not performed. Hence, the opportunity of spectrum sharing becomes smaller when

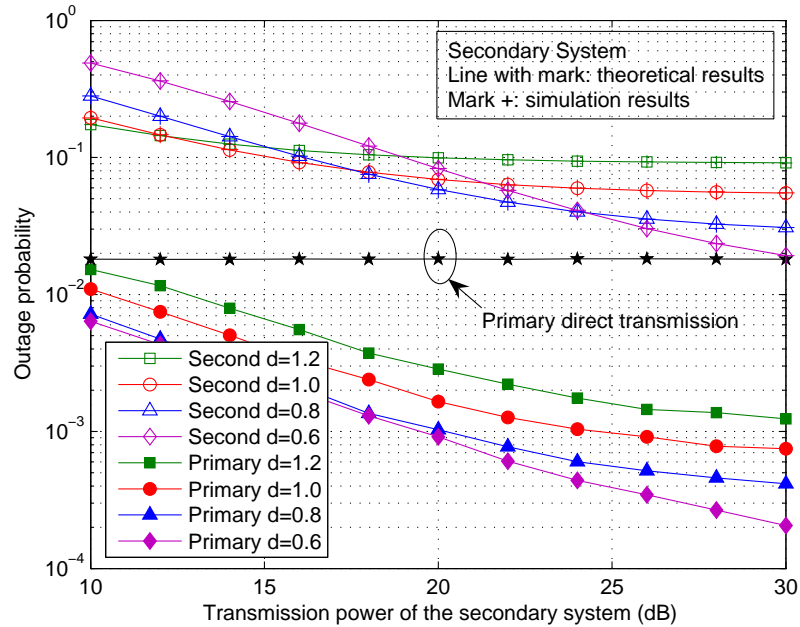


**Figure 2.6:** Outage probability w.r.t. different large-scale distances  $d = d_{PT,ST} = d_{ST,PR} = d_{PT,SR} = d_{SR,PR}$ . Small-scale distance is 0.1, primary rate  $R_p = 1.5$  bits/s/Hz, secondary rate  $R_s = 1.0$  bits/s/Hz, and primary power  $P_p = 20$  dB.

the large-scale distance gets longer.

## 2.4.2 Outage Performance vs. Secondary Transmission Power

In the following simulations, we only consider the proposed two-path cognitive spectrum sharing scheme using the optimal power allocation obtained in Section 2.3.4. Fig. 2.6 shows the outage probabilities of primary and secondary systems with respect to secondary transmission power for different large-scale distances. The figure shows that, with the increase of secondary transmission power, the outage performance of both systems are improved. The performance of the primary system improves with the smaller large-scale distance. When the secondary transmission power is low, with the increase of large-scale distance, the secondary performance gets better because the longer distance results in less interference from the primary transmitter. However, when the secondary transmission power is high, the secondary performance gets worse

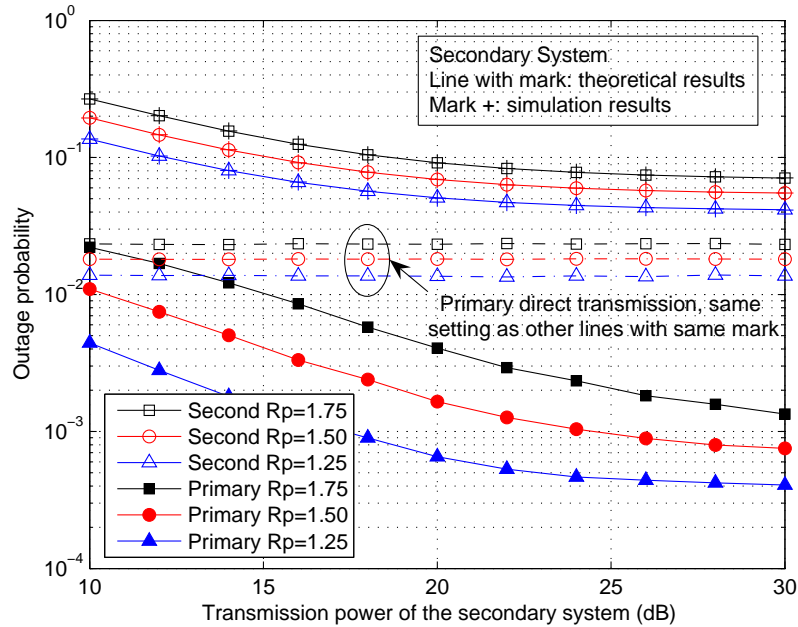


**Figure 2.7:** Outage probability w.r.t. different transmission rates  $R_p$  and  $R_s = R_p - 0.5$ . The large-scale distance is set as 1.0 while the small-scale distance is 0.1. The primary transmission power is fixed as  $P_p = 20$  dB.

with the increase of large-scale distance because, in this power range, the interference from the primary system is non-dominant for the successive decoding. However, with the increase of large-scale distance, decoding the current primary signal becomes more difficult for the secondary users. In this case, both spectrum sharing probability at ST and success decoding probability at SR become smaller, which obviously deteriorates the secondary outage performance. The performance of the secondary system analyzed in Section 2.3.3 is also validated because the theoretical results coincide exactly with the simulation results.

Fig. 2.7 shows the outage performance with respect to secondary transmission power for different target rates of primary and secondary systems. With the increase of transmission rates, the system performance deteriorates because it is more difficult for the channel to support a higher rate requirement. The numerical results also agree well with the simulation results for the secondary system, which verifies the analysis in Section 2.3.3. Compared with the direct transmission between primary transmitter

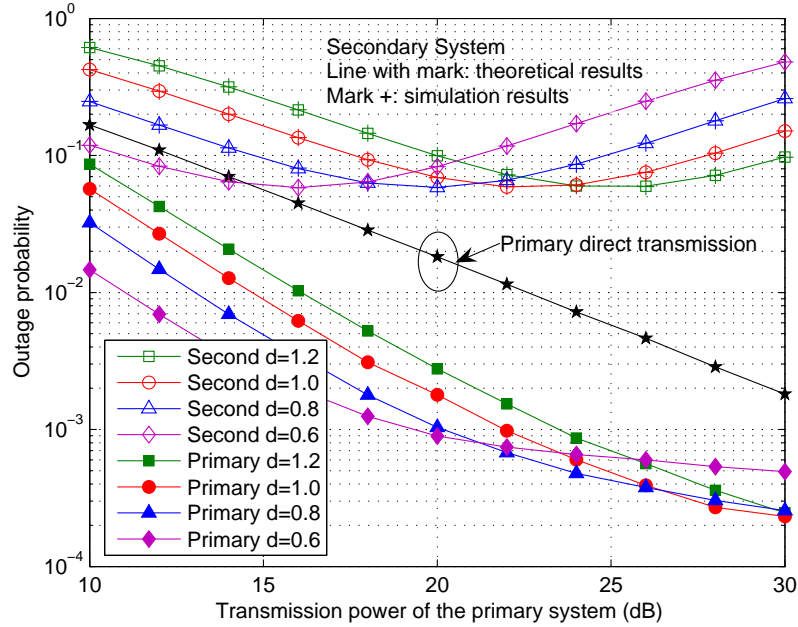


**Figure 2.8:** Outage probability w.r.t. different large-scale distance  $d$ . Small-scale distance is 0.1, primary rate  $R_p = 1.5$  bits/s/Hz, secondary rate  $R_s = 1.0$  bits/s/Hz, and secondary transmission power  $P_s = 20$  dB.

and primary receiver, the performance of the primary system is significantly improved in the proposed cognitive relaying scheme.

### 2.4.3 Outage Performance vs. Primary Transmission Power

Fig. 2.8 compares the outage probabilities of primary and secondary systems against the primary transmission power. For the secondary system, with the increase of primary transmission power, the performance first gets better and then gets worse. In the lower power range, both spectrum sharing probability and success probability become higher with the increase of primary transmission power because the channel quality between secondary users can very capably withstand the interference from primary transmission. Based on this fact, the shorter the large-scale distance, the better the average channel quality between primary transmitter and secondary user, and the smaller the outage probability of detecting the primary signal after cancel-

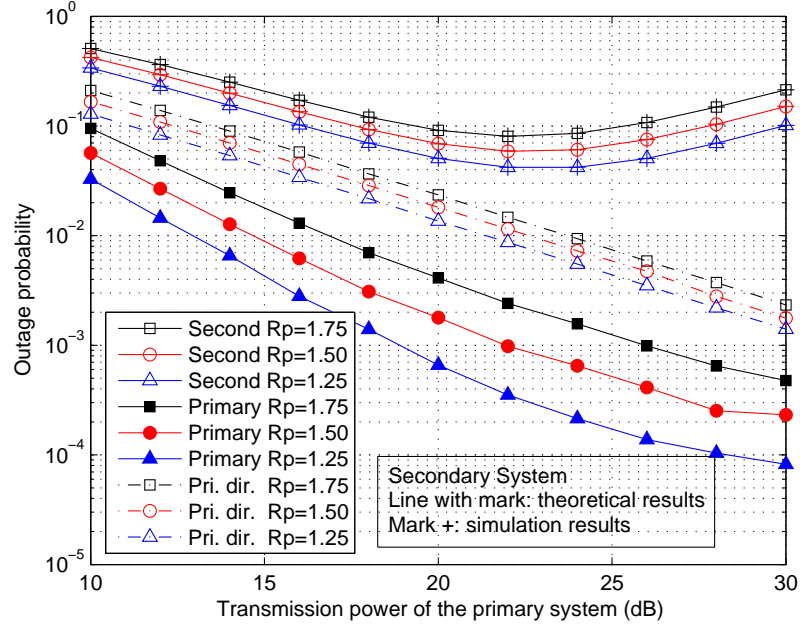


**Figure 2.9:** Outage probability w.r.t. different transmission rates  $R_p$  and  $R_s = R_p - 0.5$ . The large-scale distance is set as 1.0, while the small-scale distance is 0.1. The secondary transmission power is  $P_s = 20$  dB.

ing the composite signal from the secondary transmitter. However, in the higher power range, the interference from the primary system is very strong, which means it becomes difficult for the secondary users to apply successive interference detection and cancellation. In this case, the shorter the large-scale distance, the stronger the interference from the primary system, and the worse the outage performance.

For the primary system, the outage performance gets better with the increase of primary transmission power. However, in the high power range, the shorter the large-scale distance, the worse the performance because the shorter the distance, the smaller the probability of spectrum sharing, as shown for the secondary system. This situation means less opportunities will be encountered to achieve the space diversity brought by the cooperation of the secondary system. Moreover, our proposed scheme always outperforms direct transmission between PT and PR.

Fig. 2.9 shows the outage performance of primary and secondary systems with respect to different target rates. Similarly, the outage performance of the secondary

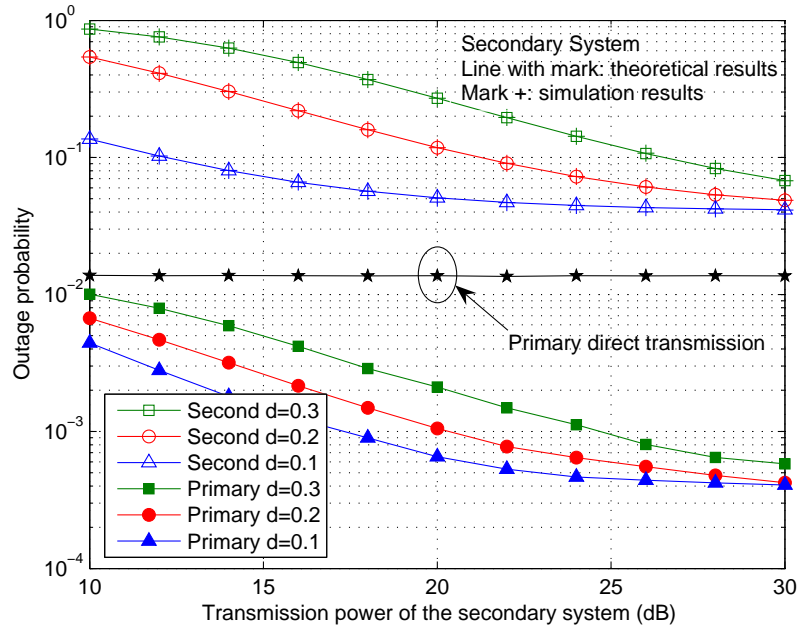


**Figure 2.10:** Outage probability w.r.t. different small-scale distance  $d$ . The large-scale distance is set as 1.0. The primary transmission power is  $P_p = 20$  dB. The transmission rates are set as  $R_p = 1.25$  bits/s/Hz and  $R_s = 0.75$  bits/s/Hz.

system gets better first and then becomes worse with the increase of primary transmission power. As expected, the performance becomes better with the decrease of the transmission rate because the smaller the target rate, the higher the probability of the channel supporting the transmission. The numerical results agree very well with the simulation results.

#### 2.4.4 Outage Performance vs. Small-Scale Distance

Fig. 2.10 compares the outage performance of both systems with different small-scale distances, while the large-scale distance is fixed as 1. With the decrease of the small-scale distance, the outage performance of both systems gets better. This is because, when the distance between secondary users is shortened, the successive interference detection and cancelation can be well performed according to the decoding order presented in Section 2.2. The primary system always outperforms the secondary

system despite the higher data transmission rate. We notice that when the secondary transmission power is very high, the impact of the small-scale distance is minor to the outage performance of both systems. This finding is caused by the fact that the average signal strength of the secondary transmission is mainly governed by the strong secondary transmission power. The small-scale distance has little impact on the signal detection at the secondary users. Again, the theoretical results coincide well with the simulation results for the secondary system.

## 2.5 Summary

A spectrum sharing scheme based on two-path successive relaying is proposed in this chapter. By linearly combining the primary and secondary signals, the two secondary transmitters not only support the secondary signal transmission, but also help the primary signal transmission via a diversity approach. The outage probabilities of the primary and secondary systems are analyzed and the optimal power allocation factor is determined. A higher spectrum efficiency can be achieved compared with the traditional multi-phase cooperative spectrum sharing schemes. Numerical and simulation results validate that the proposed spectrum sharing scheme can satisfy the data transmission requirement of the secondary system while conservatively protecting the outage performance of the primary system.

## 2.6 Appendix I: Derivation of Spectrum Sharing Probability

By substituting related terms into (2.12), we can obtain

$$\Pr \left\{ \mathcal{G}_{\text{PT},\text{ST}_0} \leq \Lambda_1(\mathcal{G}_{\text{ST}_0,\text{ST}_1}), \mathcal{G}_{\text{PT},\text{ST}_0} \leq \Lambda_2(\mathcal{G}_{\text{ST}_0,\text{ST}_1}), \frac{T}{\eta} \leq \mathcal{G}_{\text{PT},\text{ST}_0}, \right. \\ \left. \mathcal{G}_{\text{PT},\text{ST}_1} \leq \Lambda_1(\mathcal{G}_{\text{ST}_0,\text{ST}_1}), \mathcal{G}_{\text{PT},\text{ST}_1} \leq \Lambda_2(\mathcal{G}_{\text{ST}_0,\text{ST}_1}), \frac{T}{\eta} \leq \mathcal{G}_{\text{PT},\text{ST}_1} \right\}, \quad (2.35)$$

where the two intermediate terms are given as

$$\begin{aligned}\Lambda_1(\mathcal{G}_{\text{ST}_0, \text{ST}_1}) &= \frac{(1-\beta)\rho\mathcal{G}_{\text{ST}_0, \text{ST}_1}}{U} - \frac{1}{\eta} \\ \Lambda_2(\mathcal{G}_{\text{ST}_0, \text{ST}_1}) &= \frac{(\beta-T+T\beta)\rho\mathcal{G}_{\text{ST}_0, \text{ST}_1}}{T} - \frac{1}{\eta}.\end{aligned}\quad (2.36)$$

In particular, the parameters  $T = 2^{R_p} - 1$  and  $U = 2^{R_s} - 1$ .

**Case 1:** When  $\Lambda_1(\mathcal{G}_{\text{ST}_0, \text{ST}_1}) \leq \Lambda_2(\mathcal{G}_{\text{ST}_0, \text{ST}_1})$ , we can get

$$\frac{T}{\eta} \leq \frac{(1-\beta)\rho\mathcal{G}_{\text{ST}_0, \text{ST}_1}}{U} - \frac{1}{\eta} \leq \frac{(\beta-T+T\beta)\rho\mathcal{G}_{\text{ST}_0, \text{ST}_1}}{T} - \frac{1}{\eta}, \quad (2.37)$$

from which the following result is obtained

$$\frac{T(U+1)}{T(U+1)+U} \leq \beta < 1 \text{ and } \mathcal{G}_{\text{ST}_0, \text{ST}_1} \geq \mu_1 = \frac{U(T+1)}{(1-\beta)\rho\eta}. \quad (2.38)$$

In this case, the probability  $\Pr\{E_c\}$  of (2.35) is denoted as  $P_1$  and given by

$$P_1 = \Pr \left\{ \frac{T}{\eta} \leq \mathcal{G}_{\text{PT}, \text{ST}_0} \leq \Lambda_1(\mathcal{G}_{\text{ST}_0, \text{ST}_1}), \frac{T}{\eta} \leq \mathcal{G}_{\text{PT}, \text{ST}_1} \leq \Lambda_1(\mathcal{G}_{\text{ST}_0, \text{ST}_1}), \mathcal{G}_{\text{ST}_0, \text{ST}_1} \geq \mu_1 \right\}. \quad (2.39)$$

**Case 2:** When  $\Lambda_2(\mathcal{G}_{\text{ST}_0, \text{ST}_1}) \leq \Lambda_1(\mathcal{G}_{\text{ST}_0, \text{ST}_1})$ , we can get

$$\frac{T}{\eta} \leq \frac{(\beta-T+T\beta)\rho\mathcal{G}_{\text{ST}_0, \text{ST}_1}}{T} - \frac{1}{\eta} \leq \frac{(1-\beta)\rho\mathcal{G}_{\text{ST}_0, \text{ST}_1}}{U} - \frac{1}{\eta}, \quad (2.40)$$

from which the following result is obtained

$$\frac{T}{T+1} \leq \beta < \frac{T(U+1)}{T(U+1)+U} \text{ and } \mathcal{G}_{\text{ST}_0, \text{ST}_1} \geq \mu_2 = \frac{T(T+1)}{(\beta-T+T\beta)\rho\eta}. \quad (2.41)$$

In this case, the probability  $\Pr\{E_c\}$  of (2.35) is denoted as  $P_2$  and given by

$$P_2 = \Pr \left\{ \frac{T}{\eta} \leq \mathcal{G}_{\text{PT}, \text{ST}_0} \leq \Lambda_2(\mathcal{G}_{\text{ST}_0, \text{ST}_1}), \frac{T}{\eta} \leq \mathcal{G}_{\text{PT}, \text{ST}_1} \leq \Lambda_2(\mathcal{G}_{\text{ST}_0, \text{ST}_1}), \mathcal{G}_{\text{ST}_0, \text{ST}_1} \geq \mu_2 \right\}. \quad (2.42)$$

**Summary:** By uniformly writing  $\mu = \mu_1$  or  $\mu_2$ , the probability  $\Pr\{E_c\}$  with respect to different values of  $\beta$ , i.e.  $P_1$  of (2.39) and  $P_2$  of (2.42), can be generally written as

$$\begin{aligned}\Pr\{E_c\} &= \Pr \left\{ \frac{T}{\eta} \leq \mathcal{G}_{\text{PT}, \text{ST}_0} \leq \frac{T+1}{\mu\eta} \mathcal{G}_{\text{ST}_0, \text{ST}_1} - \frac{1}{\eta}, \right. \\ &\quad \left. \frac{T}{\eta} \leq \mathcal{G}_{\text{PT}, \text{ST}_1} \leq \frac{T+1}{\mu\eta} \mathcal{G}_{\text{ST}_0, \text{ST}_1} - \frac{1}{\eta}, \mathcal{G}_{\text{ST}_0, \text{ST}_1} \geq \mu \right\}.\end{aligned}\quad (2.43)$$

For the exponentially distributed random variables, the closed form expression of (2.43) can be computed as (2.13). The value of  $\mu$  is given by (2.14), which incorporates the fact that  $\beta \geq 0.5$  based on (2.38) and (2.41).

## 2.7 Appendix II: Derivation of Approximate Rate

We artificially divide the normalized equivalent MIMO channel (2.18) into blocks, for each block there are 2 transmit antennas and 3 receive antennas, and there is no interference between blocks. This is similarly with dividing the MIMO system into parallel SIMO systems where signal transmitted via each column is interference free [48, 49]. There are two different blocks included in (2.18), i.e.,

$$\mathbf{H}_0 = \begin{bmatrix} \frac{\sqrt{P_p} h_{PT,PR}}{\sqrt{N_0}} & 0 \\ \frac{\sqrt{\beta P_s} h_{ST_0,PR}}{\sqrt{\lambda_0}} & \frac{\sqrt{P_p} h_{PT,PR}}{\sqrt{\lambda_0}} \\ 0 & \frac{\sqrt{\beta P_s} h_{ST_1,PR}}{\sqrt{\lambda_1}} \end{bmatrix}, \quad \mathbf{H}_1 = \begin{bmatrix} \frac{\sqrt{P_p} h_{PT,PR}}{\sqrt{\lambda_1}} & 0 \\ \frac{\sqrt{\beta P_s} h_{ST_0,PR}}{\sqrt{\lambda_0}} & \frac{\sqrt{P_p} h_{PT,PR}}{\sqrt{\lambda_0}} \\ 0 & \frac{\sqrt{\beta P_s} h_{ST_1,PR}}{\sqrt{\lambda_1}} \end{bmatrix}. \quad (2.44)$$

The determinant of the tridiagonal matrix is thus upper bounded as

$$\det(\mathbf{I}_{L+1} + \tilde{\mathbf{H}}\tilde{\mathbf{H}}^H) \leq [\det(\mathbf{I} + \mathbf{H}_0\mathbf{H}_0^H)] [\det(\mathbf{I} + \mathbf{H}_1\mathbf{H}_1^H)]^{\frac{L-2}{2}}. \quad (2.45)$$

Since block  $\mathbf{H}_0$  is different with block  $\mathbf{H}_1$  only in the first element, we approximately have

$$\det(\mathbf{I}_{L+1} + \tilde{\mathbf{H}}\tilde{\mathbf{H}}^H) \approx [\det(\mathbf{I} + \mathbf{H}_1\mathbf{H}_1^H)]^{\frac{L}{2}}, \quad (2.46)$$

where

$$\mathbf{I} + \mathbf{H}_1\mathbf{H}_1^H = \begin{bmatrix} 1 + \frac{P_p \mathcal{G}_{PT,PR}}{\lambda_1} & \frac{\sqrt{\beta P_s P_p} h_{ST_0,PR}^* h_{PT,PR}}{\sqrt{\lambda_0 \lambda_1}} & 0 \\ \frac{\sqrt{\beta P_s P_p} h_{ST_0,PR} h_{PT,PR}^*}{\sqrt{\lambda_0 \lambda_1}} & 1 + \frac{\beta P_s \mathcal{G}_{ST_0,PR}}{\lambda_0} + \frac{P_p \mathcal{G}_{PT,PR}}{\lambda_0} & \frac{\sqrt{\beta P_s P_p} h_{ST_1,PR}^* h_{PT,PR}}{\sqrt{\lambda_0 \lambda_1}} \\ 0 & \frac{\sqrt{\beta P_s P_p} h_{ST_1,PR} h_{PT,PR}^*}{\sqrt{\lambda_0 \lambda_1}} & 1 + \frac{\beta P_s \mathcal{G}_{ST_1,PR}}{\lambda_1} \end{bmatrix}.$$

Substituting (2.46) into (2.17), we can obtain the approximate rate as (2.19).

## 2.8 Appendix III: Power Allocation Factor $\hat{\beta}$

By substituting  $\Pr\{E_c\}$  (2.15) and  $P_{\text{suc}}^s$  (2.33) into  $f(\beta)$ , the objective function is converted into

$$\mathcal{F}(\beta) = \underbrace{\exp \left[ - \left( \frac{\mu}{M} + \frac{2U(T+1)}{\rho\eta M(1-\beta)} \right) \right]}_{\mathcal{D}(\beta)} \underbrace{\frac{2M^2\xi^2}{(K+M\xi)(K+2M\xi)} \frac{\rho M(1-\beta)}{\rho M(1-\beta) + 2UK}}_{\mathcal{E}(\beta)}. \quad (2.47)$$

The derivative of  $\mathcal{F}(\beta)$  with respect to  $\beta$  is

$$\frac{d\mathcal{F}(\beta)}{d\beta} = \frac{d\mathcal{D}(\beta)}{d\beta} \mathcal{E}(\beta) + \frac{d\mathcal{E}(\beta)}{d\beta} \mathcal{D}(\beta). \quad (2.48)$$

After some mathematical manipulations, the first term of (2.48) is derived as

$$\frac{d\mathcal{D}(\beta)}{d\beta} \mathcal{E}(\beta) = \mathcal{F}(\beta) \left\{ \underbrace{\frac{T(T+1)^2}{\rho\eta M [(T+1)\beta - T]^2}}_{\tau_1(\beta)} - \underbrace{\frac{2U(T+1)}{\rho\eta M(1-\beta)^2}}_{\tau_2(\beta)} \right\}, \quad (2.49)$$

and the second term of (2.48) is derived as

$$\frac{d\mathcal{E}(\beta)}{d\beta} \mathcal{D}(\beta) = \mathcal{F}(\beta) \left\{ \underbrace{\frac{\rho K(T+1)(2K+3M\xi)}{T\xi(K+M\xi)(K+2M\xi)}}_{\tau_3(\beta)} - \underbrace{\frac{2UK}{(1-\beta)[\rho M(1-\beta) + 2UK]}}_{\tau_4(\beta)} \right\}. \quad (2.50)$$

Substitute (2.49) and (2.50) into (2.48). Note that,  $\mathcal{F}(\beta)$  is always larger than zero. Apparently, with respect to  $\beta$  in the lower range  $\max\{0.5, \frac{T}{T+1}\} \leq \beta \leq \max\left\{0.5, \frac{T(U+1)}{T(U+1)+U}\right\}$ ,  $\tau_1(\beta)$  and  $\tau_3(\beta)$  are monotonically decreasing functions, whereas  $\tau_2(\beta)$  and  $\tau_4(\beta)$  are monotonically increasing functions. Thus,  $\tau(\beta) = \tau_1(\beta) - \tau_2(\beta) + \tau_3(\beta) - \tau_4(\beta)$  is a monotonically decreasing function in the lower range of  $\beta$ . To identify the characteristic of  $\frac{d\mathcal{F}(\beta)}{d\beta}$ , we have the following observations.

- **Step 1:** Substitute  $\beta_1 = \frac{T(U+1)}{T(U+1)+U}$  into  $\tau(\beta)$ . With  $\tau(\beta_1) \geq 0$ ,  $f(\beta)$  is an increasing function in the lower range, and the optimal point is  $\hat{\beta} = \frac{T(U+1)}{T(U+1)+U}$ ; otherwise, go to Step 2.

- **Step 2:** Substitute  $\beta_0 = \max \left\{ 0.5, \frac{T}{T+1} \right\}$  into  $\tau(\beta)$ . With  $\tau(\beta_0) \leq 0$ ,  $f(\beta)$  is a decreasing function in this range, the optimal point is  $\hat{\beta} = \max \left\{ 0.5, \frac{T}{T+1} \right\}$ ; otherwise, go to Step 3.
- **Step 3:** With  $\tau(\beta_0) > 0$  and  $\tau(\beta_1) < 0$ ,  $f(\beta)$  first increases with  $\beta$ , and then decreases with  $\beta$  after reaching one extreme point, which is the optimal one, i.e.,  $\hat{\beta} = \arg_{\beta} [\tau(\beta) = 0]$ .

## Chapter 3

# Adaptive Spectrum Leasing with Secondary User Scheduling

### 3.1 Introduction

In the previous chapter, the TPSR based one-phase spectrum sharing scheme is proposed for the overlaid wireless system with one primary pair and two secondary pairs. The spectrum sharing is realized in the space domain, as the optimal transmission power of STs is determined to forward the primary data and transmit the secondary data simultaneously. Intuitively, the spectrum efficiency can be further improved in the multiuser cognitive radio network, where one primary link coexists with multiple SUs. The best SU can be scheduled to forward the primary data in the time domain to exchange for the opportunity of accessing the licensed spectrum for its own secondary data transmission. Since the multiuser scenario is considered, it is interesting to show the impacts of cognitive radio constraint to the diversity performance of both primary and secondary systems. In the stand-alone wireless network, the cooperative diversity gain on the order of the number of relays is achievable [34] and the asymptotic sum-rate capacity of the down-link scheduling scales like  $\log(\log m)$  [50]. The multiuser diversity is studied in [51–54] for the underlay spectrum sharing, where the

SU that can guarantee the interference constraint of the primary link and have the highest SNR over the secondary link is scheduled for the transmission. The multiuser diversity for the interweave spectrum sharing is studied in [55], where the SUs are allowed to opportunistically communicate over the vacant spectrum bands. However, there is no literature investigating the diversity of the multiuser spectrum leasing.

In this chapter, we propose an adaptive spectrum leasing scheme based on TPSR and DF relaying to improve the overall network throughput. Since the rate of primary system can be greatly enhanced with the help from SUs, the primary data transmission time can be shortened and the spectrum can thus be leased to the secondary data transmission in the remaining time. The TPSR or DF cooperation mode is adaptively switched to for each cognitive user. The SUs that can bring the largest achievable rate to secondary system while protecting the primary target rate are scheduled for the spectrum leasing with optimal time allocation. Cooperative diversity of primary system, and selection diversity and multiuser diversity of secondary system are analyzed. It is shown that with  $m$  SUs competing for the spectrum leasing, the cooperative diversity gain of primary system is  $m + 1$  and the selection diversity order of secondary system is  $m$ . The throughput of secondary system scales as  $\log(\log m)$  with large number of SUs.

The rest of this chapter is organized as follows. In Section 3.2, the system model is introduced. The SU scheduling with cooperation mode selection is proposed in Section 3.3. Section 3.4 analyzes the diversity gain of both systems based on the outage performance. The multiuser diversity in terms of throughput scaling is studied in Section 3.5. Numerical and simulation results are presented in Section 3.6. Section 3.7 concludes this chapter.

## 3.2 System Model

The cognitive radio network considered in this chapter has one primary link (PT  $\rightarrow$  PR) coexisting with  $m$  secondary transmitters  $ST_i, i \in \mathcal{M} = \{1, 2, \dots, m\}$ , which intend

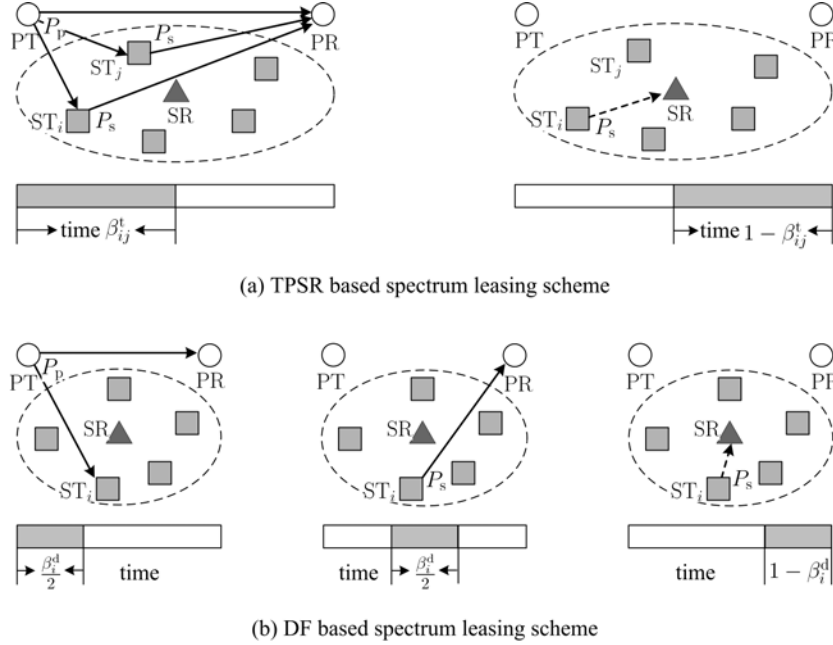


**Figure 3.1:** Spectrum leasing schemes in the cognitive radio network with one pair of PUs and multiple SUs. The solid lines represent the primary signal link, and the dashed lines represent the secondary signal link.

to communicate with a common secondary receiver SR over a single-hop link. Each user is equipped with one antenna operating with half-duplex mode. The channel between any transmitter  $u$  and receiver  $v$  is assumed to undergo independent Rayleigh block fading with channel gain  $h_{u,v}$ . The channel remains invariant in the duration of one fading block. The channel power gain is denoted as  $\mathcal{G}_{u,v} = |h_{u,v}|^2$ , which is exponentially distributed with mean  $\bar{\mathcal{G}}_{u,v} = d_{u,v}^{-\alpha}$ , where  $d_{u,v}$  is the distance and  $\alpha$  is the path loss exponent. The channel is assumed to be symmetric [34], i.e.,  $h_{u,v} = h_{v,u}$ .

The primary system is willing to share its licensed spectrum with the secondary system for a reward of cooperation gain. With the assistance from SUs, less time is needed for the transmission of primary data and hence less energy is consumed in the primary system. In return, the spectrum can be leased to the secondary transmission in the remaining time.

Two cooperation modes are considered in our proposed adaptive spectrum leasing scheme. The TPSR based spectrum leasing scheme with  $ST_i$  ( $i \in \mathcal{M}$ ) and  $ST_j$

( $j \in \mathcal{M}, j \neq i$ ) assisting the primary data transmission is shown in Fig. 3.1(a). The fraction of time used for the cooperation is  $\beta_{ij}^t \in (0, 1)$ , where the superscript “t” denotes the TPSR scheme. The primary data is encapsulated into frames, and each frame contains  $N$  symbols and lasts one unit time. One primary data frame is cooperatively transmitted in the former  $L = \beta_{ij}^t N$  time slots, while the secondary transmission between  $ST_i$  and SR is performed in the remaining  $(1 - \beta_{ij}^t)N$  time slots. Without loss of generality,  $L$  is set as an odd number. The unit-power primary signal sent in time slot  $k$  is denoted as  $x_p[k]$ . In the TPSR,  $ST_i$  receives the primary signal  $x_p[1]$  in the first time slot, and  $ST_j$  forwards the primary signal  $x_p[L - 1]$  in the last time slot  $L$ . The cooperation in other time slots is explained as follows [24].

- At even time slot  $k$ : PT sends  $x_p[k]$ ;  $ST_i$  sends  $x_p[k - 1]$ ;  $ST_j$  receives the signals, detects and cancels  $x_p[k - 1]$ , then detects  $x_p[k]$ ; PR receives the superimposed signal.
- At odd time slot  $k + 1$ : PT sends  $x_p[k + 1]$ ;  $ST_j$  sends  $x_p[k]$ ;  $ST_i$  receives the signals, detects and cancels  $x_p[k]$ , then detects  $x_p[k + 1]$ ; PR receives superimposed signal.

In the above process, the successive interference decoding and cancelation is applied at STs to retrieve the primary signals. The primary transmitter PT continuously sends its signal to PR, while  $ST_i$  and  $ST_j$  implicitly help forward the signal without interrupting the primary transmission. At the end of TPSR, PR performs the joint maximum-likelihood (ML) decoding to retrieve the primary signals received in all  $L$  time slots. From time slot  $L + 1$  to  $N$ ,  $ST_i$  sends its own secondary signal to SR, while SR performs the decoding symbol by symbol.

The DF based spectrum leasing scheme [14] with  $ST_i$  helping the primary data transmission is shown by Fig. 3.1 (b). The fraction of time used for the cooperation is  $\beta_i^d \in (0, 1)$ , where the superscript “d” denotes the DF scheme. The primary signal is broadcast in the first  $(\beta_i^d/2)N$  time slots by PT. This signal can be overheard by PR and  $ST_i$  simultaneously. Then,  $ST_i$  forwards the primary signal in the next  $(\beta_i^d/2)N$

time slots. The primary signals received in the cooperation phase are maximal ratio combined (MRC) by PR for the detection. After that,  $ST_i$  sends its own secondary signal to SR in the remaining  $(1 - \beta_i^d)N$  time slots.

### 3.3 Adaptive Spectrum Leasing with User Scheduling

In this section, we present the TPSR/DF based adaptive spectrum leasing scheme with SU scheduling. The ST that can guarantee the primary transmission rate and has the largest secondary rate towards SR is scheduled for the spectrum leasing with its preferred cooperation mode. The optimal time allocation is studied for the proposed spectrum leasing.

#### 3.3.1 Secondary User Scheduling

In the secondary system, each ST independently judges whether TPSR or DF based spectrum leasing should be performed with its participation. The cooperation mode that can bring a higher rate to the secondary system while satisfying the primary rate requirement is adaptively selected. The achievable rate of secondary system with  $ST_i$  joining in the spectrum leasing is given as

$$R_{si} = \max \{ R_{sii^*}^t, R_{si}^d \}, \quad (3.1)$$

where  $R_{sii^*}^t$  is the achievable rate of secondary system when the TPSR is jointly performed by  $ST_i$  and its best partner  $ST_{i^*}$  with  $i^* = \arg \max_{j \in \mathcal{M}, j \neq i} R_{sij}^t$ . The achievable rate of secondary system with the DF cooperation performed by  $ST_i$  is denoted as  $R_{si}^d$ . Therefore, the optimal ST scheduled for the cooperative spectrum leasing is denoted as  $ST_b$  with index

$$b = \arg \max_{i \in \mathcal{F}} R_{si}, \quad (3.2)$$

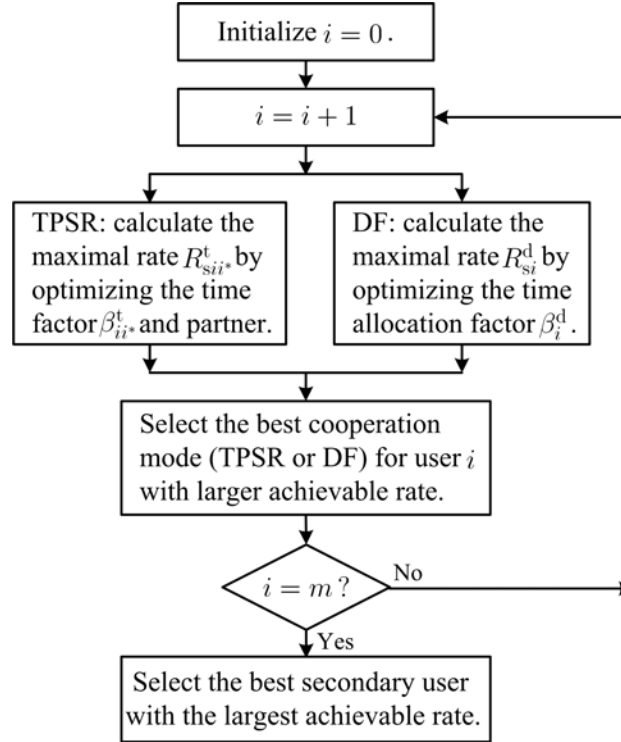


**Figure 3.2:** Flow chart illustrating the SU scheduling with adaptive mode selection between TPSR and DF protocols.

where the potential relay set is

$$\mathcal{F} = \{i | i \in \mathcal{M}, R_{si} > 0\}. \quad (3.3)$$

If the TPSR mode is selected for  $ST_b$ , then both  $ST_b$  and its best partner  $ST_{b^*}$  will participate in the cooperation. If the DF mode is selected,  $ST_b$  itself is scheduled for the cooperative transmission. Only the STs in the potential relay set  $\mathcal{F}$  could guarantee the primary target rate in the cooperation and have the opportunity for the secondary data transmission. The flow chart of user scheduling with adaptive cooperation mode selection is shown in Fig. 3.2.

We assume that the related channel state information (CSI) is available to allocate the resource and switch the cooperation mode. The active control signal exchange exists between primary and secondary systems to obtain the related channel states. The price of exchanging the CSI can be compensated by the advantage of cooperation in realizing the transmission requirements of both systems. Efficient centralized or

distributed algorithms can be designed to acquire the related CSI and make the decisions. For the centralized way, the whole CSI may be available to PT/PR/SR through signaling exchange over a control channel [14]. For the distributed way, each ST may estimate the local channel states and extract other CSI piggybacked by the control packets in the handshake process [21] [74]. The time back-off mechanism [34] or the signaling burst scheme [56] can be applied to schedule the best SU in a distributed fashion.

### 3.3.2 Optimal Time Allocation for TPSR based Scheme

For the TPSR based spectrum leasing, each  $ST_i$  ( $i \in \mathcal{M}$ ) formulates the following optimization problem considering its each possible partner  $ST_j$  ( $j \in \mathcal{M}, j \neq i$ ), i.e.,

$$\begin{aligned} \max_{\beta_{ij}^t} \quad & R_{sij}^t \\ \text{s.t.} \quad & R_{pij}^t \geq r_0, \end{aligned} \quad (3.4)$$

where  $R_{pij}^t$  is the achievable rate of primary system with the TPSR jointly performed by  $ST_i$  and its partner  $ST_j$ , and  $r_0$  is the target rate of primary system. The optimization problem aims to maximize the achievable rate of secondary system while satisfying the rate requirement of primary system. For the given channel realization, the more time allocated to the cooperation of primary signal transmission, the higher achievable rate can be obtained for the primary system, and the lower achievable rate is brought to the secondary system. Therefore, the optimal time allocation with  $ST_i$  and its partner  $ST_j$  participating in the TPSR is obtained by letting  $R_{pij}^t = r_0$ .

- If we get  $\beta_{ij}^t \geq 1$ , the TPSR jointly performed by  $ST_i$  and  $ST_j$  cannot support the primary target rate, and the achievable rate of secondary system is set as  $R_{sij}^t = 0$ .
- If we get  $0 < \beta_{ij}^t < 1$ , the primary target rate can be guaranteed and the achievable rate of secondary system is  $R_{sij}^t > 0$ . So,  $ST_i$  belongs to the potential relay set  $\mathcal{F}$ .

The maximum secondary rate achieved with the participation of  $ST_i$  in the TPSR is given as

$$R_{sii^*}^t = \max_{j \in \mathcal{M}, j \neq i} R_{sij}^t, \quad (3.5)$$

where the best partner of  $ST_i$  is denoted as  $ST_{i^*}$  with  $i^* = \arg \max_{j \in \mathcal{M}, j \neq i} R_{sij}^t$ .

Next, we determine the optimal time allocation through analyzing the achievable rates of both systems. In even time slot  $k$  ( $k < L$ ), when  $ST_i$  and PT transmit simultaneously, the signal received by  $ST_j$  is written as

$$y_{ST_j}[k] = \sqrt{P_p} h_{PT,ST_j} x_p[k] + \sqrt{P_s} h_{ST_i,ST_j} x_p[k-1] + n_{ST_j}[k], \quad (3.6)$$

where  $P_p$  and  $P_s$  represent the transmit power of primary system and secondary system, respectively. In this system, the transmit power of both systems is fixed, and  $P_s = \eta P_p$  with  $\eta > 0$  being a predefined constant. The additive white Gaussian noise (AWGN) is  $n_{SR}[k] \sim \mathcal{CN}(0, N_0)$  with  $N_0$  denoting the noise power. The SNR at PT side is denoted as  $\rho = P_p/N_0$ . We assume that the STs are close to each other, the interference between  $ST_i$  and  $ST_j$  is deemed very strong. To detect the current signal, the previous signal should be firstly detected and canceled. By viewing the current signal as noise, the achievable rate of previous signal is

$$R_{pij}^{t1} = \beta_{ij}^t \log_2 \left( 1 + \frac{\gamma_{ST_i,ST_j}}{\gamma_{PT,ST_j} + 1} \right), \quad (3.7)$$

where  $\gamma_{ST_i,ST_j} = \eta \rho \mathcal{G}_{ST_i,ST_j}$  and  $\gamma_{PT,ST_j} = \rho \mathcal{G}_{PT,ST_j}$  represent the instantaneous SNR over links  $(ST_i, ST_j)$  and  $(PT, ST_j)$ , respectively. The transmission rate of primary system is denoted as  $r_0$ , only when  $R_{pij}^{t1} \geq r_0$  could  $ST_j$  correctly detect and cancel the previous primary signal. Then, the achievable rate of current primary signal is denoted as  $R_{pij}^{t2}$  and given by

$$R_{pij}^{t2} = \beta_{ij}^t \log_2 (1 + \gamma_{PT,ST_j}). \quad (3.8)$$

$ST_j$  could correctly detect the current signal with  $R_{pij}^{t2} \geq r_0$ .

In odd time slot  $k + 1$  except the last one, when  $ST_j$  and PT transmit simultaneously, the signal received by  $ST_i$  is

$$y_{ST_i}[k + 1] = \sqrt{P_p} h_{PT,ST_i} x_p[k + 1] + \sqrt{P_s} h_{ST_i,ST_j} x_p[k] + n_{ST_i}[k + 1], \quad (3.9)$$

where  $n_{ST_i}[k + 1] \sim \mathcal{CN}(0, N_0)$  is the AWGN. By viewing the current signal as noise, the achievable rate of previous signal is given by

$$R_{p_{ij}}^{t_3} = \beta_{ij}^t \log_2 \left( 1 + \frac{\gamma_{ST_i,ST_j}}{\gamma_{PT,ST_i} + 1} \right), \quad (3.10)$$

where  $\gamma_{PT,ST_i} = \rho \mathcal{G}_{PT,ST_i}$  represents the instantaneous SNR over the link  $(PT, ST_i)$ . Only when  $R_{p_{ij}}^{t_3} \geq r_0$  could  $ST_i$  correctly detect and cancel the previous primary signal. Then, the achievable rate of current signal is denoted as  $R_{p_{ij}}^{t_4}$  and given by

$$R_{p_{ij}}^{t_4} = \beta_{ij}^t \log_2 (1 + \gamma_{PT,ST_i}). \quad (3.11)$$

$ST_i$  could correctly detect the current signal with  $R_{p_{ij}}^{t_4} \geq r_0$ .

Finally, the received signal of PR in all  $L$  time slots is

$$\mathbf{y}_{ij} = \mathbf{H}_{ij} \mathbf{x}_p + \mathbf{n}_p, \quad (3.12)$$

where  $\mathbf{x}_p = [x_p[1], x_p[2], \dots, x_p[L - 1]]^T$  is the primary signal vector with  $\mathcal{T}$  denoting the transpose operation;  $\mathbf{n}_p$  is the noise with each element modeled as independent complex Gaussian random variable  $\mathcal{CN}(0, N_0)$ ;  $\mathbf{H}_{ij}$  is the equivalent MIMO channel with size  $L \times (L - 1)$ .

$$\mathbf{H}_{ij} = \begin{bmatrix} \mathcal{C}_p & 0 & \cdots & 0 & 0 & 0 \\ \mathcal{C}_i & \mathcal{C}_p & \ddots & 0 & 0 & 0 \\ 0 & \mathcal{C}_j & \ddots & 0 & 0 & 0 \\ \vdots & \ddots & \ddots & \ddots & \ddots & \vdots \\ 0 & 0 & \ddots & \mathcal{C}_j & \mathcal{C}_p & 0 \\ 0 & 0 & \cdots & 0 & \mathcal{C}_i & \mathcal{C}_p \\ 0 & 0 & \cdots & 0 & 0 & \mathcal{C}_j \end{bmatrix}, \quad (3.13)$$

where  $C_p = \sqrt{P_p}h_{PT,PR}$ ,  $C_i = \sqrt{P_s}h_{ST_i,PR}$ , and  $C_j = \sqrt{P_s}h_{ST_j,PR}$ . In this case,  $L$  time slots are used to cooperatively transmit  $L - 1$  primary symbols and the full spatial diversity is achieved, as each signal travels two independent paths towards PR. The achievable rate of primary user is denoted as  $R_{pij}^{t_5}$  and given by

$$R_{pij}^{t_5} = \frac{1}{N} \log_2 \left[ \det(\mathbf{I} + \tilde{\mathbf{H}}_{ij} \tilde{\mathbf{H}}_{ij}^H) \right], \quad (3.14)$$

where  $\tilde{\mathbf{H}}_{ij} = \sqrt{1/N_0} \mathbf{H}_{ij}$  denotes the normalized equivalent MIMO channel. The achievable rate of primary signal in the TPSR cooperation is expressed as

$$R_{pij}^t = \min \{ R_{pij}^{t_1}, R_{pij}^{t_2}, R_{pij}^{t_3}, R_{pij}^{t_4}, R_{pij}^{t_5} \}. \quad (3.15)$$

After cooperatively transmitting the primary signal, the secondary signal is transmitted between  $ST_i$  and SR in the remaining time. The achievable rate of SU is

$$R_{sij}^t = (1 - \beta_{ij}^t) \log_2 (1 + \gamma_{ST_i,SR}). \quad (3.16)$$

The achievable rate exists for the secondary system with  $\beta_{ij}^t < 1$ . Otherwise, we set  $R_{sij}^t = 0$ .

After solving  $R_{pij}^t = r_0$ , the optimal time allocation is obtained as

$$\beta_{ij}^t = \max \{ \beta_{ij}^{t_1}, \beta_{ij}^{t_2}, \beta_{ij}^{t_3}, \beta_{ij}^{t_4}, \beta_{ij}^{t_5} \}, \quad (3.17)$$

where the five terms are derived via  $R_{pij}^{t_1} = r_0$ ,  $R_{pij}^{t_2} = r_0$ ,  $R_{pij}^{t_3} = r_0$ ,  $R_{pij}^{t_4} = r_0$ , and  $R_{pij}^{t_5} = r_0$ , respectively. The first four time allocation factors can be directly obtained, and we will derive the approximate value of  $\beta_{ij}^{t_5}$ . As  $\mathbf{I} + \tilde{\mathbf{H}}_{ij} \tilde{\mathbf{H}}_{ij}^H$  in  $R_{pij}^{t_5}$  (3.14) is a tridiagonal matrix, of which the determinant is difficult to obtain, the closed-form expression of  $R_{pij}^{t_5}$  is not available. However, we can derive the following upper bound [see Appendix I],

$$\hat{R}_{pij}^{t_5} = \frac{\beta_{ij}^t}{2} \log_2 \left[ \gamma_{ST_i,PR} (1 + \gamma_{ST_j,PR}) + (1 + \gamma_{PT,PR}) (1 + \gamma_{PT,PR} + \gamma_{ST_j,PR}) \right]. \quad (3.18)$$

Let  $\hat{R}_{pij}^{t_5} = r_0$ , we can obtain a tight lower bound of  $\beta_{ij}^{t_5}$ , which is denoted as  $\hat{\beta}_{ij}^{t_5}$ .

### 3.3.3 Optimal Time Allocation for DF based Scheme

For the DF based scheme, the optimization problem formulated by  $ST_i$  ( $\forall i \in \mathcal{M}$ ) is given as

$$\begin{aligned} \max_{\beta_i^d} \quad & R_{si}^d \\ \text{s.t.} \quad & R_{pi}^d \geq r_0, \end{aligned} \quad (3.19)$$

where  $R_{pi}^d$  is the achievable rate of primary system with the DF cooperation performed by  $ST_i$ . Similarly with the TPSR problem, this optimization aims to maximize the secondary rate while protecting the primary target rate. The optimal time allocation is obtained via setting  $R_{pi}^d = r_0$ .

- If we get  $\beta_i^d \geq 1$ , the DF relaying performed by  $ST_i$  cannot support the primary target rate, and the achievable rate of secondary system is set as  $R_{si}^d = 0$ .
- If we get  $0 < \beta_i^d < 1$ , the primary target rate can be guaranteed and the achievable rate of secondary system is  $R_{si}^d > 0$ . So,  $ST_i$  belongs to the potential relay set  $\mathcal{F}$ .

Next, we determine the optimal time allocation in the DF based spectrum leasing. When PT transmits in the former  $(\beta_i^d/2)N$  time slots, PR will receive and store this signal. Meantime,  $ST_i$  overhears the primary signal with achievable rate denoted as  $R_{pi}^{d1}$  and given by

$$R_{pi}^{d1} = \frac{\beta_i^d}{2} \log_2 (1 + \gamma_{PT,ST_i}). \quad (3.20)$$

The primary signal can be correctly detected if  $R_{pi}^{d1} \geq r_0$ . In the next  $(\beta_i^d/2)N$  time slots,  $ST_i$  will forward the primary signal to PR. The former received signal is maximal ratio combined with the latter received signal by PR [57]. For the combined signal, the achievable rate is

$$R_{pi}^{d2} = \frac{\beta_i^d}{2} \log_2 (1 + \gamma_{PT,PR} + \gamma_{ST_i,PR}). \quad (3.21)$$

The achievable rate of primary signal in the DF cooperation is thus expressed as

$$R_{\text{pi}}^{\text{d}} = \min \{R_{\text{pi}}^{\text{d}_1}, R_{\text{pi}}^{\text{d}_2}\}. \quad (3.22)$$

After cooperatively transmitting the primary signal, the secondary signal is directly transmitted between  $\text{ST}_i$  and SR, the achievable rate for the secondary transmission is given as

$$R_{\text{si}}^{\text{d}} = (1 - \beta_i^{\text{d}}) \log_2(1 + \gamma_{\text{ST}_i, \text{SR}}). \quad (3.23)$$

After solving  $R_{\text{pi}}^{\text{d}} = r_0$ , the optimal time allocation can be obtained as

$$\beta_i^{\text{d}} = \max \{\beta_i^{\text{d}_1}, \beta_i^{\text{d}_2}\}, \quad (3.24)$$

where the two terms can be obtained directly by setting  $R_{\text{pi}}^{\text{d}_1} = r_0$  and  $R_{\text{pi}}^{\text{d}_2} = r_0$ , respectively. The achievable rate exists for the secondary system with  $\beta_i^{\text{d}} < 1$ . Otherwise, we set  $R_{\text{si}}^{\text{d}} = 0$ .

**Remark:** For a certain  $\text{ST}_i$  ( $i \in \mathcal{M}$ ), the condition of it belonging to the potential relay set  $\mathcal{F}$  is  $\min\{\beta_i^{\text{d}}, \beta_{ii^*}^{\text{t}}\} < 1$ , where the lower limit is omitted as the time allocation factor is always larger than 0. Only when  $\text{ST}_i$  belongs to  $\mathcal{F}$  could it switch between TPSR and DF for the spectrum leasing. The condition of choosing DF as the cooperation mode for  $\text{ST}_i$  is  $R_{\text{sii}^*}^{\text{t}} < R_{\text{si}}^{\text{d}}$ , which is equivalent to  $\beta_i^{\text{d}} < \min\{1, \beta_{ii^*}^{\text{t}}\}$ , i.e.,

$$\max\{\beta_i^{\text{d}_1}, \beta_i^{\text{d}_2}\} < \min \left\{ 1, \min_{j \in \mathcal{M}/\{i\}} \max\{\beta_{ij}^{\text{t}_1}, \beta_{ij}^{\text{t}_2}, \beta_{ij}^{\text{t}_3}, \beta_{ij}^{\text{t}_4}, \beta_{ij}^{\text{t}_5}\} \right\}. \quad (3.25)$$

Similarly, the condition of choosing TPSR as the cooperation mode is given as

$$\min_{j \in \mathcal{M}/\{i\}} \max\{\beta_{ij}^{\text{t}_1}, \beta_{ij}^{\text{t}_2}, \beta_{ij}^{\text{t}_3}, \beta_{ij}^{\text{t}_4}, \beta_{ij}^{\text{t}_5}\} < \min \{1, \max\{\beta_i^{\text{d}_1}, \beta_i^{\text{d}_2}\}\}. \quad (3.26)$$

For each primary data transmission period, the related channel knowledge should be measured by each ST to calculate the optimal time allocation and switch between DF and TPSR. The potential SU that can bring the largest achievable rate over the secondary link is scheduled to join in the spectrum leasing with its preferred cooperation mode.

### 3.4 Diversity Performance Analysis

In this section, with the transmission rates of both systems fixed, the outage probabilities are studied to show the cooperative diversity gain of primary system and the selection diversity gain of secondary system.

#### 3.4.1 Cooperative Diversity of Primary System

When  $\mathcal{F} \neq \emptyset$ , one ST is selected for the spectrum leasing, and the primary target rate can be guaranteed. No outage event occurs to the primary system in this case. However, when  $\mathcal{F} = \emptyset$ , there is no secondary transmission and PR only receives the primary signal directly coming from PT. Therefore, the outage event occurs to primary system when  $\mathcal{F} = \emptyset$  and the direct transmission is not successful. The outage probability is denoted as  $P_{\text{out}}^{\text{P}}$  and given by

$$\begin{aligned} P_{\text{out}}^{\text{P}} &= \Pr \{ \mathcal{F} = \emptyset, \log_2(1 + \gamma_{\text{PT,PR}}) < r_0 \} \\ &= \Pr \{ \beta_{11^*}^{\text{t}} \geq 1, \beta_1^{\text{d}} \geq 1, \dots, \beta_{mm^*}^{\text{t}} \geq 1, \beta_m^{\text{d}} \geq 1, \gamma_{\text{PT,PR}} < c_0 \}, \end{aligned} \quad (3.27)$$

where  $c_0 = 2^{r_0} - 1$ . Eq. (3.27) means that no optimal time allocation can be found by each ST to support the primary target rate and the direct transmission over link (PT, PR) is unsuccessful. An upper bound of  $P_{\text{out}}^{\text{P}}$  is denoted as  $\hat{P}_{\text{out}}^{\text{P}}$ , i.e.,

$$P_{\text{out}}^{\text{P}} \leq \hat{P}_{\text{out}}^{\text{P1}} = \Pr \{ \beta_1^{\text{d}} \geq 1, \dots, \beta_m^{\text{d}} \geq 1, \gamma_{\text{PT,PR}} < c_0 \} \quad (3.28)$$

The upper bound is obtained by considering the DF based spectrum leasing protocol only.

For a given  $\Gamma_{\text{PT,PR}} = \gamma_{\text{PT,PR}}$ , which is denoted as event  $\mathcal{A}$ , the probability of  $\text{ST}_i$  ( $i \in \mathcal{M}$ ) keeping silent for the DF cooperation is calculated as

$$\begin{aligned} \Pr \{ \beta_i^{\text{d}} \geq 1 | \mathcal{A} \} &= 1 - \Pr \{ \max \{ \beta_i^{\text{d1}}, \beta_i^{\text{d2}} \} < 1 | \mathcal{A} \} \\ &= 1 - \exp \left[ - \left( \frac{c_1}{\bar{\gamma}_{\text{PT,ST}}} + \frac{c_1}{\bar{\gamma}_{\text{ST,PR}}} \right) \right] \exp \left( \frac{\gamma_{\text{PT,PR}}}{\bar{\gamma}_{\text{ST,PR}}} \right), \end{aligned} \quad (3.29)$$

where  $c_1 = 4^{r_0} - 1$ ,  $\bar{\gamma}_{\text{PT,ST}} = \rho \bar{\mathcal{G}}_{\text{PT,ST}}$  and  $\bar{\gamma}_{\text{ST,PR}} = \eta \rho \bar{\mathcal{G}}_{\text{ST,PR}}$  represent the average SNRs of link (PT, ST<sub>*i*</sub>) and (ST<sub>*i*</sub>, PR), respectively. Then, the upper bound can be further computed as

$$\begin{aligned} \hat{P}_{\text{out}}^{\text{P1}} &= \int_0^{c_0} [\text{Pr} \{ \beta_i^{\text{d}} \geq 1 | \mathcal{A} \}]^m f_{\Gamma_{\text{PT,PR}}}(\gamma_{\text{PT,PR}}) d\gamma_{\text{PT,PR}} \\ &\leq \hat{P}_{\text{out}}^{\text{P2}} = \int_0^{c_0} \left\{ 1 - \exp \left[ - \left( \frac{c_1}{\bar{\gamma}_{\text{PT,ST}}} + \frac{c_1}{\bar{\gamma}_{\text{ST,PR}}} \right) \right] \right\}^m f_{\Gamma_{\text{PT,PR}}}(\gamma_{\text{PT,PR}}) d\gamma_{\text{PT,PR}}, \end{aligned} \quad (3.30)$$

where  $f_{\Gamma_{\text{PT,PR}}}(\gamma_{\text{PT,PR}})$  is the probability density function (PDF) of the exponentially distributed random variable  $\Gamma_{\text{PT,PR}}$ . Then, the upper bound in (3.30) can be obtained as

$$\begin{aligned} \hat{P}_{\text{out}}^{\text{P2}} &= \left\{ 1 - \exp \left[ - \left( \frac{c_1}{\rho \bar{\mathcal{G}}_{\text{PT,ST}}} + \frac{c_1}{\eta \rho \bar{\mathcal{G}}_{\text{ST,PR}}} \right) \right] \right\}^m \left[ 1 - \exp \left( - \frac{c_0}{\rho \bar{\mathcal{G}}_{\text{PT,PR}}} \right) \right] \\ &\approx \frac{1}{\rho^{m+1}} \left( \frac{c_1}{\bar{\mathcal{G}}_{\text{PT,ST}}} + \frac{c_1}{\eta \bar{\mathcal{G}}_{\text{ST,PR}}} \right)^m \frac{c_0}{\bar{\mathcal{G}}_{\text{PT,PR}}}. \end{aligned} \quad (3.31)$$

The approximation of (3.31) is derived for large  $\rho$ . From the outage probability upper bound (3.31), we can get the following cooperative diversity order,

$$\hat{d}_{\text{p}} = - \lim_{\rho \rightarrow \infty} \frac{\log(\hat{P}_{\text{out}}^{\text{P2}})}{\log \rho} = m + 1, \quad (3.32)$$

from which we notice that the cooperative diversity gain of  $(m + 1)$  is achievable.

Next, we derive a lower bound of the outage probability as follows according to (3.27), i.e.,

$$P_{\text{out}}^{\text{P}} \geq \check{P}_{\text{out}}^{\text{P}} = \text{Pr} \{ \beta_{11^*}^{\text{t4}} \geq 1, \dots, \beta_{mm^*}^{\text{t4}} \geq 1, \gamma_{\text{PT,PR}} < c_0 \}. \quad (3.33)$$

It is derived since  $\beta_{ii^*}^{\text{t}} = \max \{ \beta_{ii^*}^{\text{t1}}, \beta_{ii^*}^{\text{t2}}, \beta_{ii^*}^{\text{t3}}, \beta_{ii^*}^{\text{t4}}, \beta_{ii^*}^{\text{t5}} \} \geq \beta_{ii^*}^{\text{t4}}$ , and  $\beta_i^{\text{d}} = \max \{ \beta_i^{\text{d1}}, \beta_i^{\text{d2}} \} \geq \beta_i^{\text{d1}} = 2\beta_{ii^*}^{\text{t4}}$ . For a given condition  $\mathcal{A}$ , i.e.,  $\Gamma_{\text{PT,PR}} = \gamma_{\text{PT,PR}}$ , we have

$$\text{Pr} \{ \beta_{ii^*}^{\text{t4}} \geq 1 | \mathcal{A} \} = \text{Pr} \{ \gamma_{\text{PT,ST}_i} \leq c_0 \} = 1 - \exp \left( - \frac{c_0}{\bar{\gamma}_{\text{PT,ST}}} \right). \quad (3.34)$$

Then, the lower bound  $\check{P}_{\text{out}}^{\text{P}}$  can be calculated as

$$\begin{aligned}\check{P}_{\text{out}}^{\text{P}} &= \int_0^{c_0} [\Pr \{ \beta_{ii^*}^{t_4} \geq 1 | \mathcal{A} \}]^m f_{\Gamma_{\text{PT,PR}}}(\gamma_{\text{PT,PR}}) d\gamma_{\text{PT,PR}} \\ &= \left[ 1 - \exp \left( - \frac{c_0}{\rho \bar{\mathcal{G}}_{\text{PT,ST}}} \right) \right]^m \left[ 1 - \exp \left( - \frac{c_0}{\rho \bar{\mathcal{G}}_{\text{PT,PR}}} \right) \right] \\ &\approx \frac{1}{\rho^{m+1}} \left( \frac{c_0}{\bar{\mathcal{G}}_{\text{PT,ST}}} \right)^m \frac{c_0}{\bar{\mathcal{G}}_{\text{PT,PR}}},\end{aligned}\quad (3.35)$$

where the approximation is derived in the high regime of  $\rho$ . From the outage probability lower bound (3.35), we can get the following cooperative diversity order,

$$\check{d}_{\text{p}} = - \lim_{\rho \rightarrow \infty} \frac{\log(\check{P}_{\text{out}}^{\text{P}})}{\log \rho} = m + 1, \quad (3.36)$$

from which we notice that the cooperative diversity gain of  $(m + 1)$  is achievable.

With  $m$  STs competing to forward the primary signal plus the direct link (PT  $\rightarrow$  PR), totally  $m + 1$  independent links are considered for the primary transmission. Therefore, the cooperative diversity gain of primary system is  $(m + 1)$  as can be seen from (3.32) and (3.36). The more STs contend for the spectrum leasing, the higher diversity gain is achieved for the primary system.

### 3.4.2 Selection Diversity of Secondary System

In the competition process, the potential ST with highest achievable rate is selected to relay the primary data and transmit the secondary data. If the target rate between the selected ST and the common SR is not satisfied, the outage event occurs to the secondary system [21]. Since the data length of each ST is identical and the transmit rate is fixed as  $r_1$ , this outage performance can reflect the throughput of secondary system. Denoted as  $P_{\text{out}}^{\text{s}}$ , the outage probability is given as

$$\begin{aligned}P_{\text{out}}^{\text{s}} &= \Pr \{ R_{\text{s}1} < r_1, \dots, R_{\text{s}m} < r_1 \} \\ &= \Pr \{ R_{\text{s}11^*}^{\text{t}} < r_1, R_{\text{s}1}^{\text{d}} < r_1, \dots, R_{\text{s}mm^*}^{\text{t}} < r_1, R_{\text{s}m}^{\text{d}} < r_1 \}.\end{aligned}\quad (3.37)$$

The outage probability upper bound is denoted as  $\hat{P}_{\text{out}}^{\text{s}1}$ , i.e.,

$$P_{\text{out}}^{\text{s}} \leq \hat{P}_{\text{out}}^{\text{s}1} = \Pr \{ R_{\text{s}1}^{\text{d}} < r_1, \dots, R_{\text{s}m}^{\text{d}} < r_1 \}.\quad (3.38)$$

The probability upper bound in (3.38) is derived by only considering the DF protocol. For a given condition  $\mathcal{A}$ , i.e.,  $\Gamma_{\text{PT,PR}} = \gamma_{\text{PT,PR}}$ , the probability that a certain  $\text{ST}_i$  ( $i \in \mathcal{M}$ ) cannot support the secondary transmission with DF cooperation is denoted as  $\Pr \{R_{\text{si}}^{\text{d}} < r_1 | \mathcal{A}\}$  and it is computed as

$$\begin{aligned} & \Pr \{(1 - \beta_i^{\text{d}}) \log_2(1 + \gamma_{\text{ST}_i, \text{SR}}) < r_1 | \mathcal{A}\} \\ & \leq \Pr \{\beta_i^{\text{d}} > \theta_0 | \mathcal{A}\} + \Pr \{\beta_i^{\text{d}} \leq \theta_0, \gamma_{\text{ST}_i, \text{SR}} < 2^{\frac{r_1}{1 - \beta_i^{\text{d}}}} - 1 | \mathcal{A}\} \\ & \leq 1 - \Pr \{\beta_i^{\text{d}} \leq \theta_0 | \mathcal{A}\} \Pr \{\gamma_{\text{ST}_i, \text{SR}} \geq 2^{\frac{r_1}{1 - \theta_0}} - 1 | \mathcal{A}\}, \end{aligned} \quad (3.39)$$

where  $0 < \theta_0 < 1$  is a constant. Then, we have probability

$$\begin{aligned} \Pr \{\beta_i^{\text{d}} \leq \theta_0 | \mathcal{A}\} &= \Pr \{\max\{\beta_i^{\text{d}1}, \beta_i^{\text{d}2}\} \leq \theta_0 | \mathcal{A}\} \\ &= \begin{cases} \exp\left(-\frac{v_0}{\bar{\gamma}_{\text{PT,ST}}}\right) \exp\left(-\frac{v_0 - \gamma_{\text{PT,PR}}}{\bar{\gamma}_{\text{ST,PR}}}\right), & \text{if } \gamma_{\text{PT,PR}} < v_0 \\ \exp\left(-\frac{v_0}{\bar{\gamma}_{\text{PT,ST}}}\right), & \text{if } \gamma_{\text{PT,PR}} \geq v_0, \end{cases} \end{aligned} \quad (3.40)$$

where  $v_0 = 4^{r_0/\theta_0} - 1$ . With reference to (3.40), the upper bound of (3.39) is derived as

$$\begin{aligned} \Pr \{R_{\text{si}}^{\text{d}} < r_1 | \mathcal{A}\} &\leq 1 - \Pr \{\beta_i^{\text{d}} \leq \theta_0 | \mathcal{A}\} \Pr \{\gamma_{\text{ST}_i, \text{SR}} \geq v_1 | \mathcal{A}\} \\ &\leq 1 - \exp\left(-\frac{v_0}{\bar{\gamma}_{\text{PT,ST}}}\right) \exp\left(-\frac{v_0}{\bar{\gamma}_{\text{ST,PR}}}\right) \exp\left(-\frac{v_1}{\bar{\gamma}_{\text{ST,SR}}}\right), \end{aligned} \quad (3.41)$$

where  $v_1 = 2^{\frac{r_1}{1 - \theta_0}} - 1$ . According to (3.38) and (3.41), the upper bound  $\hat{P}_{\text{out}}^{\text{S1}}$  is further derived as

$$\begin{aligned} \hat{P}_{\text{out}}^{\text{S1}} &= \int_0^\infty (\Pr \{R_{\text{si}}^{\text{d}} < r_1 | \mathcal{A}\})^m f_{\Gamma_{\text{PT,PR}}}(\gamma_{\text{PT,PR}}) d\gamma_{\text{PT,PR}} \\ &\leq \hat{P}_{\text{out}}^{\text{S2}} = \left[1 - \exp\left(-\frac{v_0}{\bar{\gamma}_{\text{PT,ST}}}\right) \exp\left(-\frac{v_0}{\bar{\gamma}_{\text{ST,PR}}}\right) \exp\left(-\frac{v_1}{\bar{\gamma}_{\text{ST,SR}}}\right)\right]^m \\ &\approx \frac{1}{\rho^m} \left(\frac{v_0}{\bar{\mathcal{G}}_{\text{PT,ST}}} + \frac{v_0}{\eta \bar{\mathcal{G}}_{\text{ST,PR}}} + \frac{v_1}{\eta \bar{\mathcal{G}}_{\text{ST,SR}}}\right)^m, \end{aligned} \quad (3.42)$$

where the approximation is derived in the high regime of  $\rho$ . Using the outage probability upper bound (3.42), we can get the following selection diversity order,

$$\hat{d}_s = - \lim_{\rho \rightarrow \infty} \frac{\log(\hat{P}_{\text{out}}^{\text{S2}})}{\log \rho} = m, \quad (3.43)$$

from which we notice that the selection diversity gain of  $m$  is achievable.

Next, we derive a lower bound of the outage probability, which is denoted as  $\check{P}_{\text{out}}^{\text{s1}}$  and given as follows according to (5.6), i.e.,

$$P_{\text{out}}^{\text{s}} \geq \check{P}_{\text{out}}^{\text{s1}} = \Pr \left\{ (1 - \beta_{11^*}^{\text{t4}}) \log_2(1 + \gamma_{\text{ST}_1, \text{SR}}) < r_1, \dots, \right. \\ \left. (1 - \beta_{mm^*}^{\text{t4}}) \log_2(1 + \gamma_{\text{ST}_m, \text{SR}}) < r_1 \right\}. \quad (3.44)$$

In the derivation of the lower bound, we use the fact  $\beta_{ii^*}^{\text{t}} \geq \beta_{ii^*}^{\text{t4}}$  and  $\beta_i^{\text{d}} \geq \beta_i^{\text{d1}} = 2\beta_{ii^*}^{\text{t4}}$ . Then, we study the outage probability with one  $\text{ST}_i$  ( $i \in \mathcal{M}$ ), i.e.,

$$\Pr \left\{ (1 - \beta_{ii^*}^{\text{t4}}) \log_2(1 + \gamma_{\text{ST}_i, \text{SR}}) < r_1 \right\} \geq \Pr \left\{ \beta_{ii^*}^{\text{t4}} \geq 1 \right\} = 1 - \exp \left( - \frac{c_0}{\bar{\gamma}_{\text{PT}, \text{ST}}} \right). \quad (3.45)$$

Considering the independence of random variables for different STs, the outage probability lower bound in (3.44) can be further derived as

$$\check{P}_{\text{out}}^{\text{s1}} \geq \check{P}_{\text{out}}^{\text{s2}} = \left[ 1 - \exp \left( - \frac{c_0}{\bar{\gamma}_{\text{PT}, \text{ST}}} \right) \right]^m \approx \frac{1}{\rho^m} \left( \frac{c_0}{\bar{\mathcal{G}}_{\text{PT}, \text{ST}}} \right)^m, \quad (3.46)$$

where the approximation is derived when  $\rho \rightarrow \infty$ . Using the outage probability lower bound (3.46), we can get the following selection diversity order,

$$\check{d}_{\text{s}} = - \lim_{\rho \rightarrow \infty} \frac{\log(\check{P}_{\text{out}}^{\text{s2}})}{\log \rho} = m, \quad (3.47)$$

from which we notice that the selection diversity gain of  $m$  is achievable.

From (3.43) and (3.47), we can see that the selection diversity order  $m$  can be achieved for the secondary system because the best user is selected among  $m$  potential STs. By observing the cooperative diversity of primary system and the selection diversity of secondary system, we note that the same diversity gain can be achieved for the overlay spectrum leasing as that of conventional stand-alone network with relay selection [34]. Therefore, the same spectrum can be utilized by two systems simultaneously without losing diversity gain for each system.

### 3.5 Multiuser Diversity: Throughput Scaling Law

In this section, with the primary target rate fixed, we study the multiuser diversity of secondary system in terms of throughput scaling with respect to the SU number. Since the potential ST with the largest rate is selected, the achievable rate of secondary system is a random variable,

$$Q = \max_{i \in \mathcal{M}} R_{si} = \max_{i \in \mathcal{M}} \max \{ R_{sii^*}^t, R_{si}^d \}. \quad (3.48)$$

We then study the throughput lower bound and upper bound based on the following Lemma.

**Lemma 1 of [58]:** Let  $Z_m = \max_{i \in \mathcal{M}} \zeta_i$  with  $\zeta_1, \zeta_2, \dots, \zeta_m$  being i.i.d. random variables with distribution  $F(x)$ . Define  $\omega(F) = \sup \{x : F(x) < 1\}$ . Assume that there is a real number  $x_1$  such that, for all  $x_1 \leq x < \omega(F)$ ,  $f(x) = F'(x)$  and  $F''(x)$  exist and  $f(x) \neq 0$ . If

$$\lim_{x \rightarrow \omega(F)} \frac{d}{dx} \left[ \frac{1 - F(x)}{f(x)} \right] = 0, \quad (3.49)$$

then there exist constants  $a_m$  and  $b_m > 0$  such that  $\frac{Z_m - a_m}{b_m}$  uniformly converges in distribution to a normalized Gumbel random variable as  $m \rightarrow \infty$ . The constants  $a_m$  and  $b_m$  are given as

$$a_m = F^{-1} \left( 1 - \frac{1}{m} \right), \quad b_m = F^{-1} \left( 1 - \frac{1}{me} \right) - a_m.$$

With  $m \rightarrow \infty$ ,  $\mathbb{E}[Z] \approx a_m + E_0 b_m$ , where  $E_0 = 0.5772\dots$  is the Euler constant.

#### 3.5.1 Throughput Lower Bound

One lower bound of the secondary rate  $Q$  is denoted as  $V$  and given by

$$V = \max_{i \in \mathcal{M}} (1 - \hat{\beta}_i^d) \log_2 (1 + \gamma_{\text{ST}_i, \text{SR}}) \leq \max_{i \in \mathcal{M}} R_{si}^d \leq Q, \quad (3.50)$$

where  $\hat{\beta}_i^d$  denotes the upper bound of the time fraction  $\beta_i^d$ , and it is given by

$$\hat{\beta}_i^d = \max \left\{ \frac{2r_0}{\log_2 (1 + \gamma_{\text{PT}, \text{ST}_i})}, \frac{2r_0}{\log_2 (1 + \gamma_{\text{ST}_i, \text{PR}})} \right\}. \quad (3.51)$$

The cumulative distribution function (CDF) of  $\hat{\beta}_i^d$  is denoted as  $F_B(\beta)$  and derived as

$$F_B(\beta) = \exp\left(\frac{1}{\bar{\gamma}_{\text{PT,ST}}} + \frac{1}{\bar{\gamma}_{\text{ST,PR}}}\right) \exp\left[-4^{r_0/\beta}\left(\frac{1}{\bar{\gamma}_{\text{PT,ST}}} + \frac{1}{\bar{\gamma}_{\text{ST,PR}}}\right)\right]. \quad (3.52)$$

For the rate lower bound  $V$ , the CDF of each i.i.d. element is denoted as  $F_V(x)$  and given by

$$\begin{aligned} F_V(x) &= \Pr\{(1-\beta)\log_2(1+\gamma_{\text{ST,SR}}) \leq x\} \\ &= \Pr\{\beta \geq 1\} + \Pr\{\beta < 1, \gamma_{\text{ST,SR}} \leq 2^{\frac{x}{1-\beta}} - 1\} \\ &= 1 - \Pr\{\beta < 1, \gamma_{\text{ST,SR}} > 2^{\frac{x}{1-\beta}} - 1\} \\ &= 1 - \exp\left(\frac{1}{\bar{\gamma}_{\text{ST,SR}}}\right) \int_0^1 \exp\left(-\frac{2^{\frac{x}{1-\beta}}}{\bar{\gamma}_{\text{ST,SR}}}\right) f_B(\beta) d\beta, \end{aligned} \quad (3.53)$$

where  $f_B(\beta)$  is the PDF of  $\hat{\beta}_i^d$ . It is nontrivial to get the closed form expression of (3.53). However, we can give an upper bound of  $F_V(x)$ . The upper bound is denoted as  $F_{V_u}(x)$  and given by

$$F_V(x) \leq F_{V_u}(x) = 1 - \Pr\{\beta \leq \beta_0, \gamma_{\text{ST,SR}} > 2^{\frac{x}{1-\beta_0}} - 1\} = 1 - k_u \exp\left(-\frac{2^{\frac{x}{1-\beta_0}}}{\bar{\gamma}_{\text{ST,SR}}}\right), \quad (3.54)$$

where  $0 < \beta_0 < 1$  is a constant and  $k_u = F_B(\beta_0) \exp\left(\frac{1}{\bar{\gamma}_{\text{ST,SR}}}\right)$  with  $F_B(\cdot)$  given by (3.52).

As proved in Appendix II, Eq. (3.49) of *Lemma 1* with  $F_V(x)$  and  $f_V(x)$  substituted is satisfied. Since the closed-form expression of  $F_V(x)$  is not available, we use  $F_{V_u}(x)$  to find the two parameters  $a_m$  and  $b_m$ , which are denoted as  $a_m^u$  and  $b_m^u$ , respectively.

$$\begin{aligned} a_m^u &= F_{V_u}^{-1}\left(1 - \frac{1}{m}\right) = (1 - \beta_0) \log_2[\bar{\gamma}_{\text{ST,SR}} \ln(k_u m)], \\ b_m^u &= F_{V_u}^{-1}\left(1 - \frac{1}{me}\right) - a_m^u = (1 - \beta_0) \log_2\left[1 + \frac{1}{\ln(k_u m)}\right]. \end{aligned} \quad (3.55)$$

With  $m \rightarrow \infty$ , the parameter  $b_m^u$  approaches zero. Therefore, the asymptotic throughput lower bound can be obtained as  $a_m^u \leq \mathbb{E}[V]$ .

### 3.5.2 Throughput Upper Bound

Since  $\beta_{ii^*}^t \geq \beta_{ii^*}^{t_4}$  and  $\beta_i^d \geq \beta_i^{d_1} = 2\beta_{ii^*}^{t_4}$ , one upper bound of the secondary rate  $Q$  is denoted as  $\Lambda$  and given by

$$Q \leq \Lambda = \max_{i \in \mathcal{M}} (1 - \beta_{ii^*}^{t_4}) \log_2 (1 + \gamma_{\text{ST},\text{SR}}). \quad (3.56)$$

Next, we investigate the throughput upper bound. The CDF of  $\beta_{ii^*}^{t_4}$  is denoted as  $F_{\tilde{B}}(\beta)$ , i.e.,

$$F_{\tilde{B}}(\beta) = \exp\left(\frac{1}{\bar{\gamma}_{\text{PT},\text{ST}}}\right) \exp\left(-\frac{2^{r_0/\beta}}{\bar{\gamma}_{\text{PT},\text{ST}}}\right). \quad (3.57)$$

The CDF of each i.i.d. element in  $\Lambda$  is denoted by  $F_{\Lambda}(x)$  and derived as

$$F_{\Lambda}(x) = 1 - \exp\left(\frac{1}{\bar{\gamma}_{\text{ST},\text{SR}}}\right) \int_0^1 \exp\left(-\frac{2^{\frac{x}{1-\beta}}}{\bar{\gamma}_{\text{ST},\text{SR}}}\right) f_{\tilde{B}}(\beta) d\beta, \quad (3.58)$$

where  $f_{\tilde{B}}(\beta)$  is the PDF of  $\beta_{ii^*}^{t_4}$ . The closed-form expression of (3.58) is not available, but we derive the lower bound, which is denoted as  $F_{\Lambda_l}(x)$  and given by

$$F_{\Lambda}(x) \geq F_{\Lambda_l}(x) = 1 - \Pr\{\beta < 1, \gamma_{\text{ST},\text{SR}} > 2^x - 1\} = 1 - k_l \exp\left(-\frac{2^x}{\bar{\gamma}_{\text{ST},\text{SR}}}\right), \quad (3.59)$$

where  $k_l = F_{\tilde{B}}(1) \exp\left(\frac{1}{\bar{\gamma}_{\text{ST},\text{SR}}}\right)$  with  $F_{\tilde{B}}(\cdot)$  given by (3.57).

With the same proof in Appendix II, Eq. (3.49) of *Lemma 1* with  $F_{\Lambda}(x)$  and  $f_{\Lambda}(x)$  substituted is also satisfied. The closed-form expression of  $F_{\Lambda}(x)$  is not available, we use  $F_{\Lambda_l}(x)$  to find  $a_m$  and  $b_m$  in *Lemma 1*. Denoted as  $a_m^l$  and  $b_m^l$ , the parameters are derived as

$$\begin{aligned} a_m^l &= F_{\Lambda_l}^{-1}\left(1 - \frac{1}{m}\right) = \log_2 [\bar{\gamma}_{\text{ST},\text{SR}} \ln(k_l m)], \\ b_m^l &= F_{\Lambda_l}^{-1}\left(1 - \frac{1}{me}\right) - a_m^l = \log_2 \left[1 + \frac{1}{\ln(k_l m)}\right]. \end{aligned} \quad (3.60)$$

With  $m \rightarrow \infty$ , the parameter  $b_m^l$  approaches zero. The asymptotic throughput upper bound can be written as  $\mathbb{E}[\Lambda] \leq a_m^l$ . Finally, we can express the system throughput as

$$a_m^u \leq \mathbb{E}[V] \leq \mathbb{E}[Q] \leq \mathbb{E}[\Lambda] \leq a_m^l. \quad (3.61)$$

Both the upper and lower bounds scale like

$$\lambda \log_2[\bar{\gamma}_{\text{ST,SR}} \ln(km)] \approx \lambda \left[ \log_2(\ln m) + \log(\bar{\gamma}_{\text{ST,SR}}) \right], \quad (3.62)$$

where the approximation is obtained when  $m$  is very large. For the rate lower bound, we have  $\lambda = 1 - \beta_0$ , while for the rate upper bound, we have  $\lambda = 1$ . Therefore, as a continuous and smooth function of  $m$ , the secondary throughput  $\mathbb{E}[Q]$  scales like  $\log_2(\bar{\gamma}_{\text{ST,SR}} \ln m)$  as  $m \rightarrow \infty$ . In other words, it scales like  $\log(\log m)$  as  $m \rightarrow \infty$ .

### 3.6 Numerical and Simulation Results

In this section, numerical and simulation results are presented to verify the efficiency of the proposed adaptive spectrum leasing scheme and validate the analysis of diversity performance. For the overlaid wireless network, we assume  $d_{\text{PT,ST}_i} = d_{\text{ST}_i,\text{PR}} = d_{\text{PT,ST}}$ ,  $d_{\text{ST}_i,\text{ST}_j} = d_{\text{ST,ST}}$ , and  $d_{\text{ST}_i,\text{SR}} = d_{\text{ST,SR}}$ , for  $\forall i \in \mathcal{M}, j \in \mathcal{M}, j \neq i$ . In the simulations, we set the noise power  $N_0 = 1$ , the path-loss exponent  $\alpha = 3$ , the power ratio  $\eta = 5$ , the total frame length  $N = 61$ , and the distance  $d_{\text{PT,PR}} = 1.0$ . The performance of this adaptive spectrum leasing scheme is compared with the DF based scheme and TPSR based scheme.

We also compare our scheme with the DF based spectrum sharing scheme [21], where two communication phases are included. In phase one, PT broadcasts its primary data with power  $P_p$ . The STs that can correctly decode the primary data and successfully forward it with power  $P_s$  are classified as potential relays. The potential ST with the largest achievable rate towards PR is selected to forward the primary data in phase two. With the cooperation of ST, the primary link can tolerate a certain amount of interference. Each remaining ST calculates the secondary transmit power under the interference constraint and the one with the best achievable rate towards SR is selected to transmit secondary data in phase two. Since the interference constraint is guaranteed, the primary rate can be satisfied in the cooperation process. If SR correctly decodes the primary data in phase one, the secondary data is decoded by

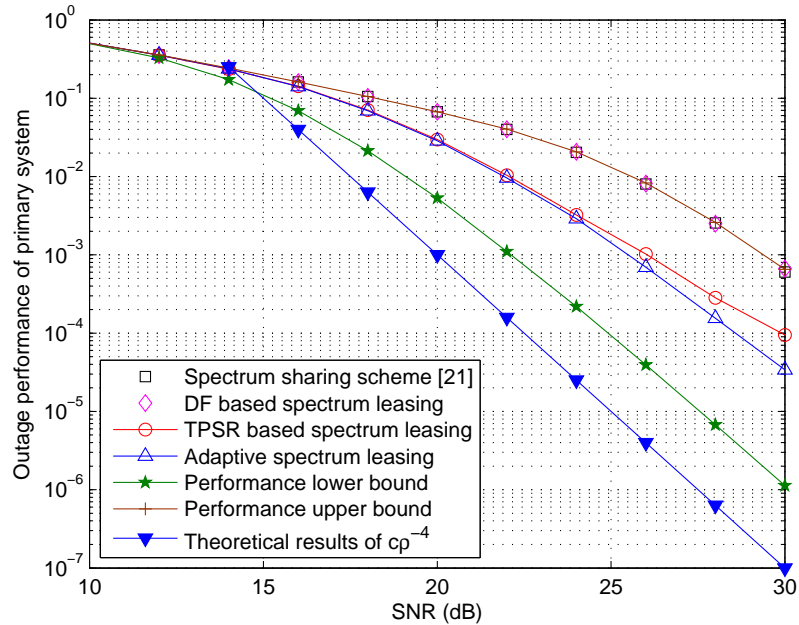


**Figure 3.3:** Outage probability of primary system with  $r_0 = 3$  and  $m = 3$ .

canceling the primary data. Otherwise, SR decodes the secondary data directly by treating the primary data as noise. In the above process, when the relaying ST is not successfully selected, the direct transmission between PT and PR is performed without interference from secondary system.

### 3.6.1 Outage Probability

Fig. 3.3 and Fig. 3.4 show the outage probability of primary system with different primary target rates. The outage performance upper bound and lower bound are plotted according to (3.31) and (3.35), respectively. Other parameters are set as  $r_1 = 1.5$ ,  $d_{PT,ST} = d_{ST,PR} = 2.0$ , and  $d_{ST,ST} = d_{ST,SR} = 0.5$ . When there are  $m = 3$  STs, the cooperative diversity gain of primary system is 4, because the simulation curves are parallel with the theoretical curves in the high regime of SNR. With the decrease of primary target rate from  $r_0 = 3$  to  $r_0 = 2$ , the outage performance gets better, since it becomes easier to support the lower rate transmission. The performance upper bound matches well with the simulation results of DF based scheme. This is

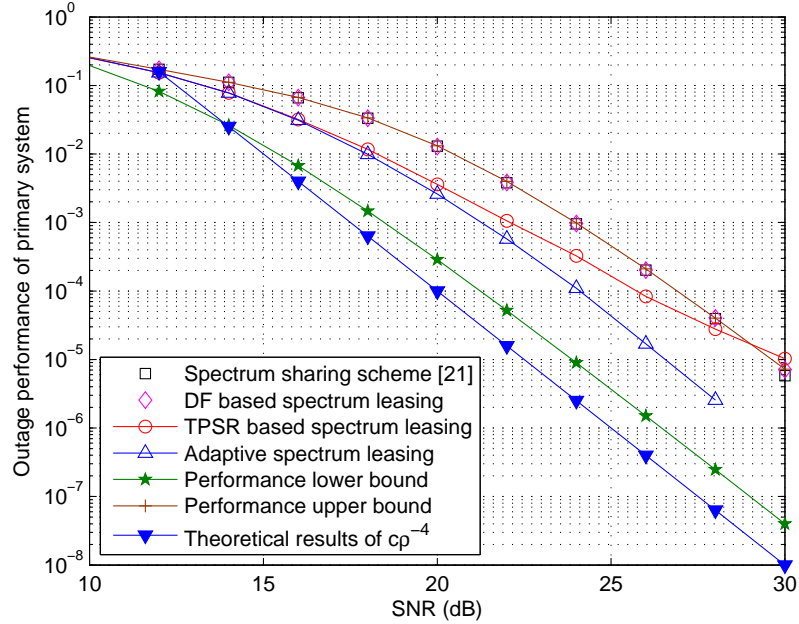


**Figure 3.4:** Outage probability of primary system with  $r_0 = 2$  and  $m = 3$ .

because the omitted term in the upper bound of (3.29) has negligible impacts to the integral over  $(0, c_0)$  in the derivation of (3.30).

Fig. 3.5 and Fig. 3.6 show the outage probability of secondary system with different primary target rates. The outage performance upper bound and lower bound are plotted according to (3.42) and (3.46), respectively. Other parameters are set as  $r_1 = 1.5$ ,  $d_{PT,ST} = d_{ST,PR} = 2.0$ , and  $d_{ST,ST} = d_{ST,SR} = 0.5$ . The selection diversity gain of secondary system is 3 when there are  $m = 3$  STs, as the simulation results are parallel with the theoretical results in the high regime of SNR. The outage performance improves with the decrease of primary rate from  $r_0 = 2$  to  $r_0 = 1.5$ . It is because when the primary rate turns smaller, it is easier for the STs to become potential relays, and as a result the opportunity of secondary transmission gets larger.

The proposed adaptive spectrum leasing scheme outperforms the DF based scheme and the TPSR based scheme. The TPSR based scheme outperforms the DF based scheme in the low to moderate SNR region, and the situation is reversed in the high SNR region. When the SNR is low, the SIC can be well performed in the TPSR as

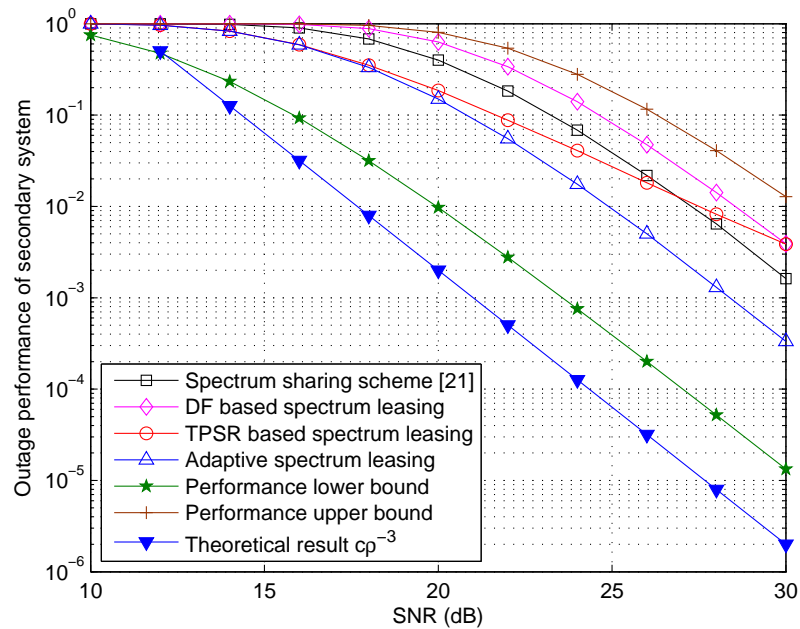


Figure 3.5: Outage probability of secondary system with  $r_0 = 2$ ,  $m = 3$ .

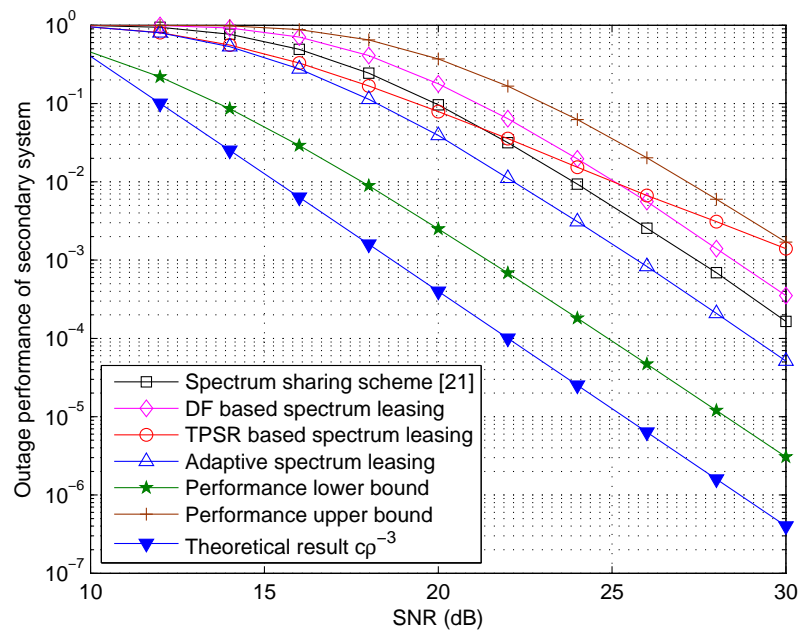
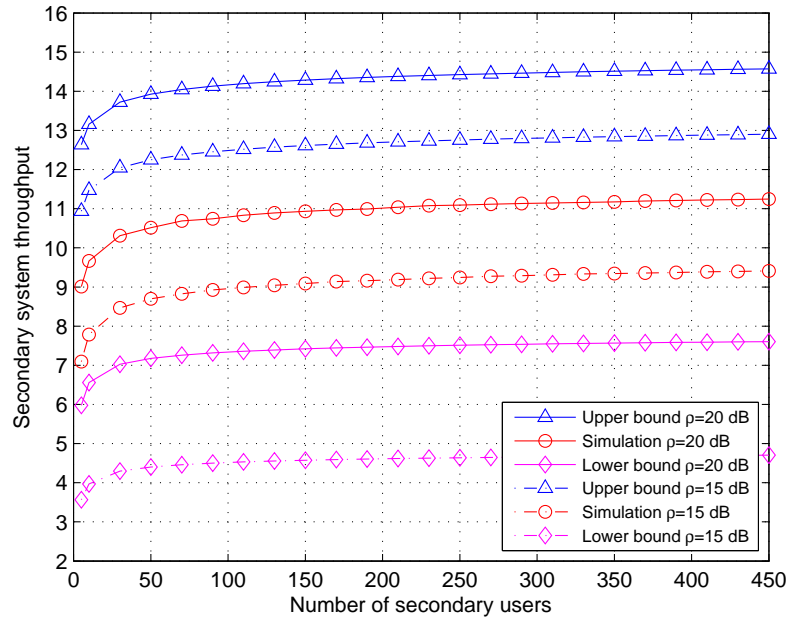


Figure 3.6: Outage probability of secondary system with  $r_0 = 1.5$ ,  $m = 3$ .



**Figure 3.7:** Throughput scaling of secondary system with  $r_0 = 1.5$  bps,  $d_{PT,ST} = d_{ST,PR} = 1.0$ , and  $d_{ST,ST} = d_{ST,SR} = 0.5$ .

the links between PT and STs are relatively weak and the TPSR scheme has a higher spectrum efficiency. However, when the SNR is large, the SIC can not work well and the DF protocol outperforms the TPSR scheme. Therefore, the proposed adaptive spectrum leasing scheme inclines to use TPSR when the power is not very strong, otherwise the DF protocol is preferred. Compared with the spatial domain spectrum sharing protocol [21], the adaptive spectrum leasing protocol in time domain has a much better performance as there is no interference between the primary data relaying and secondary data transmission.

### 3.6.2 Secondary Throughput

Fig. 3.7 shows the throughput of secondary system with respect to the increase of user number. Both the rate lower bound  $a_m^u$  (3.55) and rate upper bound  $a_m^l$  (3.60) are plotted in this figure. With the increase of SNR  $\rho$ , the performance gets better, as it becomes easier for the SUs to correctly decode the primary signal and take part

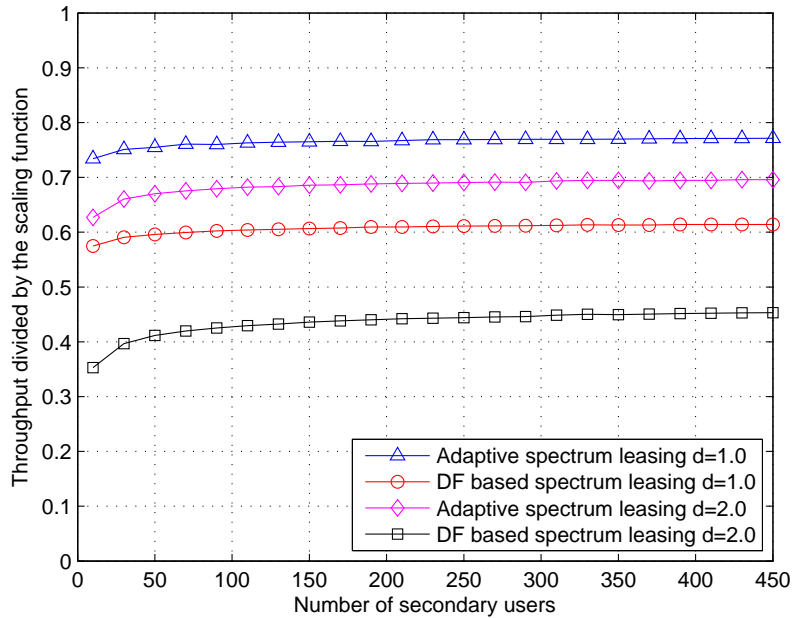


**Figure 3.8:** Throughput of secondary system divided by  $\log_2(\bar{\gamma}_{\text{ST,SR}} \ln m)$ , with  $\rho = 20$  dB,  $r_0 = 1.5$ , and  $d = d_{\text{PT,ST}} = d_{\text{ST,PR}}$ .

in the spectrum leasing. Furthermore, the channel quality between ST and SR is also better due to the increase of SNR.

Fig. 3.8 shows the throughput of secondary system divided by the scaling factor  $\log_2(\bar{\gamma}_{\text{ST,SR}} \ln m)$  with regard to the number of SUs. The performance becomes almost a horizontal line in the high regime of  $m$ . It confirms that the throughput grows linearly with  $\log_2(\bar{\gamma}_{\text{ST,SR}} \ln m)$  when the SU number  $m$  is large. The performance gets worse with the increase of distance between PUs and STs. The longer the distance, the worse the channel quality and hence the worse the performance. Again, the adaptive spectrum leasing scheme performs much better than the DF based scheme.

### 3.7 Summary

In this chapter, an adaptive spectrum leasing scheme is proposed by switching between TPSR and DF cooperation modes. The ST that can bring the largest achievable

rate while satisfying the rate requirement of primary system is scheduled for the spectrum access using the optimal cooperation mode. The cooperative diversity of primary system and selection diversity of secondary system are studied when both the primary and secondary rates are fixed. The multiuser diversity is investigated in terms of throughput for the secondary system when the primary rate is fixed. The analytical results show that, for the spectrum leasing with SU scheduling, the diversity gain is the same as that achieved in the stand-alone cooperative network without interference constraints.

### 3.8 Appendix I: Proof of the Rate Upper Bound

The equivalent channel  $\tilde{\mathbf{H}}_{ij}$  is divided into blocks, for each block there are 2 transmit antennas and 3 receive antennas, and there are no interference between blocks, i.e., the communications of different blocks are independent [48, 49]. The block included in  $\tilde{\mathbf{H}}_{ij}$  is denoted as  $\tilde{\mathbf{H}}_{bij}$ ,

$$\tilde{\mathbf{H}}_{bij} = \begin{bmatrix} a & 0 \\ b & a \\ 0 & c \end{bmatrix}, \quad (3.63)$$

where  $a = \frac{c_p}{\sqrt{N_0}}$ ,  $b = \frac{c_i}{\sqrt{N_0}}$ , and  $c = \frac{c_j}{\sqrt{N_0}}$ . As there are  $\frac{\beta_{ij}^t N-1}{2}$  same blocks in  $\tilde{\mathbf{H}}_{ij}$ , we can get

$$\begin{aligned} R_{p_{ij}}^{\text{t5}} &= \frac{1}{N} \log_2 [\det(\mathbf{I} + \tilde{\mathbf{H}}_{ij} \tilde{\mathbf{H}}_{ij}^{\mathcal{H}})] \\ &\stackrel{(\mathcal{I}_1)}{\leq} \frac{1}{N} \log_2 \left\{ \left[ \det(\mathbf{I} + \tilde{\mathbf{H}}_{bij} \tilde{\mathbf{H}}_{bij}^{\mathcal{H}}) \right]^{\frac{\beta_{ij}^t N-1}{2}} \right\} \\ &< \frac{\beta_{ij}^t}{2} \log_2 \left\{ \left[ \det(\mathbf{I} + \tilde{\mathbf{H}}_{bij} \tilde{\mathbf{H}}_{bij}^{\mathcal{H}}) \right] \right\}. \end{aligned} \quad (3.64)$$

Next, we will focus on proving the inequality  $(\mathcal{I}_1)$  of (3.64). Matrix  $\tilde{\mathbf{H}}_{ij}$  is of size  $L \times (L-1)$  with  $L = \beta_{ij}^t N$  being an odd number. For notation brevity, we set  $\mathbf{G} = \tilde{\mathbf{H}}_{ij}$  and  $\mathbf{Z} = \tilde{\mathbf{H}}_{bij}$ .

**Definition 1:** Let  $B_{(L-1)} = \det [\mathbf{M}_{(L)}]$  with  $\mathbf{M}_{(L)} = \mathbf{I}_L + \mathbf{G}\mathbf{G}^H$  being the tridiagonal matrix,

$$\mathbf{M}_{(L)} = \begin{bmatrix} 1 + |a|^2 & ab^* & \cdots & 0 \\ a^*b & 1 + |a|^2 + |b|^2 & \ddots & \vdots \\ \vdots & \ddots & \ddots & ac^* \\ 0 & \cdots & a^*c & 1 + |c|^2 \end{bmatrix}. \quad (3.65)$$

**Definition 2:** Generate  $\hat{\mathbf{G}}$  by splitting the last two columns of  $\mathbf{G}$  into one block  $\mathbf{Z}_{3 \times 2}$  as (3.63),

$$\hat{\mathbf{G}} = \left[ \begin{array}{c|c} \mathbf{G}_{(L-2) \times (L-3)} & \mathbf{0}_{(L-2) \times 2} \\ \hline \mathbf{0}_{3 \times (L-3)} & \mathbf{Z}_{3 \times 2} \end{array} \right]. \quad (3.66)$$

Let  $\hat{B}_{(L-1)} = \det [\hat{\mathbf{M}}_{(L+1)}]$  with  $\hat{\mathbf{M}}_{(L+1)} = \mathbf{I}_{L+1} + \hat{\mathbf{G}}\hat{\mathbf{G}}^H$  being the block diagonal matrix,

$$\hat{\mathbf{M}}_{(L+1)} = \left[ \begin{array}{c|c} \mathbf{M}_{(L-2)} & \mathbf{0}_{(L-2) \times 3} \\ \hline \mathbf{0}_{3 \times (L-2)} & \mathbf{I}_3 + \mathbf{Z}\mathbf{Z}^H \end{array} \right]. \quad (3.67)$$

**Definition 3:** Generate a new matrix  $\bar{\mathbf{M}}_{(L)}$  by changing the last element of  $\mathbf{M}_{(L)}$  as  $1 + |a|^2 + |c|^2$ , then let  $D_{(L-1)} = \det [\bar{\mathbf{M}}_{(L)}]$ .

Without loss of generality, we use  $a^2$ ,  $b^2$ , and  $c^2$  to represent  $|a|^2$ ,  $|b|^2$ , and  $|c|^2$ , respectively. Through (3.67), we can obtain

$$\hat{B}_{(L-1)} = B_{(L-3)} \det (\mathbf{I}_3 + \mathbf{Z}\mathbf{Z}^H) = B_{(L-3)} (1 + 2a^2 + b^2 + c^2 + a^4 + a^2c^2 + b^2c^2). \quad (3.68)$$

According to  $\mathbf{M}_{(L)}$  given by (3.65) and  $\bar{\mathbf{M}}_{(L)}$ ,  $B_{(L-1)}$  and  $D_{(L-1)}$  can be calculated as

$$\begin{cases} B_{(L-1)} = (1 + c^2)D_{(L-2)} + \Delta, \\ D_{(L-1)} = (1 + a^2 + c^2)D_{(L-2)} + \Delta, \end{cases} \quad (3.69)$$

where  $\Delta$  is a common value of  $B_{(L-1)}$  and  $D_{(L-1)}$ . Expression (3.69) tells us that

$$D_{(L-1)} = a^2D_{(L-2)} + B_{(L-1)}. \quad (3.70)$$

With reference to *Lemma 4* of [59], we can obtain

$$\begin{cases} D_{(L-1)} = (1 + a^2 + c^2)D_{(L-2)} - a^2c^2D_{(L-3)} \\ D_{(L-2)} = (1 + a^2 + b^2)D_{(L-3)} - a^2b^2D_{(L-4)} \\ D_{(L-3)} = (1 + a^2 + c^2)D_{(L-4)} - a^2c^2D_{(L-5)} \\ D_{(L-4)} = (1 + a^2 + b^2)D_{(L-5)} - a^2b^2D_{(L-6)}. \end{cases} \quad (3.71)$$

Jointly considering (3.70) and (3.71), we can get

$$\begin{aligned} B_{(L-1)} &= (1 + c^2)D_{(L-2)} - a^2c^2D_{(L-3)} \\ &= \left(1 + 2a^2 + b^2 + c^2 + b^2c^2 + \frac{a^4}{1 + c^2}\right)(1 + c^2)D_{(L-4)} \\ &\quad - (1 + a^2 + b^2 + c^2 + b^2c^2)a^2c^2D_{(L-5)}. \end{aligned} \quad (3.72)$$

Since we have  $B_{(L-3)} = (1 + c^2)D_{(L-4)} - a^2c^2D_{(L-5)}$ , substitute it into (3.68), we can obtain

$$\hat{B}_{(L-1)} = [(1 + c^2)D_{(L-4)} - a^2c^2D_{(L-5)}] (1 + 2a^2 + b^2 + c^2 + a^4 + a^2c^2 + b^2c^2). \quad (3.73)$$

Next, we compare  $\hat{B}_{(L-1)}$  of (3.73) and  $B_{(L-1)}$  of (3.72) as

$$\hat{B}_{(L-1)} - B_{(L-1)} = a^2c^2 [D_{(L-3)} - a^2(1 + a^2)D_{(L-5)}]. \quad (3.74)$$

Furthermore, according to (3.71), after some mathematical operation, we have

$$D_{(L-3)} - a^2(1 + a^2)D_{(L-5)} = a^2b^2 (D_{(L-5)} - a^2D_{(L-6)}) + B_{(L-3)}, \quad (3.75)$$

where  $B_{(L-3)} \geq 0$  is always satisfied according to (3.68), because the system rate is always no smaller than 0. Recall the iteration in (3.71), we can derive  $D_{(L-5)} - a^2D_{(L-6)} > 0$  in (3.75). As a result, we can get  $\hat{B}_{(L-1)} \geq B_{(L-1)}$  in (3.74), which means

$$\begin{aligned} B_{(L-1)} &\leq B_{(L-3)} \det(\mathbf{I}_3 + \mathbf{Z}\mathbf{Z}^H) \leq B_{(L-5)} [\det(\mathbf{I}_3 + \mathbf{Z}\mathbf{Z}^H)]^2 \leq \dots \\ &\dots \leq B_{(2)} [\det(\mathbf{I}_3 + \mathbf{Z}\mathbf{Z}^H)]^{\frac{L-3}{2}} \leq [\det(\mathbf{I}_3 + \mathbf{Z}\mathbf{Z}^H)]^{\frac{L-1}{2}}. \end{aligned} \quad (3.76)$$

So far, the inequality  $\mathcal{I}_1$  of (3.64) has been proved. Compute  $\det(\mathbf{I} + \mathbf{H}_{bij}\mathbf{H}_{bij}^H)$  and substitute it into (3.64), the rate upper bound  $\hat{R}_{pij}^{\text{ts}}$  is thus obtained as (3.18).

### 3.9 Appendix II: Proof of the Condition

Eq. (3.49) of Lemma 1 with  $F_V(x)$  and  $f_V(x)$  substituted can be expressed as

$$\lim_{x \rightarrow \infty} \frac{d}{dx} \left[ \frac{1 - F_V(x)}{f_V(x)} \right] = \lim_{x \rightarrow \infty} \left\{ -1 - \frac{[1 - F_V(x)] f'_V(x)}{f_V^2(x)} \right\}, \quad (3.77)$$

where the PDF  $f_V(x)$  is derived as follows according to  $F_V(x)$  given by (3.53).

$$f_V(x) = \frac{\ln 2}{\bar{\gamma}_{\text{ST,SR}}} \exp\left(\frac{1}{\bar{\gamma}_{\text{ST,SR}}}\right) \int_0^1 \frac{2^{\frac{x}{1-\beta}}}{1-\beta} \exp\left(-\frac{2^{\frac{x}{1-\beta}}}{\bar{\gamma}_{\text{ST,SR}}}\right) f_B(\beta) d\beta. \quad (3.78)$$

Then, the derivative of  $f_V(x)$  with respect to  $x$  is derived as

$$\begin{aligned} f'_V(x) &= \frac{(\ln 2)^2}{\bar{\gamma}_{\text{ST,SR}}} \exp\left(\frac{1}{\bar{\gamma}_{\text{ST,SR}}}\right) \int_0^1 \frac{2^{\frac{x}{1-\beta}}}{(1-\beta)^2} \exp\left(-\frac{2^{\frac{x}{1-\beta}}}{\bar{\gamma}_{\text{ST,SR}}}\right) f_B(\beta) d\beta \\ &\quad - \left(\frac{\ln 2}{\bar{\gamma}_{\text{ST,SR}}}\right)^2 \exp\left(\frac{1}{\bar{\gamma}_{\text{ST,SR}}}\right) \int_0^1 \frac{2^{\frac{2x}{1-\beta}}}{(1-\beta)^2} \exp\left(-\frac{2^{\frac{x}{1-\beta}}}{\bar{\gamma}_{\text{ST,SR}}}\right) f_B(\beta) d\beta. \end{aligned} \quad (3.79)$$

By substituting the expressions of  $F_V(x)$ ,  $f_V(x)$ , and  $f'_V(x)$  into (3.77), we have

$$\begin{aligned} &\lim_{x \rightarrow \infty} \frac{[1 - F_V(x)] f'_V(x)}{f_V^2(x)} \\ &\stackrel{(\mathcal{I}_2)}{=} \lim_{x \rightarrow \infty} \frac{\bar{\gamma}_{\text{ST,SR}} \int_0^1 \exp\left(-\frac{2^{\frac{x}{1-\beta}}}{\bar{\gamma}_{\text{ST,SR}}}\right) f_B(\beta) d\beta \int_0^1 \frac{2^{\frac{x}{1-\beta}}}{(1-\beta)^2} \exp\left(-\frac{2^{\frac{x}{1-\beta}}}{\bar{\gamma}_{\text{ST,SR}}}\right) f_B(\beta) d\beta}{\left[\int_0^1 \frac{2^{\frac{x}{1-\beta}}}{1-\beta} \exp\left(-\frac{2^{\frac{x}{1-\beta}}}{\bar{\gamma}_{\text{ST,SR}}}\right) f_B(\beta) d\beta\right]^2} \\ &\stackrel{(\mathcal{I}_3)}{=} \lim_{x \rightarrow \infty} \frac{\int_0^1 \exp\left(-\frac{2^{\frac{x}{1-\beta}}}{\bar{\gamma}_{\text{ST,SR}}}\right) f_B(\beta) d\beta \int_0^1 \frac{2^{\frac{2x}{1-\beta}}}{(1-\beta)^2} \exp\left(-\frac{2^{\frac{x}{1-\beta}}}{\bar{\gamma}_{\text{ST,SR}}}\right) f_B(\beta) d\beta}{\left[\int_0^1 \frac{2^{\frac{x}{1-\beta}}}{1-\beta} \exp\left(-\frac{2^{\frac{x}{1-\beta}}}{\bar{\gamma}_{\text{ST,SR}}}\right) f_B(\beta) d\beta\right]^2}. \end{aligned} \quad (3.80)$$

To get the limit value of  $(\mathcal{I}_2)$  in (3.80) with respect to  $x \rightarrow \infty$ , we have

$$\mathcal{I}_2 = \bar{\gamma}_{\text{ST,SR}} \lim_{\Delta\beta \rightarrow 0} \lim_{x \rightarrow \infty} \frac{\sum_{i=0}^n \mathcal{B}_i \sum_{j=0}^n \mathcal{D}_j}{\sum_{i=0}^n \mathcal{E}_i \sum_{j=0}^n \mathcal{E}_j}. \quad (3.81)$$

This equation is obtained by dividing the interval  $(0, 1)$  of  $\beta$  into a series of small intervals with equal length  $\Delta\beta$ , i.e.,  $\{(0, \beta_1], (\beta_1, \beta_2], \dots, (\beta_i, \beta_{i+1}], \dots, (\beta_{n-1}, \beta_n], (\beta_n, 1)\}$ .

The total number of small intervals is denoted as  $n$ . The related terms in (3.81) are

given as

$$\begin{aligned}\mathcal{B}_i &= \exp\left(-\frac{2^{\frac{x}{1-\beta_i}}}{\bar{\gamma}_{\text{ST,SR}}}\right) f_B(\beta_i) \Delta\beta, \\ \mathcal{D}_j &= \frac{2^{\frac{x}{1-\beta_j}}}{(1-\beta_j)^2} \exp\left(-\frac{2^{\frac{x}{1-\beta_j}}}{\bar{\gamma}_{\text{ST,SR}}}\right) f_B(\beta_j) \Delta\beta, \\ \mathcal{E}_i &= \frac{2^{\frac{x}{1-\beta_i}}}{1-\beta_i} \exp\left(-\frac{2^{\frac{x}{1-\beta_i}}}{\bar{\gamma}_{\text{ST,SR}}}\right) f_B(\beta_i) \Delta\beta.\end{aligned}\quad (3.82)$$

Then, we consider one particular term in the numerator and denominator of (3.81) with the same index. For a given  $\Delta\beta$ , we have the following expression,

$$\lim_{x \rightarrow \infty} \frac{\mathcal{B}_i \mathcal{D}_j}{\mathcal{E}_i \mathcal{E}_j} = \lim_{x \rightarrow \infty} \frac{1-\beta_i}{1-\beta_j} \frac{1}{2^{\frac{x}{1-\beta_i}}} = 0. \quad (3.83)$$

Therefore, considering all terms in the numerator and denominator of (3.81), we can get  $\mathcal{I}_2 = 0$ . Similarly with the analysis of  $\mathcal{I}_2$ , we have the following expression for  $\mathcal{I}_3$  in (3.80).

$$\mathcal{I}_3 = \lim_{\Delta\beta \rightarrow 0} \lim_{x \rightarrow 0} \frac{\sum_{i=0}^n \sum_{j=0}^k a_{ij}}{\sum_{i=0}^n \sum_{j=0}^k b_{ij}}, \quad (3.84)$$

where

$$\begin{aligned}a_{ij} &= \exp\left(-\frac{2^{\frac{x}{1-\beta_i}}}{\bar{\gamma}_{\text{ST,SR}}}\right) f_B(\beta_i) \Delta\beta \frac{2^{\frac{2x}{1-\beta_j}}}{(1-\beta_j)^2} \exp\left(-\frac{2^{\frac{x}{1-\beta_j}}}{\bar{\gamma}_{\text{ST,SR}}}\right) f_B(\beta_j) \Delta\beta, \\ b_{ij} &= \frac{2^{\frac{x}{1-\beta_i}}}{1-\beta_i} \exp\left(-\frac{2^{\frac{x}{1-\beta_i}}}{\bar{\gamma}_{\text{ST,SR}}}\right) f_B(\beta_i) \Delta\beta \frac{2^{\frac{x}{1-\beta_j}}}{1-\beta_j} \exp\left(-\frac{2^{\frac{x}{1-\beta_j}}}{\bar{\gamma}_{\text{ST,SR}}}\right) f_B(\beta_j) \Delta\beta.\end{aligned}\quad (3.85)$$

Then, we have the following observation,

$$a_{ij} = \frac{1-\beta_i}{1-\beta_j} \frac{2^{\frac{x}{1-\beta_j}}}{2^{\frac{x}{1-\beta_i}}} b_{ij}, \quad a_{ji} = \frac{1-\beta_j}{1-\beta_i} \frac{2^{\frac{x}{1-\beta_i}}}{2^{\frac{x}{1-\beta_j}}} b_{ij}. \quad (3.86)$$

Note that,  $b_{ij} = b_{ji}$  is considered in (3.86). Then, we study the difference between  $(a_{ij} + a_{ji})$  in the numerator of (3.84) and the corresponding  $(b_{ij} + b_{ji} = 2b_{ij})$  in the denominator of (3.84), i.e.,

$$\begin{aligned}\lim_{x \rightarrow \infty} a_{ij} + a_{ji} - 2b_{ij} &= \exp\left(-\frac{2^{\frac{x}{1-\beta_i}}}{\bar{\gamma}_{\text{ST,SR}}}\right) f(\beta_i) \Delta\beta \exp\left(-\frac{2^{\frac{x}{1-\beta_j}}}{\bar{\gamma}_{\text{ST,SR}}}\right) f(\beta_j) \Delta\beta \\ &\times \left[ \frac{2^{\frac{2x}{1-\beta_j}}}{(1-\beta_j)^2} + \frac{2^{\frac{2x}{1-\beta_i}}}{(1-\beta_i)^2} - 2 \left( \frac{2^{\frac{x}{1-\beta_i}}}{1-\beta_i} \right) \left( \frac{2^{\frac{x}{1-\beta_j}}}{1-\beta_j} \right) \right].\end{aligned}\quad (3.87)$$

---

It can be derived that  $\lim_{x \rightarrow \infty} a_{ij} + a_{ji} - 2b_{ij} = 0$  and the limit value of (3.84) is  $\mathcal{I}_3 = 1$ . Therefore, Eq. (3.77) equals zero and Eq. (3.49) of *Lemma 1* is satisfied with  $F_V(x)$  and  $f_V(x)$  substituted.

## Chapter 4

# Uncoordinated Cooperation with Spatially Random Relays

### 4.1 Introduction

Cooperative automatic repeat request (ARQ) [60–64] is an attractive technique that can significantly improve the link throughput by forwarding the data using the best available relay when the original transmission between source and destination fails. Moreover, space diversity can be achieved by allowing relays to do the retransmission, because the probability of relay-destination and source-destination channels undergoing deep fading simultaneously is very small. However, for the explicit relay selection [65], global knowledge of all relay metrics is needed for the source to determine which relay is the best. The overhead of exchanging the metric values, resource allocation results, and source decisions, etc. is usually very heavy, that is contrary to the goal of improving the spectral efficiency. Furthermore, if the channel coherence time is short, it is suboptimal to choose the best relay based on the outdated channel information obtained in the previous time slot. In the opportunistic relaying scheme [34], every relay node should monitor the instantaneous channel state towards the source and the destination and determines whether it is the best or not via execut-

ing a back-off mechanism. However, the overhead of coordination or synchronization becomes prohibitively large when the network size is large and the frequent coordination may negate any potential performance gains. With a priori knowledge about the spatial distribution of the nodes, an optimal uncoordinated cooperation strategy is studied in [66] to maximize the probability of successful decoding. In [66], a relay is automatically selected to do the retransmission without any coordination, and the performance is shown to be comparable to or even better than the scheme with relays preselected. Ganti *et al.* proposed four heuristic decentralized uncoordinated relay selection methods to forward the source data to the destination in a two-hop TDMA wireless system [67]. However, the retransmission probability of each relay is directly defined without theoretical backing.

In this chapter, three uncoordinated cooperative truncated ARQ schemes are proposed based on the local information of relay position or channel SNR, i.e., the distance based scheme, the sectorized scheme, and the local SNR based scheme. If the original transmission between the source and the destination fails, each potential relay accesses the channel independently according to its own retransmission probability without any coordination with other nodes. With prior knowledge of the network parameters, such as node density and transmission power etc., the retransmission probability of each potential relay is judiciously computed in a distributed fashion. If none of the relays successfully access the channel, the source will perform the retransmission. Collision does not occur if the retransmission is performed by only one node, i.e., either one potential relay or the source. The destination node combines the original erroneously received signal from the source and the retransmitted signal from either the potential relay or the source using the MRC technique. System success probabilities are derived for the sectorized and local SNR based schemes, respectively. Numerical results show that the proposed local SNR based scheme has the best performance, while the distance based scheme outperforms the sectorized scheme. The uncoordinated cooperation schemes always outperform the traditional truncated ARQ scheme with the source performing the possible retransmissions.

The rest of this chapter is organized as follows. In Section 4.2, the system model and relay protocol are introduced. In Section 4.3, three uncoordinated cooperative truncated ARQ schemes are proposed and the retransmission probabilities are studied. Section 4.4 derives the system success probabilities of the sectorized and the local SNR based schemes. Numerical and simulation results are presented in Section 4.5. Finally, Section 4.6 concludes this chapter.

## 4.2 System Model and Relay Protocol

We consider the wireless communication between one source node (denoted by  $S$ ) and one destination node (denoted by  $D$ ), which is assisted by the intermediate relay nodes if necessary. Each relay node makes decision independently on whether to participate in the cooperative communication without any coordination with other nodes.

### 4.2.1 System Model

In our system model, the locations of source and destination are fixed, and the distance between them is a deterministic value  $R$ . The locations of relay nodes are modeled as a homogeneous Poisson point process (PPP)  $\Phi$  with intensity  $\lambda$ . The source and destination do not belong to the point process  $\Phi$ . For the data transmission between a certain transmitter located at  $x$  and a certain receiver located at  $y$ , the SNR of the received signal is written as

$$\gamma_{xy} = P_0 h_{xy} g_{xy} / N_0, \quad (4.1)$$

where  $P_0$  is the transmission power,  $N_0$  denotes the power of AWGN, and  $h_{xy}$  represents the small-scale channel fading which is exponentially distributed with unit mean. The path-loss coefficient is modeled as  $g_{xy} = \|x - y\|^{-\alpha}$ , where  $\|x - y\|$  is the Euclidean distance, and  $\alpha$  is the path-loss exponent. The data transmission is deemed successful when the instantaneous SNR is no less than a threshold  $T_0$ .

### 4.2.2 Relay Protocol

The source  $S$  sends a data packet to the destination  $D$ . Due to the broadcast nature of wireless channels, the intermediate nodes and the destination can all possibly receive the packet. Those intermediate nodes that correctly receive the data packet are referred to as *potential* relays and they are denoted by

$$\Phi_r = \{x | x \in \Phi, \gamma_{sx} \geq T_0\}, \quad (4.2)$$

where  $\gamma_{sx}$  is the instantaneous SNR of the channel between  $S$  and the relay node located at  $x$ .

When the data packet is correctly decoded by the destination, a positive acknowledgment (ACK) frame will be released. After receiving the ACK frame, all the potential relays in  $\Phi_r$  will flush their memory of the stored original data packet and the source will continue to transmit a new data packet. However, when the data packet is erroneously decoded by the destination, a negative acknowledgement (NACK) frame will be broadcast by the destination. On receiving the NACK frame, all the potential relays will try to retransmit the data packet to the destination. Whether a potential relay should retransmit the data packet or not is determined independently by the retransmission probability of itself. In this phase, the following three cases may be encountered.

- If more than one potential relays simultaneously access the channel for the data retransmission, collisions occur and the retransmission is considered to be unsuccessful.
- If none of the potential relays accesses the channel in the listening period of the source, i.e., the channel keeps idle for a duration of SIFS (shorter inter-frame space), the source will retransmit the data packet.
- If only one potential relay accesses the channel to retransmit the data packet, which is the preferred scenario, the source will keep silent after sensing that the channel is busy.

The destination combines the retransmitted signal and the original erroneously received signal using the MRC technique. If the instantaneous SNR of the combined signal is no less than the threshold  $T_0$ , the retransmission is considered to be successful. Otherwise, the retransmission is deemed unsuccessful. Therefore, the retransmission probability of each potential relay should be judiciously determined in a decentralized way to reduce the collisions and maximize the success probability. The retransmission probability will be investigated in the next section. The flow chart of the protocol is shown in Fig. 4.1.

In this chapter, the following assumptions are made. The maximum retransmission attempts are set to be one. That is, a packet will be discarded if it is still incorrectly received at the destination after one retransmission. This assumption is suitable for real-time traffic, which can tolerate a certain packet loss rate, but requires very small delay [62]. The channel between any two nodes undergoes independent Rayleigh block fading, which remains invariant for the duration of two successive data packets. Moreover, the destination has enough memory to combine the original erroneously received signal and the retransmitted signal using the MRC technique for the decoding. With low rate and powerful error control, the feedback control channel is deemed as error-free [63], so the control packets can reliably reach the neighboring nodes. As the collisions are dominated by the simultaneous retransmissions of the nearby relay nodes, the data retransmission is considered as failed when collisions occur.

### 4.3 Uncoordinated Cooperation Schemes

As mentioned before, on receiving the NACK frame, each potential relay independently decides whether it should occupy the channel or not according to its own retransmission probability. In this section, three different uncoordinated cooperative communication schemes are proposed.

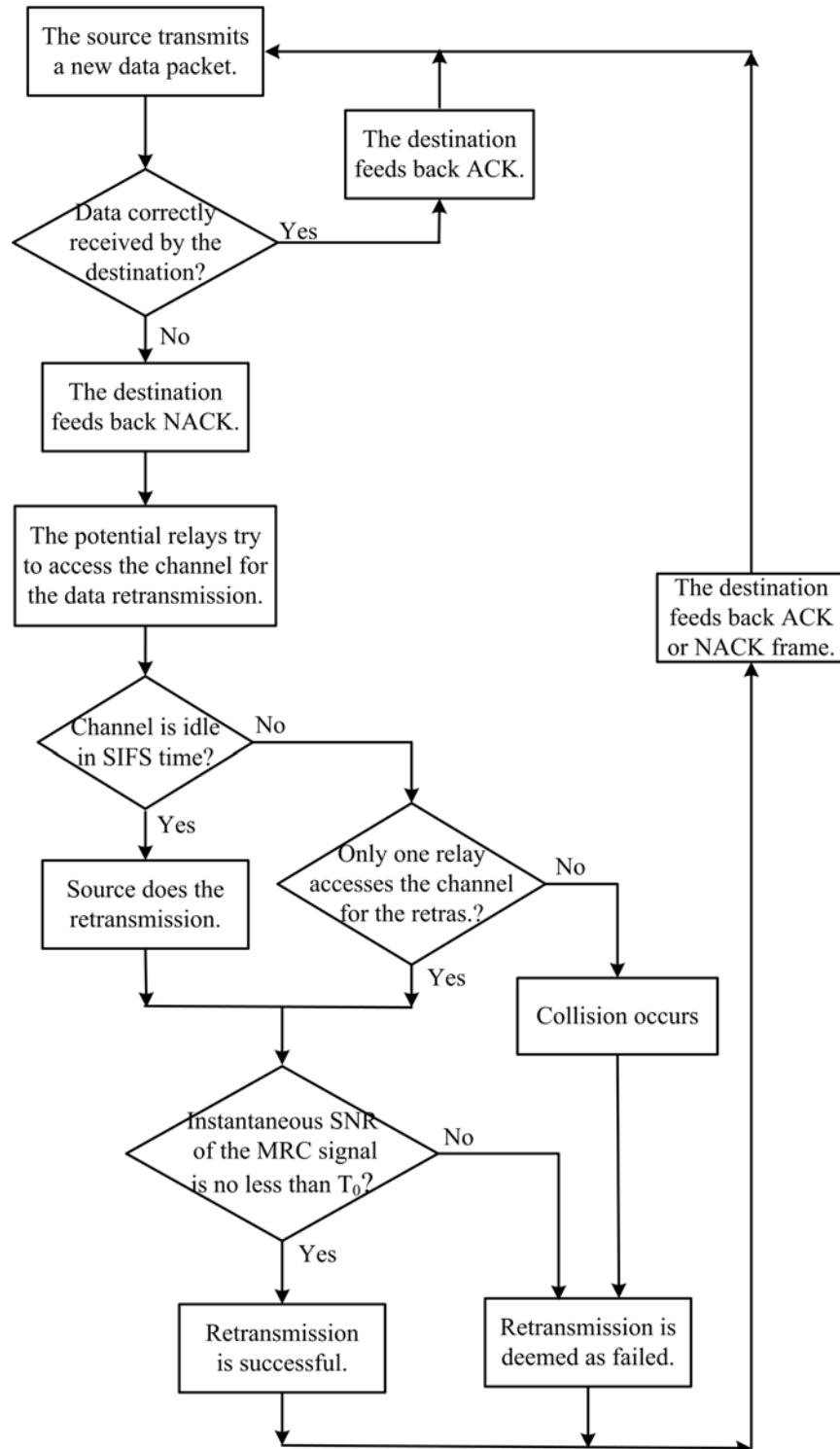


**Figure 4.1:** Flow chart of the uncoordinated cooperative truncated ARQ schemes.

### 4.3.1 Distance Based Scheme

In this scheme, we assume that each potential relay knows the distance between itself and the destination. The distance can be estimated by measuring the average strength of the received control signals from the destination, or it can be computed using the position information obtained via GPS or wireless localization techniques [68]. Positions of the destination can be included into the control packets, e.g. ACK and NACK, which can be reliably overheard by all the nearby relay nodes. In addition, each potential relay also knows the necessary parameters of the wireless network, such as the node density  $\lambda$  and the source-destination distance  $R$ .

A particular node, say node  $x \in \Phi_r$ <sup>1</sup>, will retransmit the packet with probability  $\tau_1(x)$  that no other potential relays lie in  $b(D, d_x)$ , which is a disk centered at  $D$  with radius  $d_x$ , i.e., the distance between  $x$  and the destination. Therefore,

$$\tau_1(x) = \Pr \{y \notin b(D, d_x), \forall y \in \Phi_r \setminus \{x\}\}. \quad (4.3)$$

The shorter the distance  $d_x$  is, the higher the retransmission probability is used. The main rationale behind this setting is as follows. When the potential relay  $x$  is closer to the destination, the channel quality between them is better. Moreover, fewer collisions would occur as there are less number of potential relays closer to the destination than  $x$ . Equivalently, (4.3) can be rewritten as,

$$\tau_1(x) = \Pr \{y \notin \Phi_r, \forall y \in b(D, d_x) \setminus \{x\}\}. \quad (4.4)$$

In fact, (4.3) is the probability that all potential relays except  $x$  are not in the disk  $b(D, d_x)$ , whereas (4.4) gives the probability that all relay nodes except  $x$  in the disk  $b(D, d_x)$  are not potential relays.

Suppose that a polar coordinate system with origin at  $D$  is used and that a certain relay node  $y \in b(D, d_x) \setminus \{x\}$  has the coordinate  $(r_m, \theta_n)$  as shown in Fig. 4.2. We divide the disk  $b(D, d_x)$  into many small arc regions  $\mathcal{A}_{m,n}$ , which are the intersections

---

<sup>1</sup>As each node is uniquely determined by its location, we use the location to denote the node without distinction.

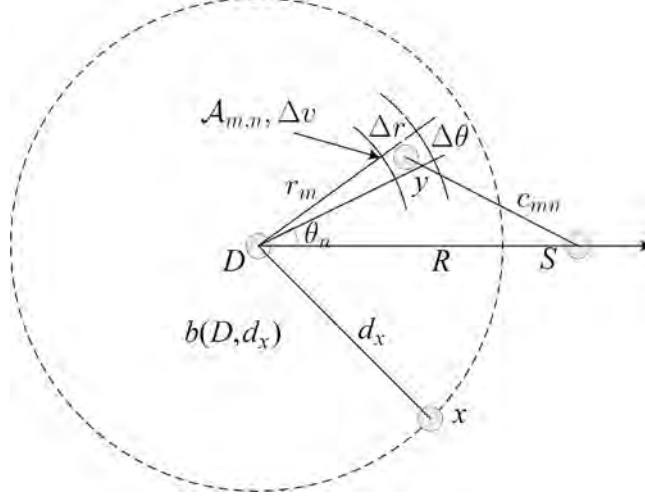


**Figure 4.2:** The coordinate system with destination located at the origin.

of rings with outer radius  $r_m$  ( $r_m \leq d_x$ ) and inner radius  $(r_m - \Delta r)$  and sectors with angle from  $\theta_n$  to  $(\theta_n + \Delta\theta)$ . Next, we calculate the probability  $\Pr\{y \in \Phi_r, y \in \mathcal{A}_{m,n}\} \forall m, n$  with  $0 < r_m \leq d_x$  and  $-\pi < \theta_n \leq \pi$ . It can be computed as  $\lambda P_{sy}(r_m, \theta_n) \Delta v + o(\Delta v)$ , where  $\Delta v$  denotes the area of the small arc region approximated as  $\Delta v \approx (r_m \Delta\theta) \Delta r$ . Conditioned on there being one node  $y$  in the small arc region  $\mathcal{A}_{m,n}$ ,  $P_{sy}(r_m, \theta_n)$  is the probability of node  $y$  correctly receiving the signal from  $S$  in the original transmission phase, given by

$$P_{sy}(r_m, \theta_n) = \Pr(\gamma_{sy} \geq T_0) = \exp(-T_0 N_0 c_{mn}^\alpha / P_0), \quad (4.5)$$

where  $\gamma_{sy}$  is the SNR between  $S$  and node  $y$ , and  $c_{mn} = \sqrt{R^2 + r_m^2 - 2Rr_m \cos|\theta_n|}$  is the distance between them.

As  $\Delta v \rightarrow 0$ , the retransmission probability  $\tau_1(x)$  in (4.4) is given by

$$\tau_1(x) = \lim_{\Delta v \rightarrow 0} \prod_{m,n} [1 - \Pr\{y \in \Phi_r, y \in \mathcal{A}_{m,n}\}] = \lim_{\Delta v \rightarrow 0} \prod_{m,n} [1 - \lambda P_{sy}(r_m, \theta_n) \Delta v]. \quad (4.6)$$

It can be further written as

$$\begin{aligned} \tau_1(x) &= \lim_{\Delta v \rightarrow 0} \exp \left[ \sum_{m,n} \ln(1 - \lambda P_{sy}(r_m, \theta_n) \Delta v) \right] \\ &= \lim_{\Delta r \rightarrow 0} \lim_{\Delta\theta \rightarrow 0} \exp \left[ \sum_{m,n} (-\lambda P_{sy}(r_m, \theta_n) r_m \Delta\theta \Delta r) \right], \end{aligned} \quad (4.7)$$

where in the second step,  $\lim_{z \rightarrow 0} \ln(1 - z) \sim -z$  is used. With  $\Delta r \rightarrow 0$  and  $\Delta\theta \rightarrow 0$ , we can obtain

$$\begin{aligned} \tau_1(x) &= \exp \left\{ -\lambda \int_0^{d_x} r \left[ \int_{-\pi}^{\pi} P_{sy}(r, \theta) d\theta \right] dr \right\} \\ &= \exp \left\{ -2\lambda \int_0^{d_x} r \int_0^{\pi} \exp \left[ -T_0 K_0 (R^2 + r^2 - 2Rr \cos \theta)^{\frac{\alpha}{2}} \right] d\theta dr \right\}, \end{aligned} \quad (4.8)$$

where  $K_0 = N_0/P_0$  is used throughout this chapter. For the general path-loss exponent, the integral in (4.8) can only be evaluated numerically and a closed-form expression is difficult to obtain. However, for the special case of  $\alpha = 2$ , the result is further derived as

$$\begin{aligned} \tau_1(x) &= \exp \left\{ -2\pi\lambda \exp(-T_0 K_0 R^2) \int_0^{d_x} r \exp(-T_0 K_0 r^2) I_0(2T_0 K_0 Rr) dr \right\} \\ &= \exp \left\{ -2\pi\lambda \exp(-T_0 K_0 R^2) \sum_{k=0}^{\infty} \frac{(T_0 K_0 R)^{2k}}{(k!)^2} \frac{\gamma(k+1, T_0 K_0 d_x^2)}{2(T_0 K_0)^{k+1}} \right\}, \end{aligned} \quad (4.9)$$

where  $I_0(z)$  is the zero-order modified Bessel function and  $\gamma(\mu, \omega)$  is the incomplete Gamma function [71]. Since we have  $I_0(z) = \sum_{k=0}^{\infty} \frac{1}{(k!)^2} \left(\frac{z}{2}\right)^{2k}$ , and  $\gamma(\mu, \omega) = (\mu - 1)! \left[1 - \exp(-\omega) \sum_{m=0}^{\mu-1} \frac{\omega^m}{m!}\right]$ , the final result can be numerically computed more efficiently using series summation instead of the integration.

Fig. 4.3 shows the retransmission probabilities of the distance based scheme with respect to the distance  $d_x$  between the potential relay  $x$  and the destination  $D$  for the given parameters  $\alpha = 2$ ,  $T_0 = 5$  and  $K_0 = 10^{-4}$ . It can be seen that the retransmission probability is a monotonically decreasing function of distance  $d_x$ . It means that the potential relays that are closer to the destination have higher retransmission probabilities. Moreover, for a given distance between the source and the destination ( $R = 50\text{m}$  or  $R = 70\text{m}$ ), the retransmission probability is larger for the smaller intensity  $\lambda$ . For a given node intensity ( $\lambda = 0.02/\text{m}^2$  or  $\lambda = 0.002/\text{m}^2$ ), the retransmission probability is larger for the longer distance  $R$ . This is because, when  $\lambda$  is smaller or  $R$  is larger, there are a smaller number of potential relays residing in the disk  $b(D, d_x)$  hereby reducing the collisions. When the distance between a potential relay node and

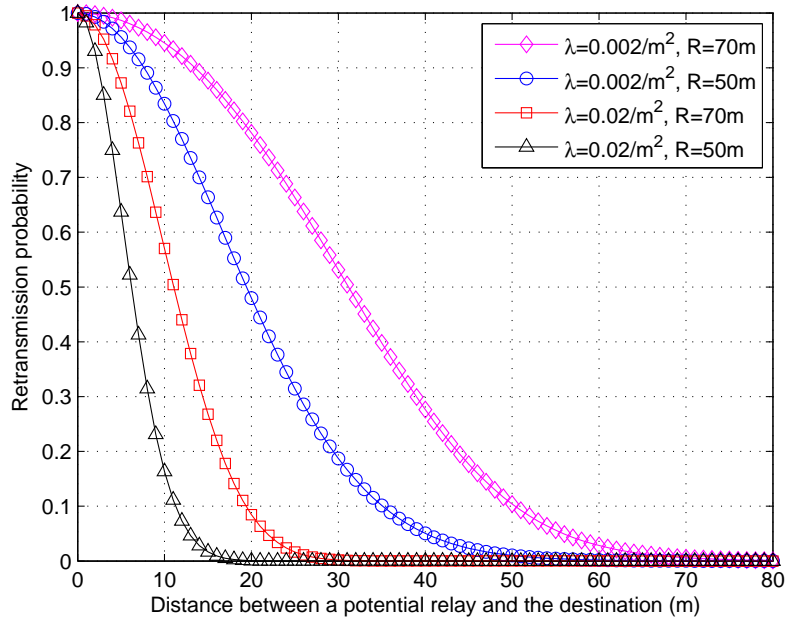


**Figure 4.3:** Retransmission probability of the distance based scheme.

the destination is comparable to the distance  $R$  between source and destination, the retransmission probability is almost zero.

### 4.3.2 Sectorized Scheme

For an efficient multi-hop routing algorithm, the information of source should be transmitted in the right direction to arrive at the destination, i.e., the next-hop neighbor should be closer to the destination [69]. So, the node of the next hop should lie in the angle interval  $(-\pi/2, \pi/2)$  symmetric with the source-destination axis. It was shown that by considering this angle information, the uncoordinated cooperative scheme proposed in [67] can achieve a good performance for the two-hop system. For the single-hop communication between  $S$  and  $D$  with the cooperation of random relays, the sectorized scheme is proposed to reduce collisions. Because the potential relays in the direction of destination are allocated higher retransmission probabilities than those in the opposite direction.

Assume that each potential relay  $x \in \Phi_r$  knows the system parameters  $(\lambda, P_0, R,$

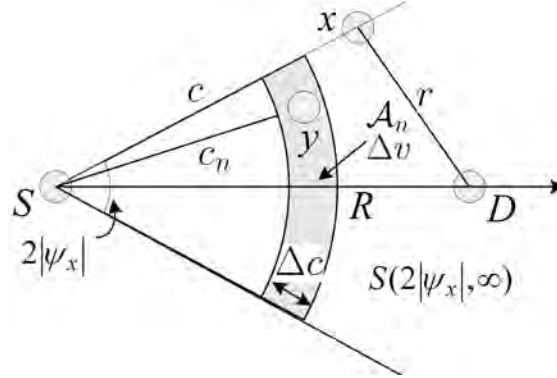


**Figure 4.4:** The coordinate system with source located at the origin.

etc.) and the angle  $\psi_x = \angle xSD$ , which can be obtained via estimating the direction of arrival (DOA) of the wanted signals [70] or computed using the positions of the source, the destination and itself. The potential relay  $x$  does the retransmission with the probability  $\tau_2(x)$  that no other potential relays reside in  $\mathcal{S}(2|\psi_x|, c)$ , which is a sector with angle spread of  $2|\psi_x|$  and edge  $c = \infty$ . Please see Fig. 4.4 for an illustration of the sector area. Therefore,

$$\tau_2(x) = \Pr \{y \notin \mathcal{S}(2|\psi_x|, \infty), \forall y \in \Phi_r \setminus \{x\}\}. \quad (4.10)$$

The smaller the angle  $|\psi_x|$  is, the higher the retransmission probability is used. This is because there are less number of potential relays in the sector area with smaller angle and as a result less collisions would be encountered. Equivalently, (4.10) can be rewritten as,

$$\tau_2(x) = \Pr \{y \notin \Phi_r, \forall y \in \mathcal{S}(2|\psi_x|, \infty) \setminus \{x\}\}. \quad (4.11)$$

In fact, (4.10) is the probability that all potential relays except  $x$  are not in the infinite sector  $\mathcal{S}(2|\psi_x|, \infty)$ , while (4.11) is the probability that all relay nodes except  $x$  in the sector  $\mathcal{S}(2|\psi_x|, \infty)$  are not potential relays.

Suppose that a polar coordinate system with origin at  $S$  is used and that a certain node  $y \in \mathcal{S}(2|\psi_x|, \infty) \setminus \{x\}$  has a distance  $c_n$  from the source as shown in Fig. 4.4. We divide the sector  $\mathcal{S}(2|\psi_x|, \infty)$  into many small strips  $\mathcal{A}_n$  with inner radius  $c_n$  and outer radius  $(c_n + \Delta c)$ . Hence, it suffices to calculate  $\Pr \{y \in \Phi_r, y \in \mathcal{A}_n\}$ ,  $\forall y$  with

$0 < c_n < \infty$ . It can be computed as  $\lambda P_{sy}(c_n)\Delta v + o(\Delta v)$ , where  $\Delta v$  denotes the area of the strip approximated as  $\Delta v \approx 2|\psi_x|c_n\Delta c$ , and  $P_{sy}(c_n)$  is the probability that node  $y$  in the strip  $\mathcal{A}_n$  correctly receives the signal of  $S$  in the original transmission phase.

As  $\Delta v \rightarrow 0$ , the retransmission probability  $\tau_2(x)$  in (4.11) is given by

$$\begin{aligned}\tau_2(x) &= \lim_{\Delta v \rightarrow 0} \prod_n [1 - \Pr \{y \in \Phi_r, y \in \mathcal{A}_n\}] \\ &= \lim_{\Delta v \rightarrow 0} \prod_n [1 - \lambda P_{sy}(c_n)\Delta v], \quad 0 < c_n < \infty.\end{aligned}\quad (4.12)$$

Similar to the derivation of (4.7), we can obtain

$$\begin{aligned}\tau_2(x) &= \lim_{\Delta c \rightarrow 0} \exp \left[ \sum_n (-\lambda P_{sy}(c_n)2|\psi_x|c_n\Delta c) \right] \\ &= \exp \left[ -2|\psi_x|\lambda \int_0^\infty c \exp(-T_0 K_0 c^\alpha) dc \right] \\ &= \exp \left[ -\frac{2|\psi_x|\lambda \Gamma(2/\alpha)}{\alpha(T_0 K_0)^{2/\alpha}} \right],\end{aligned}\quad (4.13)$$

where  $\Gamma(z) = \int_0^\infty \exp(-t)t^{z-1} dt$  is the Gamma function [71]. It can be seen from (4.13) that, the retransmission probability is an exponentially decreasing function of the absolute angle  $|\psi_x|$  and the node density  $\lambda$ . When  $|\psi_x|$  or  $\lambda$  becomes larger, there are more potential relays in the infinite sector area  $\mathcal{S}(2|\psi_x|, \infty)$  and thereby the retransmission probability gets smaller to reduce the possible collisions. In addition,  $\tau_2(x)$  is a monotonously increasing function of the product of  $T_0$  and  $K_0$ .

### 4.3.3 Local SNR Based Scheme

In this scheme, we assume that each potential relay only knows the instantaneous SNR of the channel between itself and the destination. It is assumed that pilot signals are transmitted with a constant power over the same frequency band as the data packet. Due to the reciprocity of wireless channels, the SNR information can be obtained by measuring the strength of the pilot signals transmitted by the destination [34].

Different from the aforementioned location-aware schemes where nodes lying in  $\Phi_r$  can all possibly participate in the retransmission, for this scheme only those nodes lying in the retransmission candidate set  $\Phi_N = \{x|x \in \Phi_r, \gamma_{xd} \geq T_0\}$  have the opportunity to assist the retransmission, where  $\gamma_{xd}$  is the instantaneous SNR between the potential relay  $x$  and the destination  $D$ . Thus, the potential relays in this scheme refer to those nodes belonging to  $\Phi_N$ , which is a subset of  $\Phi_r$ , i.e.,  $\Phi_N \subseteq \Phi_r$ .

In the retransmission phase, a potential relay  $x \in \Phi_N$  retransmits with probability  $\tau_3(x)$  that no other nodes in  $\Phi_N$  have an SNR larger than  $\gamma_{xd}$ , i.e., the potential relay  $x \in \Phi_N$  has the largest instantaneous SNR among all the potential relays. It follows that

$$\tau_3(x) = \Pr \{ \gamma_{xd} \geq \gamma_{yd}, \forall y \in \Phi_N \setminus \{x\} \}, \quad (4.14)$$

where  $\gamma_{yd}$  is the instantaneous SNR between potential relay  $y$  and  $D$ . The higher the instantaneous SNR is, the higher the retransmission probability is set for the potential relay  $x$ .

Next, in order to calculate  $\tau_3(x)$  we need to calculate  $\Pr \{ \gamma_{yd} > \gamma_{xd}, \forall y \in \Phi_N \setminus \{x\} \}$ . Suppose that the same coordinate system is used as the one in the distance based scheme (see Fig. 4.2), where the infinite plane is divided into small arc regions  $\mathcal{A}_{m,n}$ . Then, it suffices to calculate  $\Pr \{ \gamma_{yd} > \gamma_{xd}, y \in \Phi_N, y \in \mathcal{A}_{m,n} \}, \forall m, n$  with  $0 < r_m < \infty$  and  $-\pi < \theta_n \leq \pi$ . It can be computed as  $\lambda P_{sy}(r_m, \theta_n) \Pr(\gamma_{yd} > \gamma_{xd}) \Delta v + o(\Delta v)$ , where  $\Delta v$  denotes the area of the small arc region approximated as  $\Delta v \approx r_m \Delta \theta \Delta r$ , and  $P_{sy}(r_m, \theta_n)$  is the probability of node  $y$  correctly receiving the signal from  $S$  in the original transmission phase, conditioned on node  $y$  being located in  $\mathcal{A}_{m,n}$ . The retransmission probability  $\tau_3(x)$  is computed only when  $x \in \Phi_N$ .

With  $\Delta v \rightarrow 0$ , the retransmission probability  $\tau_3(x)$  in (4.14) is written as

$$\tau_3(x) = \lim_{\Delta v \rightarrow 0} \prod_{m,n} [1 - \lambda P_{sy}(r_m, \theta_n) \Pr(\gamma_{yd} > \gamma_{xd}) \Delta v],$$

$$0 < r_m < \infty, -\pi < \theta_n \leq \pi. \quad (4.15)$$

Similar to the derivation of (4.7), with  $\Delta v \rightarrow 0$ , using (4.5), Eq. (4.15) can be

derived as

$$\begin{aligned}
\tau_3(x) &= \lim_{\Delta r \rightarrow 0} \lim_{\Delta \theta \rightarrow 0} \exp \left\{ \sum_{m,n} [-\lambda P_{sy}(r_m, \theta_n) \Pr(\gamma_{yd} > \gamma_{xd}) r_m \Delta \theta \Delta r] \right\} \\
&= \exp \left\{ -\lambda \int_0^\infty r \left[ \int_{-\pi}^\pi P_{sy}(r, \theta) d\theta \right] \exp \left( -\frac{\gamma_{xd}}{\bar{\gamma}_{yd}(r)} \right) dr \right\} \\
&= \exp \left\{ -2\lambda \int_0^\infty r \exp \left( -\frac{\gamma_{xd}}{\bar{\gamma}_{yd}(r)} \right) \int_0^\pi \exp \left[ -T_0 K_0 (R^2 + r^2 - 2Rr \cos \theta)^{\frac{\alpha}{2}} \right] d\theta dr \right\},
\end{aligned} \tag{4.16}$$

where  $\bar{\gamma}_{yd}(r) = P_0 r^{-\alpha} / N_0$  is the average SNR between node  $y$  and the destination  $D$ . For general values of  $\alpha$ , the closed-form expression of the inner integral over  $\theta$  is difficult to derive and the above integrals in (4.16) can only be evaluated numerically. However, a succinct expression of  $\tau_3(x)$  with  $\alpha = 2$  can be derived as follows.

$$\begin{aligned}
\tau_3(x) &= \exp \left\{ -2\pi\lambda \exp(-T_0 K_0 R^2) \int_0^\infty r \exp[-K_0(\gamma_{xd} + T_0)r^2] J_0(2iT_0 K_0 Rr) dr \right\} \\
&= \exp \left[ -\frac{\pi\lambda}{K_0(\gamma_{xd} + T_0)} \exp \left( -T_0 K_0 R^2 + \frac{K_0 T_0^2 R^2}{\gamma_{xd} + T_0} \right) \right].
\end{aligned} \tag{4.17}$$

In this equation, the integral over  $\theta$  given in (4.9) is used with  $I_0(2T_0 K_0 Rr)$  being substituted by the Bessel function  $J_0(2iT_0 K_0 Rr)$  according to [71], where  $i = \sqrt{-1}$ . The integral over  $r$  is derived with reference to [71]. It can be seen from (4.17) that, the retransmission probability is a monotonically increasing function of the instantaneous SNR  $\gamma_{xd}$ .

## 4.4 System Success Probability

In this section, the system success probability is analyzed for the sectorized scheme and local SNR based scheme, respectively. Similar operation can be applied to derive the success probability of the distance based scheme. The system success probability is denoted as  $P$  and given by

$$P = P_1 + P_2 + P_3, \tag{4.18}$$

where  $P_1 = \Pr\{\gamma_{sd} \geq T_0\} = \exp(-T_0 K_0 R^\alpha)$  is the success probability of original data transmission between source and destination,  $P_2$  is the probability that the source

successfully retransmits when the original transmission fails and all the potential relays keep silent, and  $P_3$  is the probability that only one potential relay successfully retransmits when the original transmission fails.

#### 4.4.1 For the Sectorized Scheme

In order to compute  $P_2$  and  $P_3$ , we divide the network area into very small regions of size  $\Delta v$ . Suppose that each node lies in the center of a certain region [66]. Define  $q(v)$  to be the probability that a potential relay exists in the small region  $v$  and retransmits the packet. It is given by

$$q(v) = \lambda P_{sn}(v) \tau_2(v) \Delta v + o(\Delta v), \quad (4.19)$$

where  $P_{sn}(v)$  is the conditional probability that a node lying in the center of  $v$  correctly receives the original data packet given by (4.5), and  $\tau_2(v)$  is the retransmission probability of the node given by (4.13).

In the retransmission phase, if all the potential relays keep silent, the source will retransmit the original data packet. In this case, the success probability is given as follows with  $\Delta v \rightarrow 0$ .

$$\begin{aligned} P_2 &= \Pr \{T_0/2 \leq \gamma_{sd} < T_0\} \lim_{\Delta v \rightarrow 0} \prod_v [1 - q(v)] \\ &= \Pr \{T_0/2 \leq \gamma_{sd} < T_0\} \lim_{\Delta v \rightarrow 0} \prod_v [1 - \lambda P_{sn}(v) \tau_2(v) \Delta v], \end{aligned} \quad (4.20)$$

where  $\Pr \{T_0/2 \leq \gamma_{sd} < T_0\}$  is the probability that the destination correctly detects the MRC signal from the source conditioned on that the original transmission fails. When the original transmission between source and destination fails, we have  $\gamma_{sd} < T_0$ . As the channel undergoes block fading, for the source to do the retransmission, the instantaneous SNR of the MRC signal at the destination side is  $2\gamma_{sd}$ . So, for the correct retransmission from the source, we have  $2\gamma_{sd} \geq T_0$ , i.e.,  $\gamma_{sd} \geq T_0/2$ . The series product  $\prod_v [1 - q(v)]$  in (4.20) denotes the probability of all the potential relays

keeping silent. Similar to the derivation of (4.13), we continue to have

$$\begin{aligned}
P_2 &= \Pr \{T_0/2 \leq \gamma_{sd} < T_0\} \exp \left\{ - \int_{v \in \mathbb{R}^2} \lambda P_{sn}(v) \tau_2(v) dv \right\} \\
&= \Pr \{T_0/2 \leq \gamma_{sd} < T_0\} \exp \left\{ -\lambda \int_0^\infty c \left[ \int_{-\pi}^\pi \exp \left( -\frac{2|\psi| \lambda \Gamma(2/\alpha)}{\alpha (T_0 K_0)^{2/\alpha}} \right) d\psi \right] P_{sx}(c) dc \right\} \\
&= \left[ \exp(-T_0 K_0 R^\alpha / 2) - \exp(-T_0 K_0 R^\alpha) \right] \exp \left[ -1 + \exp \left( -\frac{2\pi \lambda \Gamma(2/\alpha)}{\alpha (T_0 K_0)^{2/\alpha}} \right) \right].
\end{aligned} \tag{4.21}$$

**Remark:** By formulating the problem from the perspective of stochastic geometry, the same result can be reached using the probability generating functional (PGFL) [72] [73].

Next, we consider the probability that only one potential relay successfully retransmits. If only one potential relay centered at the small region  $v$  retransmits the data packet and all the other potential relays remain silent, with  $\Delta v \rightarrow 0$ , the success probability  $P_3$  is

$$P_3 = \lim_{\Delta v \rightarrow 0} \sum_v \left\{ q(v) \Pr \{ \gamma_{vd} + \gamma_{sd} \geq T_0, \gamma_{sd} < T_0 \} \prod_{v' \neq v} [1 - q(v')] \right\}, \tag{4.22}$$

where  $q(v)$  is given by (4.19). Conditioned on the existence of a potential relay node in the center of the small area  $v$ ,  $\Pr \{ \gamma_{vd} + \gamma_{sd} \geq T_0, \gamma_{sd} < T_0 \}$  is the probability that the destination correctly detects the MRC signal with the retransmission performed by this potential relay when the original transmission between source and destination fails. Specifically,

$$\begin{aligned}
&\Pr \{ \gamma_{vd} + \gamma_{sd} \geq T_0, \gamma_{sd} < T_0 \} \\
&= \frac{R^\alpha}{R^\alpha - r^\alpha} \exp(-T_0 K_0 r^\alpha) \left\{ 1 - \exp \left[ -T_0 K_0 (R^\alpha - r^\alpha) \right] \right\},
\end{aligned} \tag{4.23}$$

where  $r$  is the distance between the potential relay and the destination.

In (4.22), with  $\Delta v \rightarrow 0$ , the probability that all the potential relays except the conditional one lying in the small region  $v$  keep silent in the retransmission phase is

computed as

$$\begin{aligned}
\lim_{\Delta v \rightarrow 0} \prod_{v' \neq v} [1 - q(v')] &= \lim_{\Delta v' \rightarrow 0} \prod_{v' \neq v} [1 - \lambda P_{sn}(v') \tau_2(v') \Delta v] \\
&= \lim_{\Delta v' \rightarrow 0} \exp \left\{ \sum_{v'} \log [1 - \lambda P_{sn}(v') \tau_2(v') \Delta v] \right\} \\
&= \lim_{\Delta v' \rightarrow 0} \exp \left\{ - \sum_{v'} \lambda P_{sn}(v') \tau_2(v') \Delta v \right\} \\
&= \exp \left\{ - \int_{\mathbb{R}^2} \lambda P_{sn}(v') \tau_2(v') dv' \right\}, \tag{4.24}
\end{aligned}$$

which is independent of  $v$ . The result of  $\lim_{\Delta v \rightarrow 0} \prod_{v' \neq v} [1 - q(v')]$  in (4.22) is the same as  $\lim_{\Delta v \rightarrow 0} \prod_v [1 - q(v)]$  in (4.20), and this reflects the infinitesimal impact of a single excluded point in a continuous space [66]. In fact,  $P_3$  given by (4.22) can also be formulated from the perspective of stochastic geometry, and the conditional PGFL of the PPP equals the PGFL according to Slivnyak's Theorem [72] [73]. Hence, without distinction between  $v$  and  $v'$ ,  $P_3$  of (4.22) can be further derived as

$$\begin{aligned}
P_3 &= \exp \left[ - \int_{\mathbb{R}^2} \lambda P_{sn}(v) \tau_2(v) dv \right] \int_{\mathbb{R}^2} \lambda P_{sn}(v) \tau_2(v) \Pr\{\gamma_{vd} + \gamma_{sd} \geq T_0, \gamma_{sd} < T_0\} dv \\
&= \exp \left[ -1 + \exp \left( - \frac{2\pi \lambda \Gamma(2/\alpha)}{\alpha (T_0 K_0)^{2/\alpha}} \right) \right] \int_0^\infty \int_{-\pi}^\pi \lambda \exp(-T_0 K_0 c^\alpha) \exp \left[ - \frac{2|\psi| \lambda \Gamma(2/\alpha)}{\alpha (T_0 K_0)^{2/\alpha}} \right] \\
&\quad \times \frac{R^\alpha}{R^\alpha - r^\alpha} \exp(-T_0 K_0 r^\alpha) \{1 - \exp[-T_0 K_0 (R^\alpha - r^\alpha)]\} c d\psi dc, \tag{4.25}
\end{aligned}$$

where the relationship between  $r$  and  $c$  is  $r = \sqrt{R^2 + c^2 - 2Rc \cos(|\psi|)}$  as shown in Fig. 4.4, and the two-dimensional integral over  $\psi$  and  $c$  can be computed numerically.

#### 4.4.2 For the Local SNR Based Scheme

To derive  $P_2$  and  $P_3$ , the infinite plane is divided into a cascade of small regions with area  $\Delta v$ . The probability that one potential relay of  $\Phi_N$  lies in a small region  $v$  and retransmits the packet is given as  $\lambda \Pr(\gamma_{sv} \geq T_0) \mathbb{E}[\mathbf{1}(\gamma_{vd} \geq T_0) \tau_3(v)] \Delta v + o(v)$ , where  $\mathbf{1}(\gamma_{sv} \geq T_0)$  is the indicator random variable, which equals 1 if  $\gamma_{sv} \geq T_0$ , and 0 otherwise.

When the original transmission between the source and the destination fails, if all the potential relays keep silent in the retransmission phase, the source will retransmit. The success probability  $P_2$  is given as follows with  $\Delta v \rightarrow 0$ .

$$P_2 = \Pr \{T_0/2 \leq \gamma_{sd} < T_0\} \lim_{\Delta v \rightarrow 0} \prod_v \{1 - \lambda \Pr(\gamma_{sv} \geq T_0) \mathbb{E}[\mathbf{1}(\gamma_{vd} \geq T_0)\tau_3(v)] \Delta v\}, \quad (4.26)$$

where the series product is the probability of all the potential relays remaining silent. The expectation is taken over the random variable  $\gamma_{vd}$ , i.e. the SNR of channel  $v \rightarrow D$ , given by

$$\mathbb{E}[\mathbf{1}(\gamma_{vd} \geq T_0)\tau_3(v)] = \int_{T_0}^{\infty} \tau_3(v) f_{\Gamma_{vd}}(\gamma_{vd}) d\gamma_{vd}, \quad (4.27)$$

where  $f_{\Gamma_{vd}}(\gamma_{vd})$  is the probability density functions (PDF) of the instantaneous SNR  $\gamma_{vd}$ . The expression of the integral (4.27) with  $\tau_3(v)$  given by (4.16) for the general  $\alpha$  is complex. However, for the special case of  $\alpha = 2$ , we have a relatively succinct expression as follows.

$$\begin{aligned} & \mathbb{E}[\mathbf{1}(\gamma_{vd} \geq T_0)\tau_3(v)] \\ &= \frac{1}{\bar{\gamma}_{vd}} \exp\left(\frac{T_0}{\bar{\gamma}_{vd}}\right) \int_{2T_0}^{\infty} \exp\left\{-\frac{t}{\bar{\gamma}_{vd}} - \frac{\pi\lambda}{K_0 t} \exp\left[-T_0 K_0 R^2 \left(1 - \frac{T_0}{t}\right)\right]\right\} dt, \end{aligned} \quad (4.28)$$

where  $\bar{\gamma}_{vd}$  is the average SNR between destination and the node located in the center of  $v$ . After taking the integral over the infinite plane, we can further get

$$P_2 = \Pr \{T_0/2 \leq \gamma_{sd} < T_0\} \exp\left\{-\int_{\mathbb{R}^2} \lambda \Pr(\gamma_{sv} \geq T_0) \mathbb{E}[\mathbf{1}(\gamma_{vd} \geq T_0)\tau_3(v)] dv\right\}. \quad (4.29)$$

The succinct expression of (4.29) with  $\alpha = 2$  is written as

$$\begin{aligned} P_2 &= [\exp(-T_0 K_0 R^2/2) - \exp(-T_0 K_0 R^2)] \exp\left\{-\frac{\pi\lambda}{K_0} \exp(-T_0 K_0 R^2)\right. \\ &\quad \left. \times \int_{2T_0}^{\infty} \left(\frac{K_0 T_0^2 R^2}{t^3} + \frac{1}{t^2}\right) \exp\left\{\frac{K_0 T_0^2 R^2}{t} - \frac{\pi\lambda}{K_0 t} \exp\left[-K_0 T_0 R^2 \left(1 - \frac{T_0}{t}\right)\right]\right\} dt\right\}. \end{aligned} \quad (4.30)$$

Next, if only one potential relay of  $\Phi_N$  occupies the channel to retransmit the data while all the other potential relays keep silent, the system success probability  $P_3$  is given by

$$P_3 = \Pr\{\gamma_{sd} < T_0\} \lim_{\Delta v \rightarrow 0} \sum_v \lambda \Pr(\gamma_{sv} \geq T_0) \mathbb{E}[\mathbf{1}(\gamma_{vd} \geq T_0) \tau_3(v)] \Delta v \\ \times \prod_{v' \neq v} \left\{ 1 - \lambda \Pr(\gamma_{sv'} \geq T_0) \mathbb{E}[\mathbf{1}(\gamma_{v'd} \geq T_0) \tau_3(v')] \Delta v \right\}, \quad (4.31)$$

where  $\Pr\{\gamma_{sd} < T_0\} = 1 - \exp(-T_0 K_0 R^\alpha)$  is the probability that the original transmission between the source and the destination is unsuccessful. If the retransmission is performed by a potential relay, with  $\gamma_{vd} \geq T_0$ , the MRC technique is not needed for the signal detection in the local SNR based scheme. As the series summation and product can be reduced to the integral and exponential integral with  $\Delta v \rightarrow 0$ , (4.31) can be further derived as

$$P_3 = \Pr\{\gamma_{sd} < T_0\} \int_{\mathbb{R}^2} \lambda \Pr(\gamma_{sv} \geq T_0) \mathbb{E}[\mathbf{1}(\gamma_{vd} \geq T_0) \tau_3(v)] dv \\ \times \exp \left[ - \int_{\mathbb{R}^2} \lambda \Pr(\gamma_{sv'} \geq T_0) \mathbb{E}[\mathbf{1}(\gamma_{v'd} \geq T_0) \tau_3(v')] dv' \right], \quad (4.32)$$

where the integral is taken over the infinite plane, and according to (4.29), for the special case of  $\alpha = 2$ , it is given by

$$\int_{\mathbb{R}^2} \lambda \Pr(\gamma_{sv} \geq T_0) \mathbb{E}[\mathbf{1}(\gamma_{vd} \geq T_0) \tau_3(v)] dv = \frac{\pi \lambda}{K_0} \exp(-T_0 K_0 R^2) \times \\ \int_{2T_0}^{\infty} \left( \frac{K_0 T_0^2 R^2}{t^3} + \frac{1}{t^2} \right) \exp \left\{ \frac{K_0 T_0^2 R^2}{t} - \frac{\pi \lambda}{K_0 t} \exp \left[ -K_0 T_0 R^2 \left( 1 - \frac{T_0}{t} \right) \right] \right\} dt. \quad (4.33)$$

For the general path-loss exponent  $\alpha$ ,  $P_3$  can also be numerically computed.

## 4.5 Numerical and Simulation Results

In this section, numerical and simulation results of the proposed uncoordinated cooperative communication schemes are presented and compared. In the comparison, the traditional truncated ARQ scheme with source performing the retransmission is

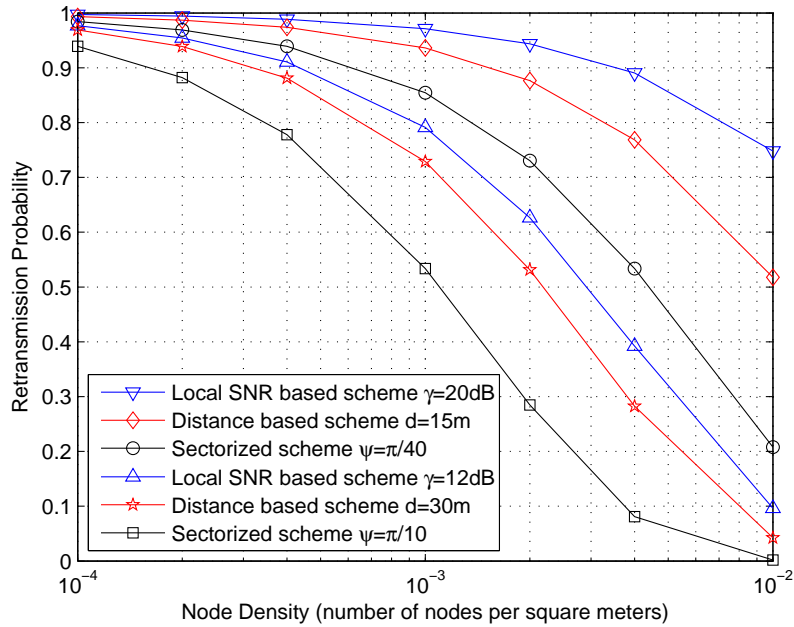


**Figure 4.5:** Retransmission probability vs. node density. The transmitter SNR is 40dB, the  $S$ - $D$  distance is  $R = 70$ m, and the decoding threshold is  $T_0 = 5$ .

also included. In the simulation, a circular area with radius 500m is considered with the destination located at the origin, and the source is located  $R$  away from the destination. All the relay nodes are uniformly distributed in the circular area, and the number of relay nodes follows Poisson distribution with mean  $\lambda\pi 500^2$ . The path-loss exponent  $\alpha = 2$  is used in the simulation.

In Fig. 4.5, the retransmission probabilities of the proposed schemes are shown with respect to the node density  $\lambda$ . Note that the theoretical retransmission probabilities of the distance based scheme, sectorized scheme, and local SNR based scheme are given in (4.9), (4.13), and (4.17), respectively. It can be seen that with the increase of  $\lambda$ , the retransmission probability of each scheme becomes smaller. For the distance based scheme, the retransmission probability gets smaller when the distance  $d$  between a potential relay and the destination increases from 15m to 30m. For the sectorized scheme, the retransmission probability turns smaller when the angle  $\psi$  increases from  $\pi/40$  to  $\pi/10$ . For the local SNR based scheme, the retransmission

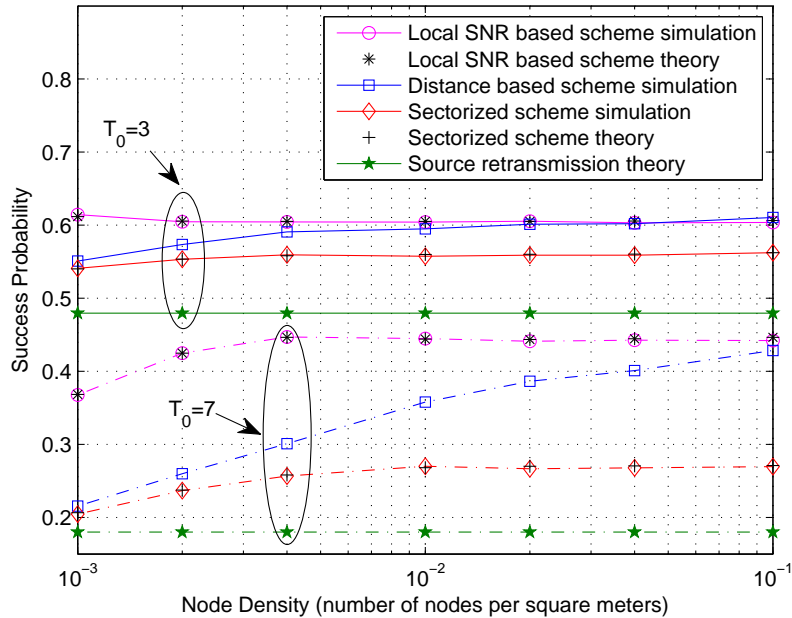


**Figure 4.6:** Success probability vs. node density. The source-destination distance is  $R = 70\text{m}$  and the transmitter SNR is 40dB.

probability becomes smaller when the instantaneous SNR  $\gamma$  between a potential relay and the destination is reduced from 20dB to 12dB.

Fig. 4.6 shows the system success probabilities of the proposed uncoordinated schemes against the node density with different SNR thresholds, while Fig. 4.7 shows the performance with different source-destination distances. The original erroneously received signal and the retransmitted signal are combined at the destination by using the MRC technique for the detection. The distance between the source and the destination is set as  $R = 70\text{m}$  in Fig. 4.6. The SNR threshold of signal detection is set as  $T_0 = 2$  in Fig. 4.7. For the sectorized and local SNR based schemes, we can see that the simulation results match well with the theoretical results presented in Section IV. Also, we can observe that, the local SNR based scheme has the best performance in general, because collisions can be greatly alleviated by allocating the retransmission task only to the nodes that have good instantaneous channel state towards the destination. Moreover, it is observed that the distance based scheme outperforms the

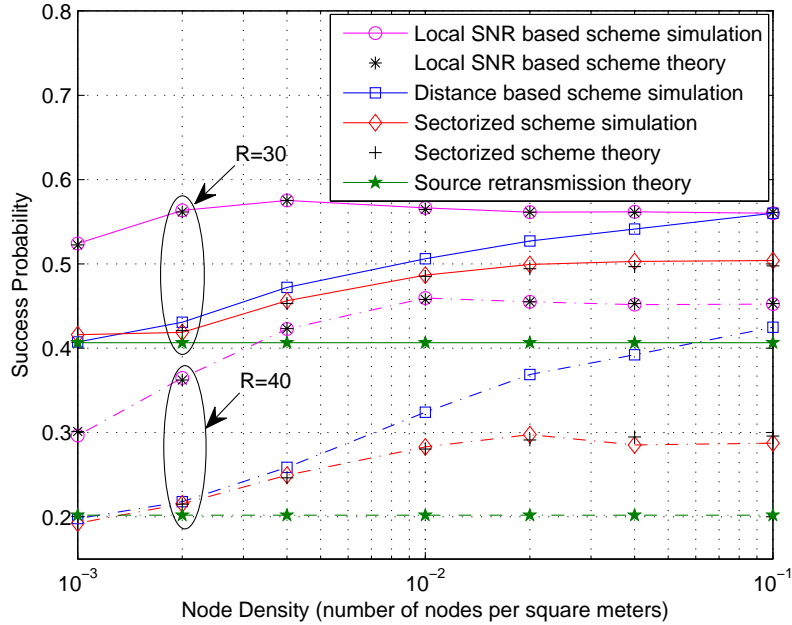


**Figure 4.7:** Success probability vs. node density. The transmitter SNR is 30dB and the decoding threshold is  $T_0 = 2$ .

sectorized scheme. The proposed uncoordinated cooperative truncated ARQ schemes outperform the source retransmission scheme.

In the whole range of  $\lambda$ , the performance of each scheme does not change greatly. The rational behind this phenomenon is explained as follows. The retransmission probabilities of the potential relays given in Section 4.3 are monotonically decreasing functions of the node density  $\lambda$ . When the node density  $\lambda$  gets larger, although more potential relays will exist in the vicinity of the source and the destination, it will not necessarily cause more collisions. This is because the retransmission probabilities of the potential relays becomes smaller with the increase of  $\lambda$ , as shown in Fig. 4.5. Consequently, the probability of only one potential relay accessing the channel for the data retransmission changes slightly with respect to different node densities. As  $T_0$  denotes the SNR threshold of successfully decoding the received signal, we can expect that more errors can be tolerated for smaller  $T_0$ . Hence, the system success probability becomes better when  $T_0$  turns smaller from 7 to 3. With the increase

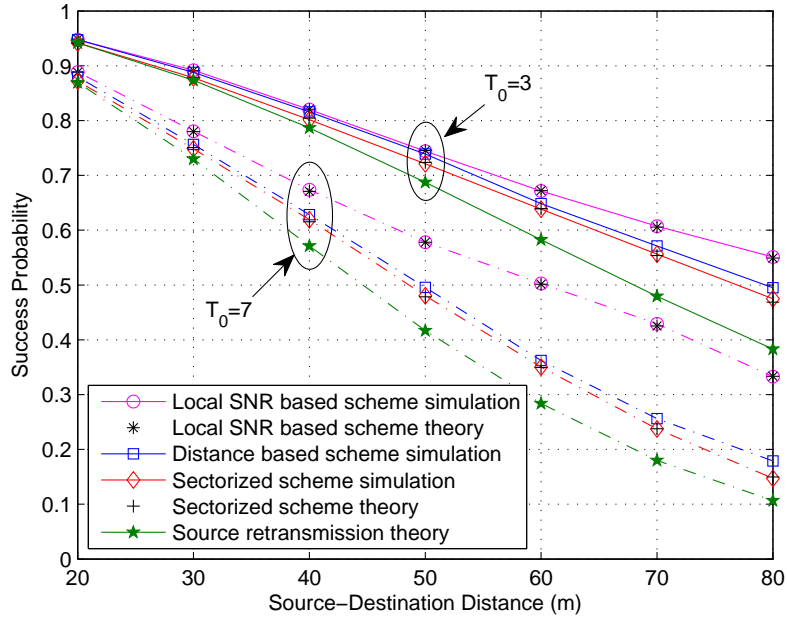


**Figure 4.8:** Success probability vs. source-destination distance. The node density is  $\lambda = 0.002/\text{m}^2$  and the transmitter SNR is 40dB.

of  $R$  from 30m to 40m, the average channel quality between source and destination deteriorates, so the system success probability gets worse.

Fig. 4.8 compares the success probabilities of the proposed schemes with respect to the source-destination distance  $R$  for  $T_0 = 3$  and  $T_0 = 7$ . The node density is set as  $\lambda = 0.002/\text{m}^2$  and the transmitter side SNR is 40dB. When the distance  $R$  is short, the original transmission between the source and the destination is successful almost all the time. However, with the increase of distance  $R$ , the success probability becomes smaller. It can be seen that the local SNR based scheme has the best performance in the whole distance range. The distance based scheme slightly outperforms the sectorized scheme. The uncoordinated schemes have a better performance than the traditional truncated ARQ scheme with only the source performing the retransmission. Because space diversity can be achieved if the signal is retransmitted by a relay node other than the source node. Apparently, when the SNR threshold becomes smaller from 7 to 3, the performance gets better. Moreover, we can observe that the

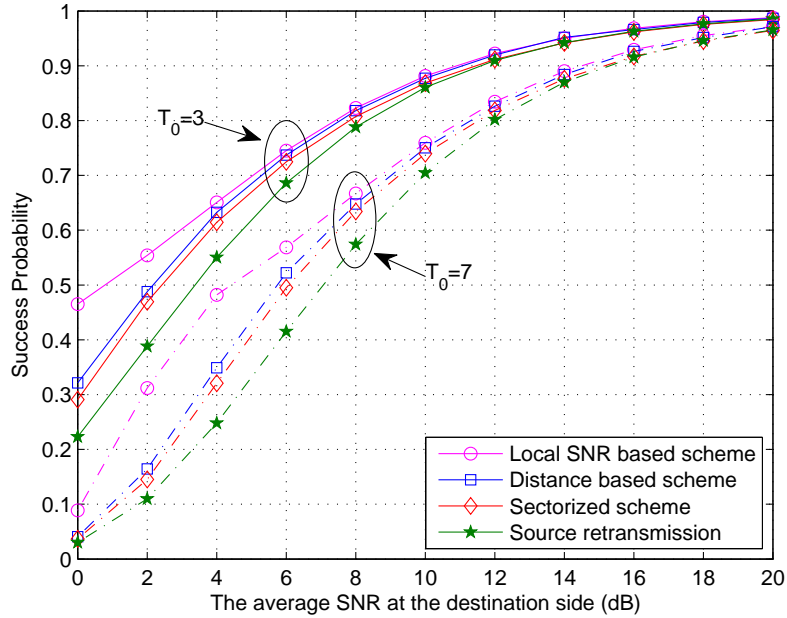


**Figure 4.9:** Success probability vs. average SNR at the destination. The node density is  $\lambda = 0.002/\text{m}^2$  and the source-destination distance is  $R = 70\text{m}$ .

numerical results coincide with the simulation results well for the sectorized and local SNR based schemes. It validates the theoretical analysis in Section 4.4.

The system success probabilities of the proposed schemes with respect to the average SNR at the destination side are shown in Fig. 4.9. The node density is set as  $\lambda = 0.002/\text{m}^2$ , and the distance between the source and the destination is fixed as  $R = 70\text{m}$ . The system success probability is small when the average SNR is very low, because the transmission power is very low. The performance improves with the increase of the average SNR. In the low to middle SNR range, we can see that the local SNR based schemes outperforms all the other schemes, and that the distance based schemes performs better than the sectorized scheme. The source retransmission schemes has the worst performance, due to its lack of cooperative diversity. When the transmission power is high enough, the original transmission between the source and the destination is successful with very high probability. Hence, in the high SNR range, the performance of all the schemes is very close.

## 4.6 Summary

In this chapter, we have proposed three uncoordinated cooperative truncated ARQ schemes in a large wireless network. If the original data packet is erroneously received by the destination, all the potential relays compete the channel for the data retransmission in a distributed fashion without coordination. Whether a potential relay should access the channel or not is determined independently by its retransmission probability, which is computed based on the local information of the potential relay, such as position or channel SNR towards the destination. Numerical and simulation results show that the local SNR based scheme has the best performance and the distance based scheme is superior to the sectorized scheme.

## Chapter 5

# Cooperative Spectrum Sharing in Ad-Hoc Network

### 5.1 Introduction

For the overlay spectrum sharing, the SUs can actively help the primary data transmission in exchange for the spectrum access in spatial domain [31], time domain [74], or frequency domain [75]. As studied in the previous chapters, the locations of users are usually fixed or restricted into a small area without suffering interference from other concurrent links. It is nontrivial to extend the cooperative spectrum sharing to the ad-hoc networks, as the topology changes frequently and the interference suffers from uncertainties caused by both random user locations and channel fading.

Transmission capacity has often been used as a major performance metric to study ad-hoc networks and it represents the area spectral efficiency constrained by the outage probability [76]. Through modeling users' locations as homogeneous PPP in the overlaid wireless system, Huang *et al.* studied the transmission capacity tradeoff between primary system and secondary system [41]. Lee *et al.* developed a comprehensive framework with multiple systems and studied the transmission capacity under the constraints of both outage probability and fair coexistence [77]. Yin *et al.*

studied the impacts of mutual interference between primary and secondary systems and found that a slight degradation of the primary outage performance can lead to a significant increase of the total transmission capacity [78]. The underlay spectrum sharing is realized in [79] by applying an exclusive region [80] around the single primary link such that the SU transmission is prohibited in the region. For the cognitive radio network with multiple primary links, the active SUs form the Poisson hole process due to the exclusive regions, and the approximate outage probability is derived in [81]. The stochastic geometry models of three types of cognitive radio networks are proposed in [42], where the single primary link, multicast primary system, or primary ad-hoc network coexists with a secondary ad-hoc network operating with the CSMA protocol. Wang *et al.* studied the DF cooperation with relays randomly distributed on the plane. A spatial QoS region around the source and destination link is applied in [83] to reduce the overhead and latency in the best relay selection. In terms of transmission capacity, the DF based incremental relaying or selection cooperation [22] significantly outperforms the non-cooperative system as shown in [84, 85].

In cognitive radio networks with users randomly distributed, the existing literatures mainly focus on the non-cooperative underlay and interweave spectrum sharing. The spectrum access of the secondary system can only degrade the performance of the primary system and will not bring any contribution to the primary system. This motivates us to study the effect of overlay spectrum sharing, where the SUs actively help the PUs with their transmissions in exchange for some spectrum release by the primary system for the secondary data transmission. However, it is a challenging issue to study the performance of an overlay spectrum sharing system, as the interferences encountered at both the relay and the receiver are dependent. Ganti *et al.* have studied the two-hop communication with relay selection to mitigate the dead-zone in the cell-edge area of the cellular network [86]. In their work, the success probability of the two-hop system is analyzed with the base stations (BSs) placed on a regular grid, which is too ideal to model the upcoming heterogenous networks [87]. To capture the increasingly random and dense placement of BSs in future networks [88], it is more

practical to model the BSs as a random spatial point process. Compared with the cellular network uplink [41], the downlink bandwidth is much broader and its data traffic is much heavier, so the spectrum efficiency can be further improved by sharing the downlink spectrum as focused on in our work.

In this work, we focus on modeling and analyzing the cooperative spectrum sharing between cellular network downlink and ad-hoc network. The cellular network is the primary system that owns the licensed spectrum, while the ad-hoc network is the secondary system. The same spectrum is reused among different cells and the interference exists over the primary data transmission. In the cellular network, the cell-edge communication is a bottleneck to guarantee the overall QoS requirement, because the desired signal is relatively weak compared with the interference [88]. To improve the quality of cell-edge communication, we apply a cooperation region between each BS and its cell-edge mobile user (MU). The SU in the cooperation region that can correctly decode the primary data and has the best channel state towards the cell-edge MU is selected for the data retransmission in case the original transmission fails. As a reward of the cooperation, a fraction of spectrum is released to the secondary system and the remaining bandwidth is kept by the primary system. Using the stochastic geometry theory, we analyze the transmission capacity of ad-hoc network and the average throughput of cellular network downlink. The optimal bandwidth allocation is obtained through maximizing the secondary transmission capacity subject to the constraints of secondary outage probability and primary throughput improvement ratio. Numerical and simulation results are provided to show the impacts of system parameters and verify the efficiency of our proposed scheme.

The rest of this chapter is organized as follows. In Section 5.2, the system model is introduced. Section 5.3 formulates the optimization problem and obtains the secondary transmission capacity. Section 5.4 derives the average throughput of primary downlink based on the analysis of success probabilities. The optimal SU density and bandwidth allocation are calculated in Section 5.5. Numerical and simulation results are presented in Section 5.6. Section 5.7 concludes this chapter.

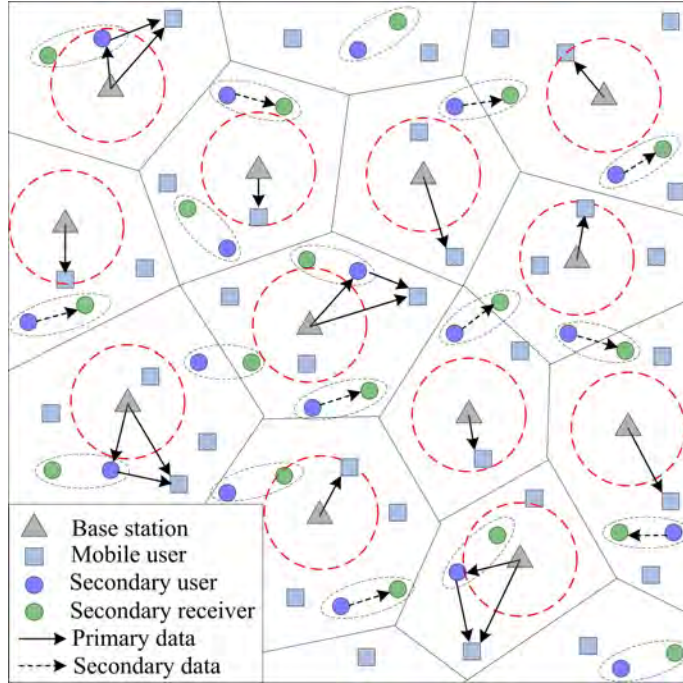


**Figure 5.1:** The overlaid wireless network with PPP modeling for both systems. The circular area around each base station represents the cell-interior area, with radius  $c_0$ . In each *Voronoi* cell, the outside of the circular area represents the cell-edge area.

## 5.2 System Description

The licensed spectrum belongs to the cellular network and it is reused by different cells. The locations of BSs and MUs are modeled as two independent homogenous PPPs  $\Pi_b = \{x_i, i \in \mathbb{Z}\}$  and  $\Pi_m = \{y_i, i \in \mathbb{Z}\}$  with intensities  $\lambda_b$  and  $\lambda_m$ , respectively. Each MU is served by its nearest BS. As plotted in Fig. 5.1, the cellular network forms a *Poisson Tessellation* of the plane and each cell is known as a *Voronoi* cell [41]. Each BS communicates with one randomly selected MU in its cell and the downlink communication is studied. An ad-hoc network is overlaid with the cellular network and it forms the secondary system. The locations of SUs follow another PPP with intensity  $\lambda_s$ , i.e.,  $\Pi_s = \{z_i, i \in \mathbb{Z}\}$ . Each SU has a receiver departed  $d$  meters away. The Aloha-type protocol is adopted in the ad-hoc network to control the channel access of SUs. Whether a SU could access the channel or not is determined by the

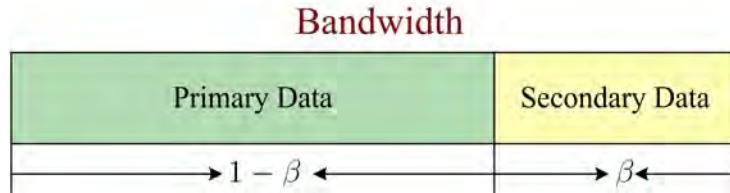


**Figure 5.2:** Bandwidth division between primary and secondary systems. The fraction  $\beta$  is released to the secondary system, while the remaining  $1 - \beta$  fraction is kept by the primary system for the direct or cooperative data transmission.

media access probability (MAP)  $\xi \in (0, 1)$ . The channel between any pair of terminals  $u_1$  and  $u_2$  undergoes small-scale block fading and large-scale path-loss. The power fading  $G_{u_1, u_2}$  is exponentially distributed with unit mean, and it is independent across links. The path-loss is  $\ell_{u_1, u_2}^{-\alpha}$ , where  $\ell_{u_1, u_2} = |u_1 - u_2|$  is the distance and  $\alpha$  is the path-loss exponent. The symbol  $u_2$  in the subscript is omitted for brevity if  $u_2$  lies at the origin. The interference-limited environment is considered and the effect of noise is neglected.

### 5.2.1 Spectrum Sharing Model

We consider the overlay spectrum sharing, where a fraction of spectrum is released to the ad-hoc network in exchange for its cooperation for the cell-edge communication [75]. Without loss of generality, the total bandwidth is set as unit and the spectrum released to the secondary system is  $\beta \in (0, 1)$ , while the remaining  $1 - \beta$  fraction of spectrum is reserved by the primary system as shown by Fig. 5.2. The primary system and secondary system do not interfere with each other as disjoint frequency bands are utilized.

If the randomly selected MU lies at the cell-interior of its serving BS, the direct transmission is performed, because the channel is usually good and the interference is relatively weak. The bandwidth release may be tolerated by the primary down-link. The interior area is defined as a circular area centered at the BS with radius  $c_0$ . However, if the MU lies at the cell-edge of its serving BS, cooperative commu-

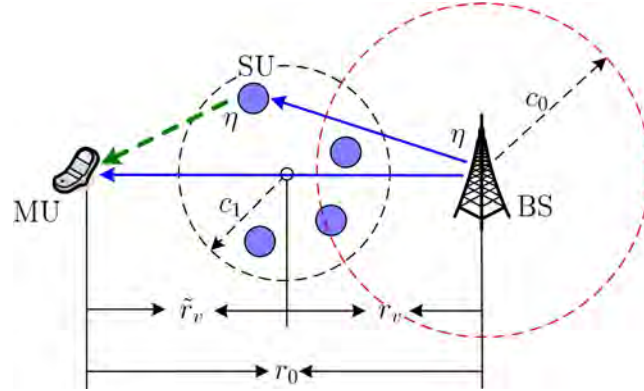


**Figure 5.3:** The cooperation model for the cell-edge MU. The corresponding receiver for each SU is not plotted in this figure.

nications are employed. With the cooperation from SUs, the throughput of primary data transmission can be enhanced to combat the strong interference. Moreover, the benefits of cooperation can be exploited to combat the negative effect of spectrum release. The more spectrum is released, the higher capacity is achieved for the secondary system. However, less capacity is retained for the primary system due to the remaining narrower bandwidth. Therefore, the bandwidth allocation should be judiciously determined to maximize the secondary capacity without violating the primary performance requirement in the cooperative spectrum sharing.

### 5.2.2 Cooperation Model

The truncated ARQ scheme with one-time retransmission is adopted for the communication between BS and its cell-interior MU. If the original transmission is successful, the acknowledgement (ACK) frame is fed back and the BS continues to transmit a new data packet. Otherwise, the negative acknowledgement (NACK) frame is released and the BS retransmits the same data packet. The received signals in both the original and the retransmission phases are maximal ratio combined (MRC) by the cell-interior MU for the detection.

The cooperative truncated ARQ scheme based on DF protocol [12], which is also known as the DF based incremental relaying [22], is adopted to help the data trans-

mission between the BS and its cell-edge MU. As shown in Fig. 5.3, a cooperation region is applied between the BS and its cell-edge MU, which can be designated by the BS through a hand-shake process or determined automatically by each SU using its estimated location obtained from the localization technique [68]. The distance between BS and the center of cooperation region is denoted as  $r_v = \zeta r_0$  with  $0 < \zeta < 1$ , while the distance between the center of cooperation region and the cell-edge MU is  $\tilde{r}_v = (1 - \zeta)r_0$ . The SUs in the cooperation region will help the primary data transmission. In the original phase, the BS broadcasts its data to the intended cell-edge MU and all the SUs in the cooperation region. The SUs that can correctly decode the original primary data are called *decoding SUs*. Three cases will occur according to whether the MU and the SUs correctly receive the primary data or not.

- Case I: The cell-edge MU correctly receives the data packet, and the ACK frame is broadcast. The SUs in the cooperation region refresh their memories and the BS continues to transmit a new data packet.
- Case II: The cell-edge MU erroneously receives the primary data and the NACK frame is fed back. There are no SUs in the cooperation region or there are no decoding SUs in the cooperation region, in this case the BS retransmits its original data packet.
- Case III: The cell-edge MU erroneously receives the primary data and the NACK frame is released. There exists at least one decoding SU in the cooperation region and the one with best channel state towards the cell-edge MU retransmits. The best decoding SU can be selected in a distributed way using the time back-off [34] or signaling burst scheme [56].

We assume that the control frame sent by the MU can be reliably received by both the BS and the relaying SUs. The channel coefficient is assumed to be available for each receiver to coherently detect signals. Each decoding SU can estimate its channel state towards the cell-edge MU through measuring the NACK frame.

### 5.3 Transmission Capacity of Secondary System

To maximize the transmission capacity [76] of secondary system while satisfying the primary performance requirement, the optimization problem is formulated as

$$\max_{\lambda_s > 0, 0 < \beta < 1} C_s^\epsilon = \xi \lambda_s (1 - \epsilon) T_1 \quad (5.1)$$

$$\text{s. t.} \quad P_{\text{out}}^s(\lambda_s, \beta) \leq \epsilon \quad (5.2)$$

$$\frac{V_c(\lambda_s, \beta) - V_d}{V_d} \geq \rho, \quad (5.3)$$

where  $C_s^\epsilon$  is the transmission capacity of secondary system. The transmission rate of each secondary link is assumed to be the same as  $T_1$ . The outage probability  $P_{\text{out}}^s(\lambda_s, \beta)$  of each secondary link should be no larger than the target outage probability  $\epsilon$ . The average throughput of primary system with and without cooperative spectrum sharing is denoted as  $V_c(\lambda_s, \beta)$  and  $V_d$ , respectively. The parameter  $\rho \geq 0$  represents the required throughput improvement ratio of the primary downlink introduced by the cooperative spectrum sharing. The optimal SU density  $\lambda_s$  and the optimal bandwidth allocation factor  $\beta$  are investigated for the optimization problem.

Since SUs transmit according to an Aloha-type protocol [56], the simultaneous transmitting SUs form a homogeneous PPP  $\tilde{\Pi}_s$  with density  $\xi \lambda_s$ , which is obtained through an independent thinning of  $\Pi_s$ . Without loss of generality, we consider and evaluate the performance of a typical secondary receiver located at the origin. According to Slivnyak's theorem [89], this artificial placement does not affect the distribution of other users. The achievable rate of secondary data transmission is given as

$$R_s = \beta \log_2 \left( 1 + \frac{G_{z_0} d^{-\alpha}}{\mathcal{I}_s} \right), \quad (5.4)$$

where  $G_{z_0}$  is the small-scale power fading. The pre-factor  $\beta$  is applied in (5.4) due to the division of bandwidth for the spectrum sharing. The interference term in (5.4) is

$$\mathcal{I}_s = \sum_{z \in \tilde{\Pi}_s / \{z_0\}} G_z \ell_z^{-\alpha}, \quad (5.5)$$

where all the active SUs except the typical one contribute to the aggregate interference. The outage probability of this typical secondary link is derived as [72],

$$\begin{aligned} P_{\text{out}}^s(\lambda_s, \beta) &= \mathbb{P}\{R_s < T_1\} = \mathbb{P}\{G_{z_0} < \tau_1 d^\alpha \mathcal{I}_s\} \\ &= 1 - \exp\left[-\xi \lambda_s \pi \tau_1^{\frac{2}{\alpha}} d^2 \frac{2\pi/\alpha}{\sin(2\pi/\alpha)}\right], \end{aligned} \quad (5.6)$$

where  $\tau_1 = 2^{T_1/\beta} - 1$  with  $T_1$  denoting the secondary target rate.

**Remarks:** (1) The increase of  $\beta$  leads to the decrease of  $\tau_1$ . With the decrease of  $\tau_1$ , the outage probability gets smaller. Therefore, the higher bandwidth allocation is beneficial to support the secondary transmission and hence reduce the outage probability. But, the primary performance gets worse with the increase of  $\beta$ , so we hope to find a trade-off of this parameter. (2) The outage performance gets worse with the increase of SU density  $\lambda_s$ , because the more concurrent secondary transmissions, the stronger the interference and hence the worse the performance.

## 5.4 Average Throughput of Primary System

In this section, we first introduce the distribution of the random distance between a BS and its intended MU. The aggregate interference encountered at the typical MU is approximated. Then, we analyze the success probabilities for the cell-interior and cell-edge communications. Finally, the average throughput of the cellular network downlink is derived.

### 5.4.1 Distance Distribution and Interference Model

One typical MU is located at the origin and the typical MU is served by its nearest BS located at  $x_0$ . Their distance is denoted as  $r_0$ , which is a realization of the random variable  $R$  (the random distance between a BS and its intended MU in the serving area). The complementary cumulative distribution function (CCDF) is given as [87]

$$\Pr\{R > r_0\} = \Pr\{\text{No BS closer than } r_0\} = \exp(-\lambda_b \pi r_0^2). \quad (5.7)$$

Then, the cumulative distribution function (CDF) is obtained as  $F_R(r_0) = 1 - \exp(-\lambda_b \pi r_0^2)$ , so the probability density function (PDF) is obtained as

$$f_R(r_0) = \frac{dF_R(r_0)}{dr_0} = 2\pi\lambda_b r_0 \exp(-\lambda_b \pi r_0^2). \quad (5.8)$$

For each BS  $x \in \Pi_b$ , a mark  $r_x$  is applied to represent the distance of its intended MU. The intended MU is a cell-interior user with  $r_x \leq c_0$ , otherwise, it is a cell-edge user.

The interference encountered at the typical MU is approximated as

$$\mathcal{I}_p \approx \sum_{x \in \Pi_b \setminus \{x_0\}} P_x G_x \ell_x^{-\alpha}, \quad (5.9)$$

where  $P_x = \mathbf{1}(r_x \leq c_0) + \eta \mathbf{1}(r_x > c_0)$ . The indicator random variable  $\mathbf{1}(\mathcal{A})$  equals 1 if condition  $\mathcal{A}$  is satisfied, otherwise it equals 0. The indicator random variable denotes whether the interfering BS communicates with a cell-interior MU with normalized unit power or communicates with a cell-edge MU with normalized power  $\eta \geq 1$ . The approximation is given because the position of the cooperative SU is not the same as its serving BS when it performs the retransmission towards the cell-edge MU. The location of the relaying SU in the cell of  $x \in \Pi_b$  (the intended MU of  $x$  is at cell-edge) is denoted as  $x_z = x + f(x)$ , where  $f(x)$  is the relative location of the selected SU from its serving BS  $x$ . Since almost surely we have  $|f(x)| < \infty$ , the distance between the selected SU and the typical MU can be approximated as the distance between its serving BS and the typical MU [86].

### 5.4.2 Success Probability of Cell-Interior Communication

Conditioned on the distance between BS  $x_0$  and its typical cell-interior MU being  $r_0$ , the achievable rate of primary data transmission is expressed as

$$R_{\text{in1}}(r_0) = (1 - \beta) \log_2 \left( 1 + \frac{G_{x_0} r_0^{-\alpha}}{\mathcal{I}_p} \right), \quad (5.10)$$

where  $(1 - \beta)$  is the fraction of bandwidth kept by the primary system. Let  $T_0$  denote the primary target rate, the success probability of original data transmission

is obtained as

$$\begin{aligned} P_{\text{in1}}(r_0) &= \mathbb{P}\{R_{\text{in1}}(r_0) \geq T_0\} = \mathbb{P}\{G_{x_0} \geq \tau_0 r_0^\alpha \mathcal{I}_p\} \\ &= \mathbb{E}[\exp(-\tau_0 r_0^\alpha \mathcal{I}_p)] = \mathcal{L}_{\mathcal{I}_p}(\tau_0 r_0^\alpha), \end{aligned} \quad (5.11)$$

where  $\tau_0 = 2^{\frac{T_0}{1-\beta}} - 1$  and  $\mathcal{L}_{\mathcal{I}_p}(\cdot)$  denotes the Laplace transform of the interference  $\mathcal{I}_p$ . The exponential distribution of  $G_{x_0}$  is considered to obtain the expectation term in (5.11), which is taken over all possible locations and channel fadings of interferers in other cells. Here, both the spatial average and the time average over the interference are performed to obtain the average success probability. The locations of MUs are coupled by the locations of their serving BSs upon the *Poisson Tessellation* over the 2-D plane. Therefore, the communication distances and transmit powers of BSs towards their intended MUs in different cells are dependent. However, the dependence in different cells is weak as validated in [90]. For different cells, the distances between BSs and their intended MUs are assumed to be independent. The Laplace transform of  $\mathcal{I}_p$  can thus be derived as

$$\begin{aligned} \mathcal{L}_{\mathcal{I}_p}(s) &= \mathbb{E}\left[\exp\left(-s \sum_{x \in \Pi_b \setminus \{x_0\}} P_x G_x \ell_x^{-\alpha}\right)\right] \\ &\stackrel{(a)}{=} \mathbb{E}_{\Pi_b}\left\{\prod_{x \in \Pi_b \setminus \{x_0\}} \mathbb{E}_{P,G}\left[\exp(-s P G \ell_x^{-\alpha})\right]\right\} \\ &\stackrel{(b)}{=} \exp\left\{-2\pi\lambda_b \mathbb{E}_{P,G}\left[\int_{r_0}^{\infty} [1 - \exp(-s P \ell^{-\alpha} G)] \ell \, d\ell\right]\right\} \\ &\stackrel{(c)}{=} \exp\left\{-2\pi\lambda_b d_1 \left[\int_0^{\infty} \int_{r_0}^{\infty} [1 - \exp(-s \ell^{-\alpha} G)] \ell \, d\ell f(G) \, dG\right]\right\} \\ &\quad \times \exp\left\{-2\pi\lambda_b d_2 \left[\int_0^{\infty} \int_{r_0}^{\infty} [1 - \exp(-s \eta \ell^{-\alpha} G)] \ell \, d\ell f(G) \, dG\right]\right\}, \end{aligned} \quad (5.12)$$

where  $d_1 = 1 - \exp(-\lambda_b \pi c_0^2)$  and  $d_2 = \exp(-\lambda_b \pi c_0^2)$ . Equality (a) is obtained due to the independence of channel fading and transmit power for each BS. Equality (b) is obtained according to the probability generating functional (PGFL) of PPP [72] and the integral is taken over  $(r_0, \infty)$  as the interfering BSs are at least  $r_0$  away from the typical MU. Taking the expectation of independent discrete random variable  $P$ , we

obtain equality (c). By substituting  $s = \tau_0 r_0^\alpha$  into (5.12) and calculating the integral over distance  $\ell$ , we can obtain

$$P_{\text{in1}}(\tau_0, r_0) = \exp[-\omega(\tau_0)r_0^2], \quad (5.13)$$

where

$$\begin{aligned} \omega(t) = -\pi\lambda_b + \frac{2\pi\lambda_b t^{\frac{2}{\alpha}}}{\alpha} \left\{ - (2/\alpha)\Gamma(2/\alpha)\Gamma(-2/\alpha)(d_1 + d_2\eta^{\frac{2}{\alpha}}) \right. \\ \left. + \int_0^\infty g^{\frac{2}{\alpha}} [d_1\Gamma(-2/\alpha, tg) + d_2\eta^{\frac{2}{\alpha}}\Gamma(-2/\alpha, \eta tg)] \exp(-g) dg \right\}. \end{aligned} \quad (5.14)$$

With  $a > 0$ , the Gamma function is  $\Gamma(a) = \int_0^\infty t^{a-1}e^{-t} dt$  and the upper incomplete Gamma function is  $\Gamma(a, x) = \int_x^\infty t^{a-1}e^{-t} dt$ . With  $-1 < a < 0$ ,  $\Gamma(a) = \Gamma(a+1)/a$  and  $\Gamma(a, x) = [\Gamma(a+1, x) - x^a \exp(-x)]/a$  [71].

If the original transmission fails, the retransmission is performed by BS with achievable rate

$$R_{\text{in2}}(r_0) = \frac{1-\beta}{2} \log_2 \left( 1 + \frac{2G_{x_0}r_0^{-\alpha}}{\mathcal{I}_p} \right), \quad (5.15)$$

where the pre-factor  $1/2$  is applied due to the retransmission and the double SIR is used due to the MRC detection. The conditional success probability of this case is derived as

$$\begin{aligned} P_{\text{in2}}(\tau_0, r_0) &= \mathbb{P}\{R_{\text{in1}}(r_0) < T_0, R_{\text{in2}}(r_0) \geq T_0/2\} \\ &= \exp[-\omega(\tau_0/2)r_0^2] - \exp[-\omega(\tau_0)r_0^2], \end{aligned} \quad (5.16)$$

where  $\omega(\cdot)$  is given by (5.14).

### 5.4.3 Success Probability of Cell-Edge Communication

The communication between a BS and its cell-edge MU includes three cases: Case I, the MU correctly receives the primary data in the original phase; Case II, the original data transmission fails, there are no decoding SUs in the cooperation region, and the BS retransmits; Case III, the original data transmission fails, and a decoding SU is successfully selected to retransmit. In the following, we analyze the three cases

separately.

**For Case I:**

Conditioned on the distance between BS  $x_0$  and its typical cell-edge MU being  $r_0$ , the achievable rate of primary data transmission is expressed as

$$R_{\text{ed}}(r_0) = (1 - \beta) \log_2 \left( 1 + \frac{\eta G_{x_0} r_0^{-\alpha}}{\mathcal{I}_p} \right). \quad (5.17)$$

Similar to (5.13), the conditional success probability of original data transmission is derived as

$$P_{\text{ed1}}(\tau_0, r_0) = \mathbb{P}\{R_{\text{ed}}(r_0) \geq T_0\} = \exp[-\omega(\tau_0/\eta)r_0^2], \quad (5.18)$$

where  $\omega(\cdot)$  is given in (5.14).

**For Case II:**

The conditional success probability is given as

$$P_{\text{ed2}}(\tau_0, r_0) = \sum_{n=0}^{\infty} \Pr\{N = n\} \mathbb{P}\{\tau_0/2 \leq \gamma_{x_0} < \tau_0, \max\{\gamma_{x_0, z_i}\} < \tau_0\}, \quad (5.19)$$

where the Poisson random variable  $N$  represents the number of SUs in the cooperation region. The probability of  $N = n$  is given as

$$\Pr\{N = n\} = \frac{(\lambda_s \pi c_1^2)^n}{n!} \exp(-\lambda_s \pi c_1^2). \quad (5.20)$$

The SIRs encountered at the typical MU and the  $i$ th SU in the cooperation region are given as

$$\gamma_{x_0} = \frac{\eta G_{x_0} r_0^{-\alpha}}{\mathcal{I}_p} \quad \text{and} \quad \gamma_{x_0, z_i} = \frac{\eta G_{x_0, z_i} r_v^{-\alpha}}{\mathcal{I}_{p_i}}, \quad (5.21)$$

where the distance between a BS and its cooperating SUs is set the same as  $r_v = \zeta r_0$  ( $0 < \zeta < 1$ ). The interference at the  $i$ th SU is denoted as  $\mathcal{I}_{p_i}$ . When  $N = 0$ , the success probability of (5.19) is reduced as  $\tilde{P}_{\text{ed2}}(\tau_0, r_0) = \mathbb{P}\{\tau_0/2 \leq \gamma_{x_0} < \tau_0\}$  and it is derived as follows similarly to (5.16),

$$\tilde{P}_{\text{ed2}}(\tau_0, r_0) = \exp[-\omega(\tau_0/(2\eta))r_0^2] - \exp[-\omega(\tau_0/\eta)r_0^2], \quad (5.22)$$

where  $\omega(\cdot)$  is given by (5.14).

When the original transmission fails, the success probability of BS doing the retransmission is obtained as (please see Appendix I for the derivation)

$$P_{\text{ed2}}(\tau_0, r_0) = \exp(-\lambda_s \pi c_1^2) \tilde{P}_{\text{ed2}}(\tau_0, r_0) + \sum_{n=1}^{\infty} \frac{(\lambda_s \pi c_1^2)^n}{n!} \exp(-\lambda_s \pi c_1^2) f_1(\tau_0, r_0, n), \quad (5.23)$$

where

$$f_1(\tau_0, r_0, n) = \sum_{k=0}^n (-1)^k \binom{n}{k} \left\{ \exp[-g(\tau_0, r_0^\alpha/2, k)] - \exp[-g(\tau_0, r_0^\alpha, k)] \right\}, \quad (5.24)$$

with

$$g(\tau_0, s, k) = 2\pi\lambda_b \int_{r_0}^{\infty} \left[ 1 - \frac{d_1}{(1 + \frac{\tau_0 s}{\eta} \ell^{-\alpha})(1 + \frac{\tau_0 r_v^\alpha}{\eta} \ell^{-\alpha})^k} - \frac{d_2}{(1 + \tau_0 s \ell^{-\alpha})(1 + \tau_0 r_v^\alpha \ell^{-\alpha})^k} \right] \ell \, d\ell. \quad (5.25)$$

Since only one-dimensional integral is included in (5.25), it can be calculated efficiently using the numerical method.

### For Case III:

In this case, the original data transmission between BS and its intended cell-edge MU fails, but at least one SU in the cooperation region correctly receives the data. Each decoding SU can estimate its channel state towards the cell-edge MU through measuring the strength of NACK frame. According to the channel quality, each SU can initiate a back-off timer [34] or transmit a burst sequence [56] to compete for the channel access. The decoding SU with the best channel state towards the cell-edge MU can be selected to retransmit.

Conditioned on the distance between BS  $x_0$  and its cell-edge MU being  $r_0$ , the success probability is

$$P_{\text{ed3}}(\tau_0, r_0) = \sum_{n=1}^{\infty} \Pr\{N = n\} \sum_{k=1}^n \mathbb{P}\left\{ \gamma_{x_0} < \tau_0, |\Phi_{x_0}| = k, \gamma_{x_0} + \max_{i \in \Phi_{x_0}} \{\gamma_{z_i}\} \geq \tau_0 \right\}, \quad (5.26)$$

where  $\gamma_{x_0}$  is the SIR between BS  $x_0$  and its typical cell-edge MU as given in (5.21). The probability of there being  $n \neq 0$  SUs in the cooperation region is given as  $\Pr\{N = n\}$  in (5.20). The inequality  $\gamma_{x_0} < \tau_0$  represents that the original transmission between BS and its cell-edge MU fails. The term  $|\Phi_{x_0}| = k$  represents that the cardinality of the decoding set is  $k$ , where  $\Phi_{x_0}$  is the decoding set of SUs in the cooperation region. The term  $\gamma_{x_0} + \max_{i \in \Phi_{x_0}} \{\gamma_{z_i}\} \geq \tau_0$  represents that the MRC detection is successful at the cell-edge MU, when the retransmission is performed by the best decoding SU. The SIR between a decoding SU  $z_i$ ,  $i \in \Phi_{x_0}$  and the typical MU is given as  $\gamma_{z_i} = \frac{\eta G_{z_i} \tilde{r}_v^{-\alpha}}{\mathcal{I}_p}$ , where  $\tilde{r}_v = r_0 - r_v = (1 - \zeta)r_0$  is the distance between the center of the cooperation region and the cell-edge MU. Since the relaying SUs lie in the cooperation region with small radius, the distance between each decoding SU in the cooperation region and the cell-edge MU can be set the same as  $\tilde{r}_v$ .

If the original transmission fails and one decoding SU in the cooperation region is selected to retransmit, the success probability is obtained as (please see Appendix II for the derivation)

$$P_{\text{cd3}}(\tau_0, r_0) = \sum_{n=1}^{\infty} \frac{(\lambda_s \pi c_1^2)^n}{n!} \exp(-\lambda_s \pi c_1^2) f_2(\tau_0, r_0, n), \quad (5.27)$$

where

$$\begin{aligned} f_2(\tau_0, r_0, n) &= \sum_{k=1}^n \binom{n}{k} \sum_{m=0}^{n-k} \binom{n-k}{m} (-1)^m \\ &\times \left\{ \exp[-g(\tau_0, 0, m+k)] - \left[ \sum_{t=0}^k \binom{k}{t} \frac{(-1)^t r_0^\alpha}{t \tilde{r}_v^\alpha - r_0^\alpha} + 1 \right] \right. \\ &\times \left. \exp[-g(\tau_0, r_0^\alpha, m+k)] + \sum_{t=0}^k \binom{k}{t} \frac{(-1)^t r_0^\alpha}{t \tilde{r}_v^\alpha - r_0^\alpha} \exp[-g(\tau_0, t \tilde{r}_v^\alpha, m+k)] \right\}, \end{aligned} \quad (5.28)$$

with the function  $g(\cdot, \cdot, \cdot)$  given by (5.25).

#### 5.4.4 Average Throughput of Primary System

If there is no spectrum sharing, the traditional truncated ARQ scheme with one-time retransmission is applied in the stand-alone cellular network. By averaging over the

random variable  $R$ , we can obtain the average throughput of primary system as

$$V_d = \underbrace{\int_0^{c_0} T_0 [P_{\text{in1}}(\hat{\tau}_0, r_0) + (1/2)P_{\text{in2}}(\hat{\tau}_0, r_0)] f_R(r_0) dr_0}_{V_{\text{din}}(\hat{\tau}_0)} + \underbrace{\int_{c_0}^{\infty} T_0 [P_{\text{ed1}}(\hat{\tau}_0, r_0) + (1/2)\tilde{P}_{\text{ed2}}(\hat{\tau}_0, r_0)] f_R(r_0) dr_0}_{V_{\text{ded}}(\hat{\tau}_0)}, \quad (5.29)$$

where  $\hat{\tau}_0 = 2^{T_0} - 1$ . The conditional success probabilities of original data transmission and retransmission for the cell-interior MU and cell-edge MU are given as  $P_{\text{in1}}(\hat{\tau}_0, r_0)$ ,  $P_{\text{in2}}(\hat{\tau}_0, r_0)$ ,  $P_{\text{ed1}}(\hat{\tau}_0, r_0)$ , and  $\tilde{P}_{\text{ed2}}(\hat{\tau}_0, r_0)$ , which can be obtained by replacing  $\tau_0$  in (5.13), (5.16), (5.18), and (5.22) with  $\hat{\tau}_0$ , respectively. By substituting the related expressions into (5.29), the average throughput of cell-interior communication is derived as

$$V_{\text{din}}(\hat{\tau}_0) = \frac{T_0 \lambda_b \pi}{2[\lambda_b \pi + \omega(\hat{\tau}_0)]} \{1 - \exp[-(\lambda_b \pi + \omega(\hat{\tau}_0))c_0^2]\} + \frac{T_0 \lambda_b \pi}{2[\lambda_b \pi + \omega(\hat{\tau}_0/2)]} \{1 - \exp[-(\lambda_b \pi + \omega(\hat{\tau}_0/2))c_0^2]\}. \quad (5.30)$$

The average throughput of cell-edge communication is derived as

$$V_{\text{ded}}(\hat{\tau}_0) = \frac{T_0 \lambda_b \pi}{2[\lambda_b \pi + \omega(\hat{\tau}_0/\eta)]} \exp\{-[\lambda_b \pi + \omega(\hat{\tau}_0/\eta)]c_0^2\} + \frac{T_0 \lambda_b \pi}{2[\lambda_b \pi + \omega(\hat{\tau}_0/(2\eta))]} \exp\{-[\lambda_b \pi + \omega(\hat{\tau}_0/(2\eta))]c_0^2\}. \quad (5.31)$$

The average throughput of primary system with cooperative spectrum sharing is obtained as

$$V_c(\lambda_s, \beta) = \underbrace{\int_0^{c_0} T_0 [P_{\text{in1}}(\tau_0, r_0) + (1/2)P_{\text{in2}}(\tau_0, r_0)] f_R(r_0) dr_0}_{V_{\text{cin}}(\tau_0)} + \underbrace{\int_{c_0}^{\infty} T_0 [P_{\text{ed1}}(\tau_0, r_0) + (1/2)P_{\text{ed2}}(\tau_0, r_0) + (1/2)P_{\text{ed3}}(\tau_0, r_0)] f_R(r_0) dr_0}_{V_{\text{ced}}(\tau_0)}, \quad (5.32)$$

where  $V_{\text{cin}}(\tau_0) = V_{\text{din}}(\tau_0)$  is obtained by replacing  $\hat{\tau}_0$  with  $\tau_0$  in (5.30). The other

integral in (5.32) is derived as

$$\begin{aligned}
V_{\text{ced}}(\tau_0) &= \frac{T_0 \lambda_b \pi [2 - \exp(-\lambda_s \pi c_1^2)]}{2 [\lambda_b \pi + \omega(\tau_0/\eta)]} \exp \{ - [\lambda_b \pi + \omega(\tau_0/\eta)] c_0^2 \} \\
&\quad + \frac{T_0 \lambda_b \pi \exp(-\lambda_s \pi c_1^2)}{2 [\lambda_b \pi + \omega(\tau_0/(2\eta))]} \exp \{ - [\lambda_b \pi + \omega(\tau_0/(2\eta))] c_0^2 \} \\
&\quad + \frac{T_0 \lambda_b \pi}{\exp(\lambda_s \pi c_1^2)} \sum_{n=1}^{\infty} \frac{(\lambda_s \pi c_1^2)^n}{n!} \int_{c_0}^{\infty} r_0 [f_1(\tau_0, r_0, n) + f_2(\tau_0, r_0, n)] \exp(-\lambda_b \pi r_0^2) dr_0,
\end{aligned} \tag{5.33}$$

where  $f_1(\tau_0, r_0, n)$  and  $f_2(\tau_0, r_0, n)$  are given by (5.24) and (5.28), respectively. The closed form expression of the integral in (5.33) is not available, but it can be numerically calculated. Without losing accuracy, the last term of (5.33) can be calculated with limited number of  $n$ .

## 5.5 Solution to the Optimization Problem

In this section, we will find the optimal  $\lambda_s$  and  $\beta$  that can maximize the secondary transmission capacity (5.1) while satisfying the constraints (5.2) and (5.3). The transmission capacity of secondary system is a monotonically increasing function of the SU density  $\lambda_s$ . Therefore, the higher the SU density, the higher the transmission capacity. However, the outage performance of secondary system gets worse with higher SU density as more interference is introduced. The maximum SU density that can satisfy the outage constraint (5.2) is obtained via  $P_{\text{out}}^s(\lambda_s, \beta) = \epsilon$ . Then, we can obtain one critical point of the SU density as

$$\lambda_{s1}(\beta) = -\frac{\ln(1 - \epsilon) \sin(2\pi/\alpha)}{\xi \pi d^2 \tau_1^{2/\alpha} 2\pi/\alpha}. \tag{5.34}$$

This critical density is a function of the bandwidth allocation factor  $\beta$  included in  $\tau_1 = 2^{T_1/\beta} - 1$ . We note that the outage constraint is guaranteed only when  $\lambda_s \leq \lambda_{s1}(\beta)$ .

The higher the SU density, the more SUs lying in the cooperation region and the higher the average throughput of primary downlink. Through setting  $V_c(\lambda_s, \beta) = (1 + \rho)V_d$  in the constraint (5.3), we can find another critical point  $\lambda_{s2}(\beta)$ , which

is also a function of  $\beta$ . For a given  $\beta$ , the throughput improvement requirement of primary system can be satisfied only when  $\lambda_s \geq \lambda_{s2}(\beta)$ .

Therefore, for a given  $\beta \in (0, 1)$ , both constraints (5.2) and (5.3) can be satisfied with  $\lambda_{s2}(\beta) \leq \lambda_s \leq \lambda_{s1}(\beta)$ . To maximize the transmission capacity of secondary system, we need to search for the values of  $\beta$  and its corresponding  $\lambda_{s1}(\beta)$  and  $\lambda_{s2}(\beta)$ . A given  $\beta$  belongs to the potential allocation set  $\mathcal{S}$  if we have  $\lambda_{s2}(\beta) \leq \lambda_{s1}(\beta)$ , i.e.,  $\mathcal{S} = \{\beta \in (0, 1) : \lambda_{s2}(\beta) \leq \lambda_{s1}(\beta)\}$ . The optimal bandwidth allocation factor is denoted as  $\beta^*$  and obtained as  $\beta^* = \arg \max_{\beta \in \mathcal{S}} \lambda_{s1}(\beta)$ . The optimal SU density is obtained as  $\lambda_{s1}(\beta^*)$  and the transmission capacity of secondary system can thus be derived as  $C_s^\epsilon = \xi \lambda_{s1}(\beta^*) (1 - \epsilon) T_1$ . Using this solution, the throughput of primary system can be improved by at least the ratio  $\rho$ . However, if  $\mathcal{S} = \emptyset$ , the two constraints of the optimization problem cannot be satisfied simultaneously and the cellular network will utilize the whole spectrum band for its own data transmission without secondary access.

To numerically search the optimal bandwidth allocation factor and the maximum SU density, we use the following approach. For each value of  $\beta \in (0, 1)$ , we calculate  $\lambda_{s1}(\beta)$  according to (5.34) and  $\hat{\rho} = [V_c(\lambda_{s1}(\beta), \beta) - V_d]/V_d$ . If  $\hat{\rho} < \rho$  occurs,  $\lambda_{s2}(\beta)$  is larger than  $\lambda_{s1}(\beta)$ , so this bandwidth allocation factor is not a potential point, i.e.,  $\beta \notin \mathcal{S}$ . If  $\hat{\rho} \geq \rho$  occurs,  $\lambda_{s2}(\beta)$  is no larger than  $\lambda_{s1}(\beta)$ , so this bandwidth allocation factor is potential, i.e.,  $\beta \in \mathcal{S}$ . Over the whole potential allocation set  $\mathcal{S}$ , we can find the one that brings the largest SU density.

## 5.6 Numerical and Simulation Results

In this section, we show the impacts of system parameters to the primary performance and verify our theoretical analysis of Section 5.4. The transmission capacities of secondary system with different system settings are plotted by solving the optimization problem of Section 5.3. The simulation results are obtained by averaging over the topology iterations for  $10^5$  times, and the overlaid network is modeled as a circular

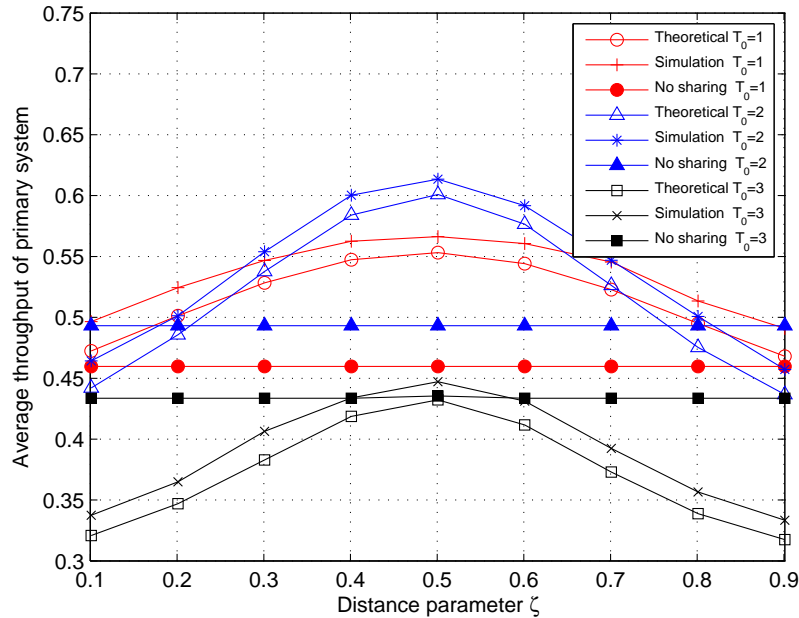


**Figure 5.4:** Average throughput of the primary system w.r.t. the relative distance  $\zeta$ . The system settings are  $\alpha = 3$ ,  $c_0 = 9$  m,  $c_1 = 1$  m,  $\lambda_b = 10^{-3}$ ,  $\lambda_m = 10^{-2}$ , and  $\lambda_s = 0.9$ . The bandwidth allocation  $\beta = 0.2$  is used for the cooperative spectrum sharing, while it is zero for the stand-alone cellular network without spectrum sharing.

area over the 2-D plane with radius  $\sqrt{10} \times 10^2$  m. Similarly to reference [88], the optimal power ratio is set as  $\eta^* = \arg \max_{\eta \in [1, 20]} V_d$ .

### 5.6.1 Average Throughput of Primary System

Fig. 5.4 shows the average throughput of cellular network downlink with respect to the distance factor  $\zeta$ . In the cooperative spectrum sharing, the best performance of primary system can be achieved when  $\zeta = 0.5$ . The cooperation region should be located in the middle between each BS and its cell-edge MU. When  $\zeta$  is small, the cooperation region is close to the BS and it is more likely to select one decoding SU to help the primary data transmission. As the distance towards the cell-edge MU is far, the robustness of cooperative communication is weak. On the other hand, when  $\zeta$  is large, the cooperation region is far from the BS and the decoding set is

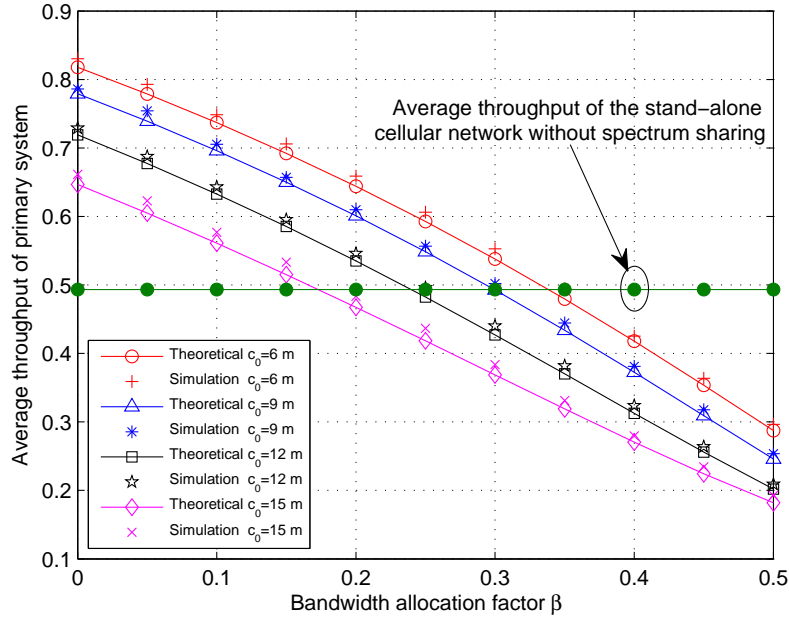


**Figure 5.5:** Average throughput of the primary system w.r.t. the bandwidth allocation factor  $\beta$ . The system settings are  $\alpha = 3$ ,  $c_1 = 1$  m,  $\zeta = 0.501$ ,  $T_0 = 2$  bits/s/Hz,  $\lambda_b = 10^{-3}$ ,  $\lambda_m = 10^{-2}$ , and  $\lambda_s = 0.9$ .

more likely empty. As a result, the opportunity of cooperation is small. Therefore, the primary performance is worse in both the small and large regions of  $\zeta$ . The throughput is defined as the product of target rate  $T_0$  and success probability, which gets worse with the increase of  $T_0$ . With the variation of  $T_0$ , the primary throughput is a trade-off between target rate and success probability. Since a fraction of spectrum is released for the secondary data transmission, the throughput of primary system may be worse than that without spectrum sharing.

Fig. 5.5 shows the primary average throughput with respect to the bandwidth allocation factor  $\beta$  in the cooperative spectrum sharing. The higher the bandwidth allocation, the less throughput is obtained for the primary system, as it becomes more difficult to support the primary target rate with the remaining narrower bandwidth  $1 - \beta$ . When  $\beta = 0$ , no spectrum is allocated to the secondary system, but the primary transmission is assisted by SUs, so the throughput greatly outperforms the stand-alone cellular network without spectrum sharing. The average throughput of

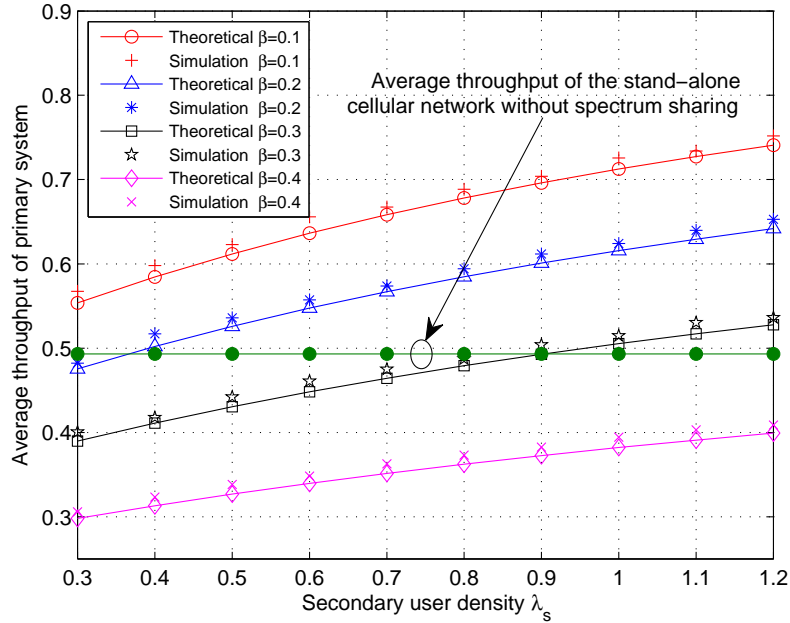


**Figure 5.6:** Average throughput of the primary system w.r.t. the SU density  $\lambda_s$ . The system settings are  $\alpha = 3$ ,  $c_0 = 9$  m,  $c_1 = 1$  m,  $\zeta = 0.501$ ,  $T_0 = 2$  bits/s/Hz,  $\lambda_b = 10^{-3}$ , and  $\lambda_m = 10^{-2}$ .

primary down-link improves with the decrease of the division radius  $c_0$ . The smaller the cell-interior area, the larger the cell-edge area, and hence more benefits can be brought by the cooperation from SUs. The numerical results of Section 5.4 are tight to the simulation results.

Fig. 5.6 shows the impact of SU density  $\lambda_s$  on the primary performance. The region division radius of each cell is set as  $c_0 = 9$  m, while the radius of the cooperation region is set as  $c_1 = 1$ . Due to the Poisson distribution on the 2-D plane, the average number of SUs in the cooperation region is  $\lambda_s \pi c_1^2$ . Obviously, the smaller the SU density  $\lambda_s$ , the less average number of SUs residing in the cooperation region for the possible retransmission of primary data. Therefore, the average throughput of the primary downlink deteriorates with the decrease of the SU density  $\lambda_s$ . It also shows that the larger time allocation factor  $\beta$  results in the smaller primary throughput. It verifies that our theoretical analysis can well match the simulation results.

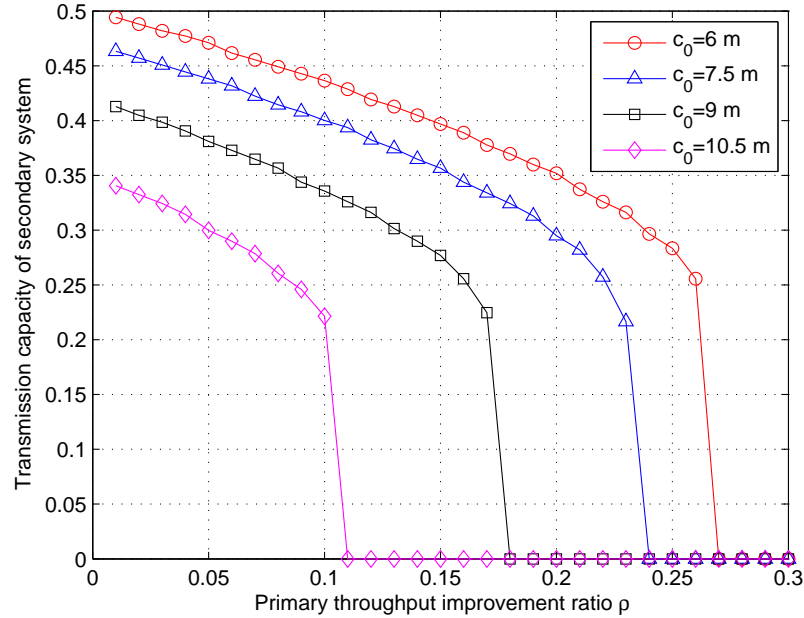


**Figure 5.7:** Transmission capacity of secondary system w.r.t. the primary throughput improvement ratio  $\rho$  for different  $c_0$ . The system settings are  $\alpha = 3$ ,  $c_1 = 1$  m,  $\zeta = 0.501$ ,  $T_0 = 2$  bits/s/Hz,  $T_1 = 1$  bits/s/Hz,  $\epsilon = 0.1$ ,  $\xi = 0.2$ ,  $d = 0.1$ , and  $\lambda_b = 10^{-3}$ .

### 5.6.2 Transmission Capacity of Secondary System

Fig. 5.7 shows the secondary transmission capacity against the primary throughput improvement ratio  $\rho$  with different cell division radius  $c_0$ . The secondary transmission capacity gets worse with the increase of  $\rho$  and it becomes zero when  $\rho$  is larger than a critical point, which is an upper bound of the primary throughput improvement ratio. In other words, the throughput improvement ratio larger than this critical point cannot be achieved by the cooperative spectrum sharing scheme. The secondary transmission capacity deteriorates with the increase of radius  $c_0$ . The cell-edge area is small when  $c_0$  is large, so the potential improvement of primary performance is small due to the small opportunity of cooperative data transmission. Therefore, the secondary performance gets worse as more resource is reserved to meet the primary QoS requirement.

Fig. 5.8 shows the secondary transmission capacity versus the primary through-

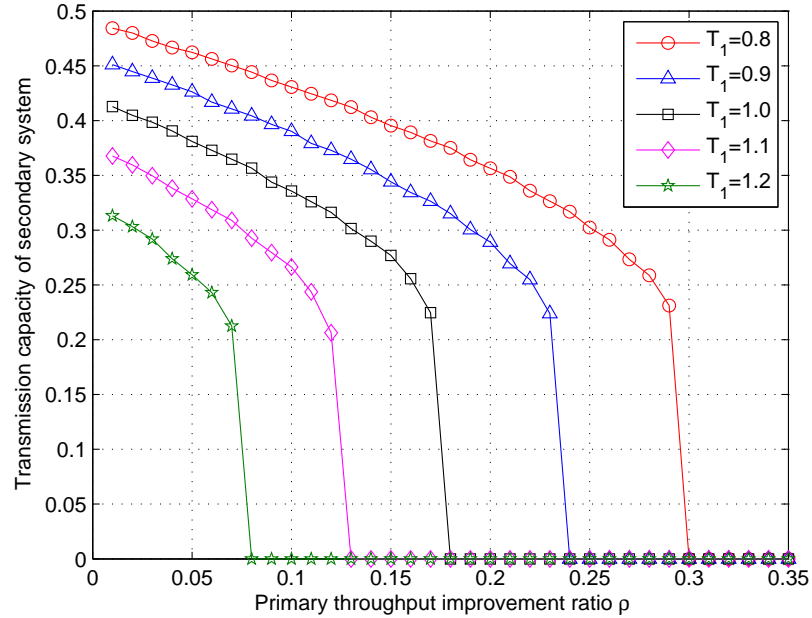


**Figure 5.8:** Transmission capacity of secondary system w.r.t. the primary throughput improvement ratio  $\rho$  for different  $T_1$ . The system settings are  $\alpha = 3$ ,  $c_0 = 9$  m,  $c_1 = 1$  m,  $\zeta = 0.501$ ,  $T_0 = 2$  bits/s/Hz,  $\epsilon = 0.1$ ,  $\xi = 0.2$ ,  $d = 0.1$ , and  $\lambda_b = 10^{-3}$ .

put improvement ratio  $\rho$  for different secondary target rate  $T_1$ . Similarly, there is an upper bound of the parameter  $\rho$ , above which the primary requirement can not be satisfied and the cooperative spectrum sharing is inactive. The secondary transmission capacity gets smaller with the increase of target rate  $T_1$ . This phenomenon is attributable to a trade-off between the maximum allowable SU density and the transmission rate. The outage probability of secondary data transmission gets worse with the increase of  $T_1$  as shown by (5.6). Therefore, the allowable maximum SU density  $\lambda_s$  becomes smaller to satisfy the constraint of target outage probability  $\epsilon$  as can be seen from (5.34). Since the negative effect of SU density reduction dominates over the positive effect of transmission rate increase, the secondary transmission capacity gets worse.

Fig. 5.9 shows the secondary transmission capacity with respect to the secondary target outage probability  $\epsilon$  for different Aloha MAP  $\xi$ . With the primary throughput

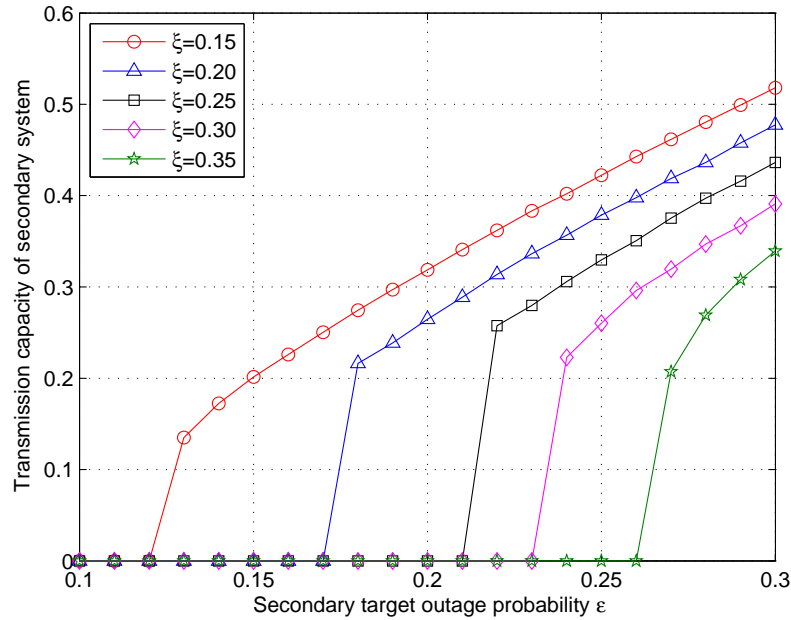


**Figure 5.9** Transmission capacity of secondary system w.r.t. the secondary target outage probability  $\epsilon$  for different  $\xi$ . The system settings are  $\alpha = 3$ ,  $c_0 = 9$  m,  $c_1 = 1$  m,  $\zeta = 0.501$ ,  $T_0 = 2$  bits/s/Hz,  $T_1 = 1$  bits/s/Hz,  $d = 0.15$ ,  $\rho = 0.1$ , and  $\lambda_b = 10^{-3}$ .

improvement ratio fixed, there exists a critical value of  $\epsilon$ , below which the primary performance improvement requirement can not be guaranteed and the cooperative spectrum sharing is not valid. Above this critical point, the secondary transmission capacity gets larger with the increase of target outage probability  $\epsilon$ . The larger the target outage probability, the larger the maximum allowable SU density as shown by (5.34). Although the success probability of secondary data transmission becomes worse with the increase of  $\epsilon$ , the benefits brought by the SU density increase can beat against the degradation of success probability. As a compromise, the secondary transmission capacity gets better. With the increase of  $\xi$ , the maximum allowable SU density gets smaller and less cooperation is performed for the primary cell-edge communication. As a result, less resource is allocated for the secondary data transmission, and hence the secondary transmission capacity gets worse.

Fig. 5.10 shows the secondary transmission capacity against the secondary target

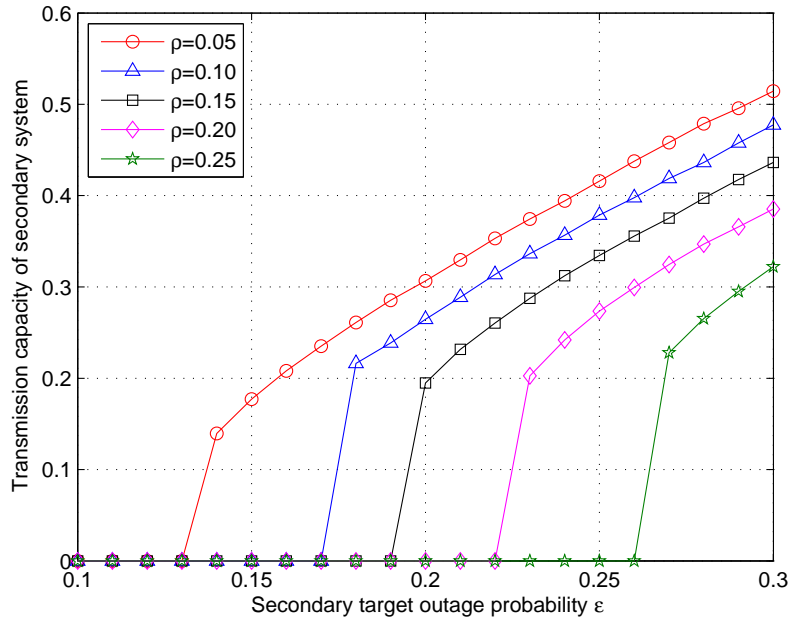


**Figure 5.10** Transmission capacity of secondary system w.r.t. the secondary target outage probability  $\epsilon$  for different  $\rho$ . The system settings are  $\alpha = 3$ ,  $c_0 = 9$  m,  $c_1 = 1$  m,  $\zeta = 0.501$ ,  $T_0 = 2$  bits/s/Hz,  $T_1 = 1$  bits/s/Hz,  $d = 0.15$ ,  $\xi = 0.2$ , and  $\lambda_b = 10^{-3}$ .

outage probability  $\epsilon$  with different primary throughput improvement ratio  $\rho$ . Similarly, there is a critical point of  $\epsilon$ , below which the cooperative spectrum sharing cannot be performed, because the primary performance constraint is violated. The secondary transmission capacity deteriorates with the increase of  $\rho$ , because it is more difficult to meet the primary performance requirement and more resource is kept for the primary data transmission. In this situation, less resource is available for the secondary data transmission and hence the secondary transmission capacity gets smaller.

## 5.7 Summary

In this chapter, we design a cooperative spectrum sharing scheme between cellular network downlink and ad-hoc network. The secondary users can actively help the

primary cell-edge communication to improve the primary performance by a predefined ratio. As a reward, a fraction of disjoint bandwidth can be released for the secondary data transmission. The transmission capacity of secondary system and the average throughput of primary downlink are analyzed using the stochastic geometry theory. The optimization problem is formulated to maximize the secondary transmission capacity under the QoS constraints of secondary outage probability and primary throughput improvement. The optimal secondary user density and bandwidth allocation are numerically calculated. Performance results are provided to demonstrate that the primary performance can be conservatively improved and the secondary transmission can be well accommodated.

## 5.8 Appendix I: Success Probability of Case II

We assume that the distance between an interferer and each SU in the cooperation region is the same as the distance between this interferer and the typical cell-edge MU. The path-loss from an interferer to the cooperative SUs and to the typical MU is the same, while the channel fading is independent. The success probability in (5.19) is derived as

$$\begin{aligned}
& \mathbb{P} \left\{ \frac{\tau_0}{2} \leq \gamma_{x_0} < \tau_0, \max_{i=1 \rightarrow n} \{ \gamma_{x_0, z_i} \} < \tau_0 \right\} \\
&= \mathbb{P} \left\{ \frac{\tau_0}{2} \leq \frac{\eta G_{x_0} r_0^{-\alpha}}{\mathcal{I}_p} < \tau_0, \max \left\{ \frac{\eta G_{x_0, z_i} r_v^{-\alpha}}{\mathcal{I}_{p_i}} \right\} < \tau_0 \right\} \tag{5.35} \\
&= \Pr \left\{ \frac{\tau_0 r_0^\alpha}{2\eta} \mathcal{I}_p \leq G_{x_0} < \frac{\tau_0 r_0^\alpha}{\eta} \mathcal{I}_p, G_{x_0, z_1} < \frac{\tau_0 r_v^\alpha}{\eta} \mathcal{I}_{p_1}, \dots, G_{x_0, z_n} < \frac{\tau_0 r_v^\alpha}{\eta} \mathcal{I}_{p_n} \right\} \\
&= \mathbb{E}_{\Pi_b, P} \left\{ \underbrace{\mathbb{E}_G \left[ \exp \left( - \frac{\tau_0 r_0^\alpha}{2\eta} \mathcal{I}_p \right) - \exp \left( - \frac{\tau_0 r_0^\alpha}{\eta} \mathcal{I}_p \right) \right]}_{\mathcal{A}_1} \prod_{i=1}^n \underbrace{\mathbb{E}_G \left[ 1 - \exp \left( - \frac{\tau_0 r_v^\alpha}{\eta} \mathcal{I}_{p_i} \right) \right]}_{\mathcal{A}_2} \right\},
\end{aligned}$$

where the inner expectations are taken over the independent channel fading from each interferer to the cell-edge MU and each cooperative SU. The outside expectation of (5.35) is taken over the point process and the transmit power of interferers. The expectation over the independent channel fading between interferers and the typical

cell-edge MU, i.e.,  $\mathcal{A}_1$  of (5.35), is derived as

$$\mathcal{A}_1 = \prod_{x \in \Pi_b \setminus \{x_0\}} \frac{1}{1 + \frac{\tau_0 r_0^\alpha}{2\eta} P_x \ell_x^{-\alpha}} - \prod_{x \in \Pi_b \setminus \{x_0\}} \frac{1}{1 + \frac{\tau_0 r_0^\alpha}{\eta} P_x \ell_x^{-\alpha}}, \quad (5.36)$$

where this result is obtained by substituting the interference  $\mathcal{I}_p$  (5.9) and taking the expectation over the independent channel fading. Similarly, the expectation over the channel fading between interferers and SUs in the cooperation region, i.e.,  $\mathcal{A}_2$  of (5.35), is derived as

$$\mathcal{A}_2 = \left\{ 1 - \prod_{x \in \Pi_b \setminus \{x_0\}} \frac{1}{1 + \frac{\tau_0 r_v^\alpha}{\eta} P_x \ell_x^{-\alpha}} \right\}^n. \quad (5.37)$$

Substitute (5.36) and (5.37) into (5.35), we can get the result as

$$\begin{aligned} & \mathbb{P} \left\{ \frac{\tau_0}{2} \leq \gamma_{x_0} < \tau_0, \max_{i=1 \rightarrow n} \{\gamma_{x_0, z_i}\} < \tau_0 \right\} \\ &= \sum_{k=0}^n (-1)^k \binom{n}{k} \left\{ \underbrace{\mathbb{E}_{\Pi_b, P} \left[ \prod_{x \in \Pi_b \setminus \{x_0\}} \frac{1}{\left(1 + \frac{\tau_0 r_0^\alpha}{2\eta} P_x \ell_x^{-\alpha}\right) \left(1 + \frac{\tau_0 r_v^\alpha}{\eta} P_x \ell_x^{-\alpha}\right)^k} \right]}_{\mathcal{B}_1} \right. \\ & \quad \left. - \underbrace{\mathbb{E}_{\Pi_b, P} \left[ \prod_{x \in \Pi_b \setminus \{x_0\}} \frac{1}{\left(1 + \frac{\tau_0 r_0^\alpha}{\eta} P_x \ell_x^{-\alpha}\right) \left(1 + \frac{\tau_0 r_v^\alpha}{\eta} P_x \ell_x^{-\alpha}\right)^k} \right]}_{\mathcal{B}_2} \right\}, \quad (5.38) \end{aligned}$$

where the binomial expansion of  $\mathcal{A}_2$  is utilized. Then, applying the PGFL of PPP and taking the expectation over the BS transmit power, we can get the result of  $\mathcal{B}_1$  of (5.38) as

$$\begin{aligned} \mathcal{B}_1 = \exp \left\{ -2\pi\lambda_b \int_{r_0}^{\infty} \left[ 1 - \frac{d_1}{\left(1 + \frac{\tau_0 r_0^\alpha}{2\eta} \ell^{-\alpha}\right) \left(1 + \frac{\tau_0 r_v^\alpha}{\eta} \ell^{-\alpha}\right)^k} \right. \right. \\ \left. \left. - \frac{d_2}{\left(1 + \frac{\tau_0 r_0^\alpha}{2\eta} \ell^{-\alpha}\right) \left(1 + \tau_0 r_v^\alpha \ell^{-\alpha}\right)^k} \right] \ell \, d\ell \right\}, \quad (5.39) \end{aligned}$$

where the integral plus the pre-factor is denoted as a function  $g(\tau_0, r_0^\alpha/2, k)$ . Similarly, another expectation of (5.38) can be directly obtained as

$$\mathcal{B}_2 = \exp \left[ -g(\tau_0, r_0^\alpha, k) \right]. \quad (5.40)$$

Then, jointly considering  $\Pr\{N = n\}$  in (5.20) and the probability of (5.38), the success probability of Case II can thus be derived as (5.23).

## 5.9 Appendix II: Success Probability of Case III

The probability of (5.26) is given as follows and it is further divided into two parts.

$$\begin{aligned} & \mathbb{P}\left\{\gamma_{x_0} < \tau_0, |\Phi_{x_0}| = k, \gamma_{x_0} + \max_{i \in \Phi_{x_0}}\{\gamma_{z_i}\} \geq \tau_0\right\} \\ &= \underbrace{\mathbb{P}\left\{\gamma_{x_0} < \tau_0, |\Phi_{x_0}| = k\right\}}_{\mathcal{C}_1} - \underbrace{\mathbb{P}\left\{\gamma_{x_0} < \tau_0, |\Phi_{x_0}| = k, \gamma_{x_0} + \max_{i \in \Phi_{x_0}}\{\gamma_{z_i}\} < \tau_0\right\}}_{\mathcal{C}_2}. \end{aligned} \quad (5.41)$$

Conditioned on the PPP  $\Pi_b$  and the transmit power  $P$  of interferers, the probability of a cooperating SU  $z_i$  correctly receiving the primary data is given as

$$\mathbb{P}\left\{\gamma_{x_0, z_i} \geq \tau_0 | \Pi_b, P\right\} = \prod_{x \in \Pi_b \setminus \{x_0\}} \frac{1}{1 + \frac{\tau_0 r_x^\alpha}{\eta} P_x \ell_x^{-\alpha}}. \quad (5.42)$$

Then, the conditional probability of the cardinality of decoding set being  $k$  is derived as

$$\begin{aligned} \mathbb{P}\left\{|\Phi_{x_0}| = k | \Pi_b, P\right\} &= \binom{n}{k} \left[ \mathbb{P}\left\{\gamma_{x_0, z_i} \geq \tau_0 | \Pi_b, P\right\} \right]^k \left[ 1 - \mathbb{P}\left\{\gamma_{x_0, z_i} \geq \tau_0 | \Pi_b, P\right\} \right]^{n-k} \\ &= \binom{n}{k} \sum_{m=0}^{n-k} \binom{n-k}{m} (-1)^m \prod_{x \in \Pi_b \setminus \{x_0\}} \frac{1}{\left(1 + \frac{\tau_0 r_x^\alpha}{\eta} P_x \ell_x^{-\alpha}\right)^{m+k}}, \end{aligned} \quad (5.43)$$

where the binomial expansion is considered. The distance between an interferer and each SU in the cooperation region is set the same as the distance between this interferer and the typical cell-edge MU. Jointly considering the events that the original transmission fails and the decoding set has  $k$  SUs, taking expectation over the discrete random variable  $P$  and applying the PGFL of PPP, the first probability of (5.41) is derived as

$$\mathcal{C}_1 = \binom{n}{k} \sum_{m=0}^{n-k} \binom{n-k}{m} (-1)^m \left\{ \exp\left[-g(\tau_0, 0, m+k)\right] - \exp\left[-g(\tau_0, r_0^\alpha, m+k)\right] \right\}, \quad (5.44)$$

where the function  $g(\cdot, \cdot, \cdot)$  is given in (5.25).

Conditioned on the PPP  $\Pi_b$  and transmit power  $P$  of interferers, we can derive the following probability when there are  $k$  SUs in the decoding set  $\Phi_{x_0}$ .

$$\begin{aligned}
& \mathbb{P}\left\{\gamma_{x_0} < \tau_0, \gamma_{x_0} + \max_{i \in \Phi_{x_0}}\{\gamma_{z_i}\} < \tau_0 \mid |\Phi_{x_0}| = k, \Pi_b, P\right\} \\
&= \mathbb{E}_G \left\{ \int_0^{\frac{\tau_0 r_0^\alpha}{\eta} \mathcal{I}_p} \left\{ 1 - \exp \left[ - \frac{(\tau_0 - \gamma_{x_0}) \tilde{r}_v^\alpha}{\eta} \mathcal{I}_p \right] \right\}^k \exp(-G_{x_0}) dG_{x_0} \right\} \\
&= \sum_{t=0}^k \binom{k}{t} \frac{(-1)^t r_0^\alpha}{t \tilde{r}_v^\alpha - r_0^\alpha} \left[ \prod_{x \in \Pi_b \setminus \{x_0\}} \frac{1}{1 + \frac{\tau_0 r_0^\alpha}{\eta} P x \ell_x^{-\alpha}} - \prod_{x \in \Pi_b \setminus \{x_0\}} \frac{1}{1 + \frac{\tau_0 t \tilde{r}_v^\alpha}{\eta} P x \ell_x^{-\alpha}} \right], \quad (5.45)
\end{aligned}$$

where the binomial expansion is used in the derivation. In the derivation of (5.45), we assume that  $t \tilde{r}_v^\alpha \neq r_0^\alpha$  for  $\forall t \in \{0, 1, \dots, k\}$ . Jointly considering (5.43) and (5.45), the second probability of (5.41) can be derived as  $\mathcal{C}_2 = \mathcal{D}_1 - \mathcal{D}_2$ , where

$$\mathcal{D}_1 = \binom{n}{k} \sum_{m=0}^{n-k} \binom{n-k}{m} (-1)^m \sum_{t=0}^k \binom{k}{t} \frac{(-1)^t r_0^\alpha}{t \tilde{r}_v^\alpha - r_0^\alpha} \exp \left[ -g(\tau_0, r_0^\alpha, m+k) \right]. \quad (5.46)$$

In the derivation of  $\mathcal{D}_1$ , the PGFL of PPP is applied and the expectation over discrete random variable  $P$  is taken. Another term  $\mathcal{D}_2$  is derived as

$$\mathcal{D}_2 = \binom{n}{k} \sum_{m=0}^{n-k} \binom{n-k}{m} (-1)^m \sum_{t=0}^k \binom{k}{t} \frac{(-1)^t r_0^\alpha}{t \tilde{r}_v^\alpha - r_0^\alpha} \exp \left[ -g(\tau_0, t \tilde{r}_v^\alpha, m+k) \right]. \quad (5.47)$$

Combine the first probability  $\mathcal{C}_1$  and second probability  $\mathcal{C}_2$  of (5.41) and consider the probability of  $\Pr\{N = n\}$ , the result of (5.27) is obtained.

# Chapter 6

## Conclusion and Future Work

### 6.1 Thesis Conclusion

Cognitive radio techniques have been intensively studied to improve the utilization efficiency of the scarce spectrum so as to accommodate the increasing wireless data transmission requirements. In this context, cooperative techniques have been adopted as an effective way to facilitate the spectrum sharing, as the space diversity can be achieved. However, the overlay spectrum sharing based on the traditional cooperative protocols is proved to be inefficient, as multiple communication phases are usually included to transmit the same signal. This thesis aims to propose a variety of relay based spectrum sharing designs in space, time, and frequency domains to significantly improve the bandwidth efficiency of the cognitive radio network.

In Chapter 2, the two-path successive relaying based spectrum sharing protocol is proposed, where one primary communication pair coexists with two secondary communication pairs. Both the superposition coding and successive interference cancellation techniques are adopted to realize the simultaneous primary signal relaying and secondary signal transmission. The primary signal transmission is continuous over the whole time slots without interruption from secondary transmitters. The optimal secondary transmission power allocation is investigated in the space domain to

maximize the secondary success probability under the constraint that the primary outage performance should be protected. Numerical and simulation results demonstrate that this novel relay based spectrum sharing scheme can significantly outperform the conventional multi-phase cooperative spectrum sharing schemes.

In Chapter 3, the relay based spectrum leasing is designed in the multiuser cognitive radio network, where one primary link coexists with multiples secondary users. The best secondary user is selected to help the primary data transmission in the time domain through adaptively switching between two-path successive relaying and decode-and-forward relaying protocols. As a reward of the cooperation, the licensed spectrum can be released to the secondary data transmission in a fraction of time. The cooperative diversity gain of primary system and the selection diversity of secondary system are analyzed when the transmission rates of both systems are fixed. However, if the secondary transmission rate can be adjusted instantaneously according to the channel states, the multiuser diversity performance in terms of throughput scaling law is studied when there are large number of secondary users. Numerical results show that the same diversity gain can be achieved as that of the stand-alone multiuser wireless system without the cognitive radio constraint.

In Chapter 4, the uncoordinated cooperative communications are studied for the spatially random relay network, where each potential relay node determines independently whether it should cooperate with the source in the signal transmission or not based on its own local information. Three uncoordinated relay selection schemes are developed, namely distance-based, angle-based, and local SNR-based schemes. By using the local information each relay competes for the cooperation with the source governed by its own retransmission probability. The proposed uncoordinated cooperative communications require no coordination of the relay nodes but outperform the conventional cooperative communications by giving higher success transmission probability. It is expected that the proposed schemes have wide applications to wireless local area network or cellular networks to improve the coverage area and transmission efficiency with little computational complexity.

In Chapter 5, the relay based spectrum sharing between cellular network downlink and ad-hoc network is designed. All the users are assumed to randomly distribute on the two-dimensional plane following independent Poisson point processes. Between each cellular network base station and its cell-edge mobile users, a cooperation region is applied, among which the ad-hoc users can actively help the cell-edge data transmission using the cooperative truncated ARQ to combat the strong interference. In return, a fraction of spectrum bands can be allocated for the ad-hoc data transmissions. Since there are many concurrent transmission links, the aggregate interference is incorporated to study the average performance using the stochastic geometry theory. The impacts of system parameter settings to both the cellular and ad-hoc networks are investigated and the optimal bandwidth allocation factor is obtained. It shows that the secondary data transmission requirement can be well satisfied while the primary performance can be conservatively improved.

## 6.2 Future Work

Apart from the problems addressed in this thesis, there are some interesting and challenging topics to be investigated in the immediate future.

- For the adaptive spectrum leasing in the multiuser cognitive radio network, the best secondary user is selected based on the assumption that the perfect channel state information (CSI) is available. However, it is interesting to relax this ideal assumption and study the secondary user selection with imperfect CSI obtained through the limited feedback. The more flexible coordination protocols can be designed for the practical implementation. The multiuser diversity performance of this cognitive radio system has not yet been revealed if the limited feedback is considered to select the best secondary user.
- The overlay spectrum sharing between cellular network downlink and ad-hoc network is designed in this thesis. However, it is also interesting to study the

---

relay-based underlay spectrum sharing, where the exclusive region should be applied around each mobile user. The ad-hoc transmissions are prohibited in the exclusive regions to avoid severely interfering the cellular network transmissions. The successive interference cancelation can be performed by the ad-hoc users to extract their desired secondary signals when they lie close to the base stations. The more intelligent carrier sense multiple access (CSMA) protocol can be used by the ad-hoc network to avoid the strong mutual interference between the concurrent ad-hoc transmissions. In addition, the cooperation can be adopted among the ad-hoc users to combat the interference so as to struggle for more opportunities of accessing the licensed spectrum. The optimization problem can be formulated to determine the exclusive region radius and the CSMA sensing radius. These points can make the spectrum sharing more practical, but it becomes more challenging to solve these problems.

# Bibliography

- [1] A. Rabbachin, T. Q. S. Quek, H. Shin, and M. Z. Win, “Cognitive network interference,” *IEEE J. Sel. Areas Commun.*, vol. 29, pp. 480–493, Feb. 2011.
- [2] A. Ghasemi and E. S. Sousa, “Interference aggregation in spectrum-sensing cognitive wireless networks,” *IEEE J. Sel. Topics Signal Process.*, vol. 2, pp. 28–40, Feb. 2008.
- [3] W. Zhang, X.-G. Xia, and K. B. Letaief, “Space-time/frequency coding for MIMO-OFDM in next generation broadband wireless systems,” *IEEE Wireless Commun.*, vol. 14, pp. 32–43, Jun. 2007.
- [4] C. Zhai, J. Liu, L. Zheng, and H. Xu, “Lifetime maximization via a new cooperative MAC protocol in wireless sensor networks,” in *Proc. IEEE Global Communications Conference (GLOBECOM)*, Hawaii, USA, pp. 1–6, Dec. 2009.
- [5] W. Zhang and K. B. Letaief, “Full-rate distributed space-time codes for cooperative communications,” *IEEE Trans. Wireless Commun.*, vol. 7, pp. 2446–2451, Jul. 2008.
- [6] Y. Jing and B. Hassibi, “Distributed space-time coding in wireless relay networks,” *IEEE Trans. Wireless Commun.*, vol. 5, pp. 3524–3536, Dec. 2006.
- [7] K. B. Letaief and W. Zhang, “Cooperative communications for cognitive radio networks,” *Proc. of the IEEE*, vol. 97, pp. 878–893, May 2009.
- [8] J. M. Peha, “Approaches to spectrum sharing,” *IEEE Commun. Mag.*, vol. 43, pp. 10–12, Feb. 2005.
- [9] I. F. Akyildiz, W.-Y. Lee, M. C. Vuran, and S. Mohanty, “A survey on spectrum management in cognitive radio networks,” *IEEE Commun. Mag.*, vol. 46, pp. 40–48, Apr. 2008.
- [10] Q. Zhao and B. M. Sadler, “A survey of dynamic spectrum access,” *IEEE Signal Process. Mag.*, vol. 24, pp. 79–89, May 2007.
- [11] A. Goldsmith, S. A. Jafar, I. Maric, and S. Srinivasa, “Breaking spectrum gridlock with cognitive radios: An information theoretic perspective,” *Proc. of the IEEE*, vol. 97, pp. 894–914, May 2009.

- [12] C. Zhai, H. Xu, J. Liu, L. Zheng, and Y. Zhou, "Performance of opportunistic relaying with truncated ARQ over Nakagami-m fading channels," *Trans. Emerg. Telecommun. Techns.*, vol. 23, pp. 50–66, Jan. 2012.
- [13] M. Dohler, "Virtual Antenna Arrays," Ph.D. dissertation, King's College, London, U.K., 2003.
- [14] O. Simeone, I. Stanojev, S. Savazzi, Y. Bar-Ness, U. Spagnolini, and R. L. Pickholtz, "Spectrum leasing to cooperating secondary ad hoc networks," *IEEE J. Sel. Areas Commun.*, vol. 26, pp. 203–213, Jan. 2008.
- [15] I. Stanojev, O. Simeone, U. Spagnolini, Y. Bar-Ness, and R. L. Pickholtz, "Cooperative ARQ via auction-based spectrum leasing," *IEEE Trans. Commun.*, vol. 58, pp. 1843–1856, Jun. 2010.
- [16] D. Chiarotto, O. Simeone, and M. Zorzi, "Spectrum leasing via cooperative opportunistic routing techniques," *IEEE Trans. Wireless Commun.*, vol. 10, pp. 2960–2970, Sep. 2011.
- [17] S. K. Jayaweera, G. Vazquez-Vilar, and C. Mosquera, "Dynamic spectrum leasing: A new paradigm for spectrum sharing in cognitive radio networks," *IEEE Trans. Veh. Technol.*, vol. 59, pp. 2328–2339, Jun. 2010.
- [18] Y. Yi, J. Zhang, Q. Zhang, T. Jiang, and J. Zhang, "Cooperative communication-aware spectrum leasing in cognitive radio networks," in *Proc. IEEE New Frontiers in Dynamic Spectrum Access Networks (DySPAN)*, Singapore, pp. 1–11, Apr. 2010.
- [19] Y. Han, A. Pandharipande, and S. H. Ting, "Cooperative decode-and-forward relaying for secondary spectrum access," *IEEE Trans. Wireless Commun.*, vol. 8, pp. 4945–4950, Oct. 2009.
- [20] Y. Han, A. Pandharipande, and S. H. Ting, "Cooperative spectrum sharing via controlled amplify-and-forward relaying," in *Proc. IEEE International Symposium on Personal, Indoor, Mobile Radio Communications (PIMRC)*, Cannes, France, pp. 1–5, Sep. 2008.
- [21] Y. Han, S. H. Ting, and A. Pandharipande, "Cooperative spectrum sharing protocol with secondary user selection," *IEEE Trans. Wireless Commun.*, vol. 9, pp. 2914–2923, Sep. 2010.
- [22] J. N. Laneman, D. Tse, and G. W. Wornell, "Cooperative diversity in wireless networks: Efficient protocols and outage behavior," *IEEE Trans. Inf. Theory*, vol. 50, pp. 3062–3080, Dec. 2004.
- [23] B. Rankov and A. Wittneben, "Spectral efficient protocols for half-duplex fading relay channels," *IEEE J. Sel. Areas Commun.*, vol. 25, pp. 379–389, Feb. 2007.

- [24] Y. Fan, C. Wang, J. Thompson, and H. V. Poor, "Recovering multiplexing loss through successive relaying using repetition coding," *IEEE Trans. Wireless Commun.*, vol. 6, pp. 4484–4493, Dec. 2007.
- [25] F. Tian, W. Zhang, W.-K. Ma, P. C. Ching, and H. V. Poor, "An effective distributed space-time code for two-path successive relay network," *IEEE Trans. Commun.*, vol. 59, pp. 2254–2263, Aug. 2011.
- [26] L. Shi, W. Zhang, and P. C. Ching, "Single-symbol decodable distributed STBC for two-path successive relaying networks," in *Proc. IEEE International Conference on Acoustics, Speech and Signal Processing (ICASSP)*, Prague, Czech, pp. 3324–3327, May 2011.
- [27] R. Zhang, "On achievable rates of two-path successive relaying," *IEEE Trans. Commun.*, vol. 57, pp. 2914–2917, Oct. 2009.
- [28] H. Wicaksana, S. H. Ting, C. K. Ho, W. H. Chin, and Y. L. Guan, "AF two-path half duplex relaying with inter-relay self interference cancellation: Diversity analysis and its improvement," *IEEE Trans. Wireless Commun.*, vol. 8, pp. 4720–4729, Sep. 2009.
- [29] H. Wicaksana, S. H. Ting, Y. L. Guan, and X.-G. Xia, "Decode-and-forward two-path half-duplex relaying: Diversity-multiplexing tradeoff analysis," *IEEE Trans. Commun.*, vol. 59, pp. 1985–1994, Jul. 2011.
- [30] C. Luo, Y. Gong, and F. Zheng, "Full interference cancellation for two-path relay cooperative networks," *IEEE Trans. Veh. Technol.*, vol. 60, pp. 343–347, Jan. 2011.
- [31] C. Zhai, W. Zhang, and P. C. Ching, "Cooperative spectrum sharing based on two-path successive relaying," *IEEE Trans. Commun.*, vol. 61, pp. 2260–2270, Jun. 2013.
- [32] C. Zhai and W. Zhang, "Adaptive spectrum leasing with secondary user scheduling in cognitive radio networks," *IEEE Trans. Wireless Commun.*, vol. 12, pp. 3388–3398, Apr. 2013.
- [33] C. Zhai, J. Liu, L. Zheng, H. Xu, and H. Chen, "Maximize lifetime of wireless sensor networks via a distributed cooperative routing algorithm," *Trans. Emerg. Telecommun. Technol.*, vol. 23, pp. 414–428, Feb. 2012.
- [34] A. Bletsas, A. Khisti, D. P. Reed, A. Lippman, "A simple cooperative diversity method based on network path selection," *IEEE J. Sel. Areas Commun.*, vol. 24, pp. 659–672, Mar. 2006.

- [35] C. Zhai, W. Zhang, and G. Mao, "Uncoordinated cooperative communications with spatially random relays," *IEEE Trans. Wireless Commun.*, vol. 11, pp. 3126–3135, Sep. 2012.
- [36] C. Zhai, W. Zhang, and G. Mao, "Cooperative spectrum sharing between cellular and ad-hoc networks," *IEEE Trans. Wireless Commun.*, submitted, Jul. 2013.
- [37] J. Huang, R. A. Berry, and M. L. Honig, "Auction-based spectrum sharing," *Mobile Networks and Applications*, vol. 11, pp. 405–418, Apr. 2006.
- [38] F. Wang, M. Krunz, and S. Cui, "Spectrum sharing in cognitive radio networks," in *Proc. IEEE International Conference on Computer Communications (INFOCOM)*, Phoenix, USA, pp. 36–40, Apr. 2008.
- [39] D. Niyato and E. Hossain, "Competitive spectrum sharing in cognitive radio networks: a dynamic game approach," *IEEE Trans. Wireless Commun.*, vol. 7, pp. 2651–2660, Jul. 2008.
- [40] R. Menon, R. M. Buehrer, and J. H. Reed, "On the impact of dynamic spectrum sharing techniques on legacy radio systems," *IEEE Trans. Wireless Commun.*, vol. 7, pp. 4198–4207, Nov. 2008.
- [41] K. Huang, V. K. N. Lau, and Y. Chen, "Spectrum sharing between cellular and mobile ad hoc networks: transmission-capacity trade-off," *IEEE J. Sel. Areas Commun.*, vol. 27, pp. 1256–1267, Sep. 2009.
- [42] T. V. Nguyen and F. Baccelli, "A stochastic geometry model for cognitive radio networks," *The Computer Journal*, vol. 55, pp. 534–552, Jul. 2011.
- [43] K. Hamdi, W. Zhang, and K. B. Letaief, "Opportunistic spectrum sharing in cognitive MIMO wireless networks," *IEEE Trans. Wireless Commun.*, vol. 8, pp. 4098–4109, Aug. 2009.
- [44] R. Zhang and Y.-C. Liang, "Exploiting multi-antennas for opportunistic spectrum sharing in cognitive radio networks," *IEEE J. Sel. Topics Signal Process.*, vol. 2, pp. 88–102, Feb. 2008.
- [45] K. T. Phan, S. A. Vorobyov, N. D. Sidiropoulos, and C. Tellambura, "Spectrum sharing in wireless networks via QoS-aware secondary multicast beamforming," *IEEE Trans. Signal Process.*, vol. 57, pp. 2323–2335, Jun. 2009.
- [46] J. C. F. Li, W. Zhang, and J. Yuan, "Opportunistic spectrum sharing in cognitive radio networks based on primary limited feedback," *IEEE Trans. Commun.*, vol. 59, pp. 3272–3277, Dec. 2011.
- [47] W. Zhang, R. K. Mallik, and K. B. Letaief, "Optimization of cooperative spectrum sensing with energy detection in cognitive radio networks," *IEEE Trans. Wireless Commun.*, vol. 8, pp. 5761–5766, Dec. 2009.

- [48] G. J. Foschini and M. J. Gans, "On limits of wireless communications in a fading environment when using multiple antennas," *Wireless Pers. Commun.*, vol. 6, pp. 311–335, Feb. 1998.
- [49] A. F. Molisch, M. Z. Win, Y.-S. Choi, and J. H. Winters, "Capacity of MIMO systems with antenna selection," *IEEE Trans. Wireless Commun.*, vol. 4, pp. 1759–1772, Jul. 2005.
- [50] S. Sanayei and A. Nosratinia, "Exploiting multiuser diversity with only 1-bit feedback," in *Proc. IEEE Wireless Communications and Networking Conference (WCNC)*, New Orleans, USA, pp. 978–983, Mar. 2005.
- [51] T. W. Ban, W. Choi, B. C. Jung, and D. K. Sung, "Multi-user diversity in a spectrum sharing system," *IEEE Trans. Wireless Commun.*, vol. 8, pp. 102–106, Jan. 2009.
- [52] A. Tajer and X. Wang, "Multiuser diversity gain in cognitive networks," *IEEE Trans. Network.*, vol. 18, pp. 1766–1779, Dec. 2010.
- [53] Y. Li and A. Nosratinia, "Hybrid opportunistic scheduling in cognitive radio networks," *IEEE Trans. Wireless Commun.*, vol. 11, pp. 328–337, Jan. 2012.
- [54] R. Zhang and Y.-C. Liang, "Investigation on multiuser diversity in spectrum sharing based cognitive radio networks," *IEEE Commun. Letters*, vol. 14, pp. 133–135, Feb. 2010.
- [55] J.-P. Hong and W. Choi, "Capacity scaling law by multiuser diversity in cognitive radio systems," in *Proc. IEEE International Symposium on Information Theory (ISIT)*, Austin, Texas, USA, pp. 2088–2092, Jun. 2010.
- [56] F. Baccelli, B. Błaszczyszyn, and P. Mühlethaler, "An aloha protocol for multihop mobile wireless networks," *IEEE Trans. Inf. Theory*, vol. 52, pp. 421–436, Feb. 2006.
- [57] W. Su, A. K. Sadek, and K. J. R. Liu, "Cooperative communication protocols in wireless networks: performance analysis and optimum power allocation," *Wireless Personal Commun.*, vol. 44, pp. 181–217, Jan. 2008.
- [58] G. Song and Y. G. Li, "Asymptotic throughput analysis for channel-aware scheduling," *IEEE Trans. Commun.*, vol. 54, pp. 1827–1834, Oct. 2006.
- [59] S. Yang and J.-C. Belfiore, "Towards the optimal amplify-and-forward cooperative diversity scheme," *IEEE Trans. Inf. Theory*, vol. 53, pp. 3114–3126, Sep. 2007.
- [60] B. Zhao and M. C. Valenti, "Practical relay networks: a generalization of hybrid-ARQ," *IEEE J. Sel. Areas Commun.*, vol. 23, pp. 7–18, Jan. 2005.

- [61] M. Dianati, X. Ling, K. Naik, and X. Shen, "A node-cooperative ARQ scheme for wireless ad hoc networks," *IEEE Trans. Veh. Technol.*, vol. 55, pp. 1032–1044, May 2006.
- [62] G. Yu, Z. Zhang, and P. Qiu, "Cooperative ARQ in wireless networks: protocols description and performance analysis," in *Proc. IEEE International Conference on Communications (ICC)*, Istanbul, Turkey, pp. 3608–3614, Jun. 2006.
- [63] Q. Liu, S. Zhou, and G. B. Giannakis, "Cross-layer combining of adaptive modulation and coding with truncated ARQ over wireless links," *IEEE Trans. Wireless Commun.*, vol. 3, pp. 1746–1755, Sep. 2004.
- [64] J. Alonso-Zárate, E. Kartsakli, Ch. Verikoukis, and L. Alonso, "Persistent RC-SMA: a MAC protocol for a distributed cooperative ARQ scheme in wireless networks," *EURASIP Journal on Advanced Signal Processing*, pp. 1–13, Dec. 2008.
- [65] A. S. Ibrahim, A. K. Sadek, W. Su, and K. J. Ray Liu, "Cooperative communications with relay-selection: when to cooperate and whom to cooperate with?" *IEEE Trans. Wireless Commun.*, vol. 7, pp. 2814–2827, Jul. 2008.
- [66] L. Xiong, L. Libman, and G. Mao, "On uncoordinated cooperative communication strategies in wireless ad-hoc networks," *IEEE J. Sel. Areas Commun.*, vol. 32, pp. 280–288, Feb. 2012.
- [67] R. K. Ganti and M. Haenggi, "Analysis of uncoordinated opportunistic two-hop wireless ad hoc systems," in *Proc. IEEE International Symposium on Information Theory (ISIT)*, Seoul, Korea, pp. 1020–1024, Jun. 2009.
- [68] G. Mao, B. Fidan, and B. Anderson, "Wireless sensor network localization techniques," *Computer Networks*, vol. 51, pp. 2529–2553, Jul. 2007.
- [69] M. Haenggi, "On distances in uniformly random networks," *IEEE Trans. Inf. Theory*, vol. 51, pp. 3584–3586, Oct. 2005.
- [70] Z. Chen, G. Gokeda, and Y. Yu, *Introduction to Direction-of-Arrival Estimation*, Artech House, 2010.
- [71] I. S. Gradshteyn and I. M. Ryzhik, *Talbe of Integrals, Series, and Products*, 7th Edition, Academic Press, 2007.
- [72] M. Haenggi and R. K. Ganti, "Interference in Large Wireless Networks," *Foundations and Trends in Networking (NOW Publishers)*, vol. 3, pp. 127–248, 2008.
- [73] M. Haenggi, J. G. Andrews, F. Baccelli, O. Dousse, and M. Franceschetti, "Stochastic geometry and random graphs for the analysis and design of wireless networks," *IEEE J. Sel. Areas Commun.*, vol. 27, pp. 1029–1046, Sep. 2009.

- [74] C. Zhai and W. Zhang, "Spectrum and energy efficient cognitive relay for spectrum leasing," in *Proc. IEEE International Conference on Communication Systems (ICCS)*, Singapore, pp. 240-244, Nov. 2012.
- [75] W. Su, J. D. Matyjas, and S. Batalama, "Active cooperation between primary users and cognitive radio users in heterogeneous ad-hoc networks," *IEEE Trans. Signal Process.*, vol. 60, pp. 1796-1805, Apr. 2012.
- [76] S. P. Weber, X. Yang, J. G. Andrews and G. de Veciana, "Transmission capacity of wireless ad hoc networks with outage constraints," *IEEE Trans. Inf. Theory*, vol. 51, pp. 4091-4102, Dec. 2005.
- [77] J. Lee, J. G. Andrews, and D. Hong, "Spectrum sharing transmission capacity," *IEEE Trans. Wireless Commun.*, vol. 10, pp. 3053-3063, Sep. 2011.
- [78] C. Yin, C. Chen, T. Liu and S. Cui, "Generalized results of transmission capacities for overlaid wireless networks," in *Proc. IEEE International Symposium on Information Theory (ISIT)*, Seoul, Korea, pp. 1774-1778, Jun. 2009.
- [79] M. Vu, N. Devroye, and V. Tarokh, "On the primary exclusive region of cognitive networks," *IEEE Trans. Wireless Commun.*, vol. 8, pp. 3380-3385, Jul. 2009.
- [80] X. Hong, C.-X. Wang, and J. Thompson, "Interference modeling of cognitive radio networks," in *Proc. IEEE Vehicular Technology Conference (VTC Spring)*, Singapore, pp. 1851-1855, May 2008.
- [81] C.-H. Lee and M. Haenggi, "Interference and outage in poisson cognitive networks," *IEEE Trans. Wireless Commun.*, vol. 11, pp. 1392-1401, Apr. 2012.
- [82] H. Wang, S. Ma, and T.-S. Ng, "On performance of cooperative communication systems with spatial random relays," *IEEE Trans. Commun.*, vol. 59, pp. 1190-1199, Apr. 2011.
- [83] S.-R. Cho, W. Choi, and K. Huang, "QoS provisioning relay selection in random relay networks," *IEEE Trans. Veh. Technol.*, vol. 60, pp. 2680-2689, Jul. 2011.
- [84] Z. Sheng, Z. Ding, and K. K. Leung, "Transmission capacity of decode-and-forward cooperation in overlaid wireless networks," in *Proc. IEEE International Conference on Communications (ICC)*, Cape Town, South Africa, pp. 1-5, May 2010.
- [85] Y. Xu, P. Wu, L. Ding, and L. Shen, "Capacity analysis of selection cooperation in wireless ad-hoc networks," *IEEE Commun. Letters*, vol. 15, pp. 1212-1214, Nov. 2011.
- [86] R. K. Ganti and M. Haenggi, "Spatial analysis of opportunistic downlink relaying in a two-hop cellular system," *IEEE Trans. Commun.*, vol. 60, pp. 1443-1450, May 2012.

- 
- [87] J. G. Andrews, F. Baccelli, and R. K. Ganti, “A tractable approach to coverage and rate in cellular networks,” *IEEE Trans. Commun.*, vol. 59, pp. 3122–3134, Nov. 2011.
- [88] T. D. Novlan, R. K. Ganti, A. Ghosh, and J. G. Andrews, “Analytical evaluation of fractional frequency reuse for OFDMA cellular networks,” *IEEE Trans. Wireless Commun.*, vol. 10, pp. 4294–4305, Dec. 2011.
- [89] D. Stoyan, W. Kendall, and J. Mecke, *Stochastic Geometry and Its Applications*, 2nd Edition. New York: Wiley, 1996.
- [90] H. S. Dhillon, T. D. Novlan, and J. G. Andrews, “Coverage probability of uplink cellular networks,” in *Proc. IEEE Global Communications Conference (GLOBECOM)*, Anaheim, California, USA, pp. 2203–2208, Dec. 2012.